SYNTHESIS, CHARACTERIZATION AND REACTIVITY OF METAL MODIFIED HETEROPOLYACID CATALYSTS FOR ORGANIC TRANSFORMATION REACTIONS

by

Ms. Jhansi Pedada

Submitted in fulfillment of the academic requirement for
the degree of Doctor of Philosophy
in the
School of Chemistry and Physics
University of KwaZulu-Natal
Durban
South Africa

April 2018

Note: This thesis has been written according to Format 3, as outlined in the guidelines from the Faculty of Science and Agriculture, University of KwaZulu-Natal, which states: This is a thesis in which the chapters are written as a set of discrete research papers, with an overall introduction and final conclusions. These research papers would not all have been published yet, but at least one paper have already been submitted for publication. The references are reformatted to a uniform standard.

As the candidate's supervisor I have approved this thesis for submission

Name	Signature	Date

DEDICATED

TO

MY BELOVED PARENTS

ABSTRACT

In the present investigation, eco-friendly, sustainable and recyclable heteropolyacid catalysts have been developed for a series of organic transformations such as the production of ethyl acetate by solvent free liquid phase esterification and the formation of benzaldehyde by the oxidation of styrene and benzyl alcohol. All these reactions were carried out at room temperature. Various metal exchanged heteropolyacid catalysts with different metal loadings were prepared by the ion-exchange method and characterized by spectroscopic and adsorptions methods such as powder X-ray diffraction, scanning electron and transition electron microscopy, ^{31}P NMR spectroscopy, elemental analysis, Bright Field-STEM analysis, infrared spectroscopy, ex-situ pyridine adsorbed infrared spectroscopy, pore size distribution studies and BET surface area measurements to understand their structural and surface properties, together with their acidity and to relate this to the catalytic performance.

A series of K and Cs exchanged phosphotungstic acid (PTA) and phosphomolybdic acid (PMA) catalysts were synthesized for the esterification reaction. XRD patterns and infrared spectra showed that the crystallites and characteristic bands of the Keggin ion, respectively, were maintained after exchange of protons in the heteropolyacids with metal at all loadings of the catalysts. From pyridine adsorbed infrared spectroscopy, Brønsted and Lewis acid sites were present on the surface of the catalyst. Bright field STEM analysis showed a uniform distribution of the chemical composition which correlated well with theoretical atomic values of the metal loadings of all the catalysts, verified by ICP results. The efficiency of various metal exchanged heteropolyacid catalysts were assessed for the esterification reaction using various substrates and the Cs exchanged phosphotungstic acid catalysts showed superior activity compared to the other catalysts. In particular, the Cs exchanged phosphotungstic acid with a 1 wt.% loading showed the highest activity and was most tolerant to the presence of water that was produced in the reaction. The catalytic activity showed some correlation to the Brønsted and Lewis acidity, as well as Keggin ion density of catalysts.

A series of alkali metal exchanged phosphomolybdic acid catalysts were synthesized by ion exchange, characterized by various physico-chemical techniques and used in the solvent free

oxidation of styrene to benzaldehyde. XRD and infrared results showed that the primary structure of the Keggin ion usually present in phosphomolybdic acid is retained after metal exchange. HR-TEM analysis show a well-constructed spherical morphology of the materials with a lower degree of crystalinity. Type IV isotherms with mesoporous structure are observed from nitrogen adsorption-desorption isotherm studies and *ex-situ* pyridine adsorption experiments reveal that Brønsted acidic sites increased after metal exchange. The K exchanged phosphomolybdic acid catalysts were most efficient in the conversion of styrene to benzaldehyde and the order of reactivity of the alkali metal exchanged phosphomolybdic acid catalysts was K > Rb > Cs. Insight into the reaction pathway was obtained by investigating the oxidation styrene oxide. The results showed that phenyl acetaldehyde together with benzaldehyde are produced, providing some evidence that styrene oxidation proceeds via C=C cleavage to selectively produce benzaldehyde. The catalyst was easily recovered and was reused for up to three cycles showing stable activity.

Copper and zinc exchanged heteropolyacid catalysts were used in the oxidation of benzyl alcohol to benzaldehyde. The Zn exchanged phosphomolybdic acid catalysts showed higher oxidation activity that correlated well with the acidity of the catalysts. The catalysts were synthesized by the ion exchange method and were subjected to X-ray diffraction, infrared spectroscopy, pyridine adsorbed infrared spectroscopy, BET surface studies, ^{31}P NMR spectroscopy and inductively coupled plasma-optical emission spectroscopy to determine its physico-chemical properties. XRD diffractograms showed that crystallites of the Keggin ion of the heteropolyacid were present and were retained after metal modification, as observed by infrared spectroscopy. From pyridine adsorbed infrared, the Brønsted/Lewis acid site ratio increased in the metal exchanged phosphomolybdic acid catalysts, whereas there was a decrease in the ratio for the modified phosphotungstic acid catalysts. ^{31}P NMR spectra results showed that the metal was successfully exchanged with protons and was not incorporated in the primary structure of heteropolyacid catalyst, thus maintaining the Keggin ion. ICP analysis indicated a correlation of the theoretical metal content with the experimental loadings of the catalysts.

ACKNOWLEDGEMENTS

My sincere thanks go to my parents; I could not have done this without their love, patience, encouragement and understanding.

I would like to thank my supervisor Prof. Holger B. Friedrich and my co-supervisor Dr. S. Singh for their guidance and valuable advice throughout the course of my PhD. I am also indebted to my supervisor, Prof. Holger B. Friedrich for giving me the great opportunity to join his group, His patience, sharp eye and interpersonal skills in handling such a large and diverse group are unequalled. I also express my gratitude to my co-supervisor, Dr. S. Singh for his support, encouragement and scientific contribution.

Special thanks also go to the following organization and individuals:

- SASOL and University of KwaZulu-Natal for funding of project.
- Catalysis Research Group for their contribution in various ways, especially to Dr.Viswanadham Balaga for his scientific contribution.
- School of Chemistry and Physics, University of KwaZulu-Natal for providing facilities.

Most importantly, I would like to thank God for this blessings and guidance.

PREFACE

The experimental work described in this thesis has been done in the School of Chemistry and Physics, University of KwaZulu-Natal (Westville campus) from July 2015 to November 2017, under the supervision of Professor Holger B. Friedrich and Dr. Sooboo Singh.

The study mentioned in the thesis represents original work by the author and have not otherwise been submitted in any form for any degree or diploma to any other tertiary institution. Where use has been made of the work of others are duly acknowledged in the text.

Author: Ms. Jhansi Pedada

25 April 2018

DECLARATION-1

I, Ms. Jhansi Pedada, declare that:

1 The research reported in this thesis, except where otherwise indicated is my original research.

2 This thesis has not been submitted for any degree or examination at any other university.

3 This thesis does not contain other persons' data, pictures, graphs or other information, unless specifically acknowledged as being sourced from other persons.

4 This thesis does not contain other persons' writing unless specifically acknowledged as being sourced from other researchers. Where other written sources have been quoted, then:

   (a) Their words have been re-written but the general information attributed to them has been referenced.

   (b) Where their exact words have been used, then their writing has been placed in italics and inside quotation marks, and referenced.

5 This thesis does not contain text, graphics or tables copied and pasted from the internet, unless specifically acknowledged, and the source being detailed in the thesis and in the Reference sections.

25 April 2018

DECLARATION-2

Work from this thesis has been accepted for publication or submitted to journals as detailed below and are indicated in Appendix A:

Paper 1: Jhansi Pedada, Holger B. Friedrich and Sooboo Singh*, Synergistic role of Brønsted and Lewis acidity in Cs exchanged heteropolyacid catalysts for esterification of acetic acid at room temperature, Journal of Iranian Chemical Society, doi.org/10.1007/s13738-018-1341-z.

Paper 2: Jhansi Pedada, Holger B. Friedrich and Sooboo Singh*, The role of alkali metal exchanged phosphomolybdic acid catalysts in the solvent free oxidation of styrene to benzaldehyde at room temperature, Catalysis Letters, doi.org/10.1007/s10562-018-2352-1.

Paper 3: Jhansi Pedada, Holger B. Friedrich and Sooboo Singh*, Solvent free oxidation of benzyl alcohol to benzaldehyde over copper and zinc modified phosphomolybdic acid catalysts at room temperature. (Submitted: Bulletin of Chemical Society of Ethiopia)

[redacted]

25 April 2018

DECLARATION-3

I, Jhansi Pedada was also co-author of the following papers which will be included as part of a short-review of the Knoevenagel condensation reaction in Chapter Two of this thesis and are attached in Appendix B.

- Balaga Viswanadham, Pedada Jhansi, Komandur V. R. Chary, Holger B. Friedrich, Sooboo Singh, Efficient Solvent Free Knoevenagel Condensation Over Vanadium Containing Heteropolyacid Catalysts, *Catal Lett* (2016) 146:364–372.
  Co-author contribution: Catalyst synthesis and characterization studies.

- Balaga Viswanadham, Jhansi Pedada, Holger B. Friedrich, Sooboo Singh, The Role of Copper Exchanged Phosphomolybdic Acid Catalyst for Knoevenagel Condensation, *Catal Lett* (2016) 146:1470-1477.
  Co-author contribution: Catalyst synthesis and characterization studies.

- Viswanadham Balaga, Jhansi Pedada, Holger B. Friedrich, Sooboo Singh, Tuning surface composition of Cs exchanged phosphomolybdic acid catalysts in C-H bond activation of toluene to benzaldehyde at room temperature, *J Mol Catal A: Chem* 425 (2016) 116-123.
  Co-author contribution: Catalyst synthesis and characterization studies.

[redacted]

25 April 2018

TABLE OF CONTENTS

Page No.

LIST OF ABBREVATIONS AND TERMS

XRD	:	X-ray diffraction
ATR	:	Attenuated total reflectance
BET	:	Brunauer-Emmett-Teller
BJH	:	Barrett-Jonyer-Halenda
EDX	:	Energy dispersive X-ray spectroscopy
FTIR	:	Fourier transform infrared
Py-FTIR	:	Pyridine adsorbed Fourier transform infrared
GC	:	Gas chromatography
SEM	:	Scanning electron microscopy
TEM	:	Transmission electron microscopy
HR-TEM	:	High resolution - transmission electron microscopy
BF-STEM	:	Bright field- scanning transmission electron microscopy
Wt %	:	Weight percent
PMA	:	Phosphomolybdic acid
PTA	:	Phosphotungstic acid
CsPMA	:	Cs exchanged phosphomolybdic acid
CuPMA	:	Cu exchanged phosphomolybdic acid
KPMA	:	K exchanged phosphomolybdic acid
RbPMA	:	Rb exchanged phosphomolybdic acid
ZnPMA	:	Zn exchanged phosphomolybdic acid
CuPTA	:	Cu exchanged phosphotungstic acid
CsPTA	:	Cs exchanged phosphotungstic acid
KPTA	:	K exchanged phosphotungstic acid
ZnPTA	:	Zn exchanged phosphotungstic acid

LIST OF TABLES

Page No.

Page No.

LIST OF FIGURES

Page No.

Page No.

Page No.

CHAPTER ONE

INTRODUCTION AND LITERATURE SURVEY

Catalysis is a key area for chemical sciences and plays an important role in academic and industrial development. The majority of the specialty chemicals and also fuels are produced through catalytic means in chemical industries. Catalysts are employed at some stage in their process, as well in product development, for a greener and cleaner technology. This area is extended further to fine chemical synthesis by replacing stoichiometric processes that generate undesirable waste products.

Organic transformation reactions such as esterification and selective oxidation are important reactions in academia as well as industry. Among the various chemicals that are produced by these reactions, ethyl acetate and benzaldehyde stand out as important starting materials in the chemical, pharmaceutical and cosmetic industries.

1.1 Esterification reaction

Esters are prepared by the reaction of a carboxylic acid and an alcohol with the elimination of water. Esters are also formed by a number of other reactions utilizing acid anhydrides, acid chlorides, amides, nitriles, unsaturated hydrocarbons, ethers, aldehydes, ketones, alcohols, and esters (via ester interchange). One of the valuable esters produced industrially is ethyl acetate.

1.1.1 Manufacturing process and production of ethyl acetate

The main method in the manufacture of ethyl acetate involves the esterification of ethanol with acetic acid. It can also be produced by the catalytic condensation of acetaldehyde with alkoxides. In the main esterification process, a mixture of acetic acid and ethanol with a small amount of sulfuric acid is preheated and fed to an esterification column under reflux. The mixture is then removed and placed into a second refluxing column where a ternary azeotrope containing 85% ethyl acetate is removed. Water is mixed with the

distillate after which it separates into two layers. The top layer is fed to a refluxing column from which the residue containing 95% ethyl acetate is distilled to remove any impurities.

A number of new technologies for the manufacture of ethyl acetate have been commercialised. In its 220 000 tons per year plant at Hull, BP employs a process that uses ethylene and acetic acid with a solid acid catalyst. This process, called Avada, is targeted at areas where there is a shortage of ethanol for esterification.

Kvaerner's new process, which only uses an ethanol feedstock, has been implemented by Sasol in a 50 000 tons per year plant at Secunda, South Africa. In this process, ethanol is dehydrogenated to acetaldehyde which further reacts to form ethyl acetate. Chinese National Petroleum has developed a one-step ethanol process where the ethanol is partially oxidised to acetic acid and subsequently esterified with excess ethanol [1].

Generally, two categories of catalysts have been used for the production of ethyl acetate, viz. homogeneous acid catalysts which include mineral acids such as HCl, H_2SO_4, alkyl sulfonic acid, aromatic sulfonic acid, methane sulfonic acid, benzene sulfonic acid and *p*-toluene sulfonic acid and heterogeneous acid catalysts such as Rohm Q-16® and Hass A-16®.

Esterification of ethanol with acetic acid on silica-alumina, alumina-boria, silica-alumina poisoned with sodium and alumina has been investigated by the pulse technique and compared with ethanol dehydration [2]. The catalysts were classified into two groups based on their catalytic behavior. Silica-alumina, alumina-boria, and sodium poisoned silica-alumina were placed in one group and alumina in the other. With regards to the silica-alumina group, poisoning them with organic bases still resulted in esterification proceeding on weaker acid sites, rather than promoting other acid catalyzed reactions such as de-alkylation and dehydration. This was supported with data from adopting a Linear Free Energy Relationship (LFER) approach.

Shirai *et al*. [3] prepared niobium catalysts for the formation of ethyl acetate from ethanol and acetic acid. The niobium catalysts were prepared by the reaction between surface OH groups of SiO_2 and $Nb(\eta^3\text{-}C_3H_5)_4$, $[Nb(\eta^5\text{-}C_5H_5)H\text{-}\mu\text{-}(\eta^5, \eta^1\text{-}C_5H_4)]_2$, and $Nb(OC_2H_5)_5$, respectively. The Nb sites attached to the surface through oxygen atoms, showing Nb-Si bonding. The Nb monomers on SiO_2 were active for ethanol dehydrogenation which proceeded on Nb=O bonds

which possessed basic character, while dehydration of diethyl ether to ethene took place on the Nb dimers which had acidic character. The Nb monolayers on SiO_2 produced ethyl acetate from ethanol. The monolayer catalyst also showed a high activity for the formation of ethyl acetate from ethanol and acetic acid.

The work by Mazzotti *et al.* [4] indicated that ion-exchange resins can be useful in catalysis. The authors infer that the resin not only catalyzes the esterification reaction, but also to shifts the corresponding equilibrium conversion due to its swelling capability. This approach is thought to be applicable to a various reactions catalyzed by polymeric resins and it is suitable for the optimal design of the subsequent process.

An acidic ion-exchange resin, Amberlyst-15, was used by Kirbaslar *et al.* [5] for the esterification of acetic acid with ethanol carried out in a batch reactor at temperatures between 50°C and 80°C at various starting compositions. The resultant kinetic model correlated with the experimental data and the activation energy was found to be 104.129 kJ $kmol^{-1}$ for the formation of ethyl acetate. Removal of acetic acid from ethyl acetate and ethanol (95%) has been investigated using polymeric ion-exchange resins by Anasthas and Gaikar [6], with the idea of possibly applying it the general use of removing acetic acid impurities from organic solvents. The resins contain tertiary or quaternary amino functional groups on a styrene–divinyl benzene copolymer matrix. Equilibrium adsorption studies showed selective adsorption with a high loading capacity for acetic acid. The uptake of the acid from the organic solutions is by sorption, reinforced by specific interaction with the functional groups on the polymer matrix. The specific interaction takes place by a hydrogen bonded complex formed between the acidic proton and the lone pair of electrons on the amino group. An efficient application of these ion-exchange resins is indicated clearly in the purification by ethyl acetate by selective removal of acetic acid.

Esterification reactions are normally carried out under homogeneous conditions using acids such as sulphuric acid [7]. However, since catalyst separation poses a problem, the use of heterogeneous catalysts is clearly preferred. Koster *et al.* [8] investigated the use of MCM-41 as a solid esterification catalyst. To better understand the mechanism using solid catalysts transient and steady state experiments, temperature programmed desorption (TPD) and isotopic labelling experiments were conducted. It was shown that the reaction proceeds via a Langmuir-Hinshelwood-type mechanism, involving a protonated acetic acid intermediate. A one step synthesis of ethyl acetate from ethane, oxygen and water over a Pd supported silicotungstic

acid catalyst showed a 25% ethane conversion with an ethyl acetate selectivity of 46% at 180°C, together about 34% acetic acid and ethanol that is produced and which can be recycled. The catalyst was said to be a bi-functional catalyst with Pd providing the oxidation function, with silicotungstic acid providing the acidic function [9].

Esterification reactions are normally hindered by thermodynamic limitations and encounter many challenges with regards to product purification. These setbacks have prompted scientists to seek for much more efficient protocols to address these issues, as a result, research into the formation of ethyl acetate has progressed considerably. Chilev and Simeonov [10] described a model and devised a calculation technique that allows the use of reactive distillation columns. This approach is suitable for the production of ethyl acetate where the use of a reactive distillation column, which combines the reaction and separation into a single stage, is proposed. The advantage of this combination is that ethyl acetate is always distilled and withdrawn out of the reaction zone, allowing the equilibrium to be shifted to the right, thus improving the reactants conversion. The influence of the different parameters such as pressure, reflux ratio, feed stage location were also investigated and the effect of reactant excess on the conversion and the ethyl acetate production was also studied. The study of Konakom *et al*. [11] was similar to that of Chilev. They used a batch reactive distillation column for the production of high purity ethyl acetate, where combining the reaction and separation into a single stage is also proposed. The ethyl acetate is always distilled and withdrawn out the reaction zone and the equilibrium is shifted to the right which, improved conversion.

The kinetics and mechanism of an eco-benign clay catalyst was studied by Chidi and Peter [12] for the synthesis of ethyl acetate. The results showed that the conversion of acetic acid was dependent on the catalyst weight, reaction time and mole ratio. The maximum conversion of acetic acid was obtained for a mole ratio (acid: alcohol) of 2:1. It was also shown that the reaction was second-order and followed the single step, Eley-Rideal reaction mechanism. Hua *et al*. [13] used $(NH_4)_6[MnMo_9O_{32}]\cdot 8H_2O$ with a Waugh structure as a catalyst for synthesizing ethyl acetate. A control variation method was adopted to determine reaction conditions and the optimum conditions determined were a mole ratio of acid: alcohol of 3:1. Under these conditions, selectivity was 100% at a conversion of 91%.

Inui *et al*. [14] investigated the direct synthesis of ethyl acetate from ethanol with the reaction being carried out under pressure. The selectivity to ethyl acetate and its space-time yield

increased with an increase in reaction pressure, but ethanol conversion decreases. The highest space-time yield recorded was at a reaction pressure of about 0.8 MPa with maximum selectivity of 93 wt%. During this process, they suggested that ethanol is first dehydrogenated to acetaldehyde and is then coupled with another ethanol molecule to form a hemiacetal, which is further dehydrogenated to ethyl acetate. In the process, the concentration of by-products such as 1-butanol and butanone, which form after the aldol addition of acetaldehyde decreases with an increase in pressure.

However, challenges still exist to develop efficient and eco-friendly materials to catalyse esterification. This will discussed towards the latter part of this chapter.

1.1.2 Possible mechanistic pathways for formation of ethyl acetate

The overall reaction scheme for the formation of ethyl acetate from acetic acid and ethanol is shown in Figure 1.1.

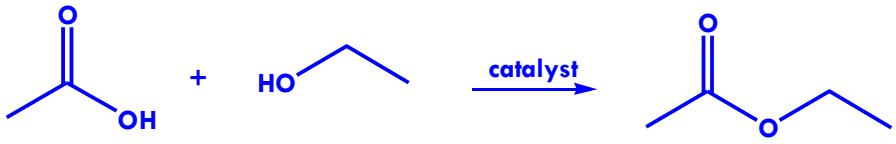

Figure 1.1 Scheme showing acetic acid esterification reaction over acidic sites of solid acid catalysts.

This reaction proceeds via two pathways, one on Brønsted acidic sites, while the other on Lewis acid sites of catalyst (Figure 1.2). Pathway 1 shows a lone pair on the carbonyl oxygen abstracts a proton from the catalyst to form a bond between hydrogen and oxygen and, thereafter, the alcoholic oxygen lone pair attacks the carbonyl carbon, followed by elimination of water to form the ester. Pathway 2 shows the formation of a partial dative bond between the Lewis acid sites of catalyst with the carbonyl oxygen in the carboxylic acid to form a transition state, the electron deficient carbonyl carbon then reacts with the alcohol oxygen lone pair, followed by removal of water to form the product.

Pathway 1:

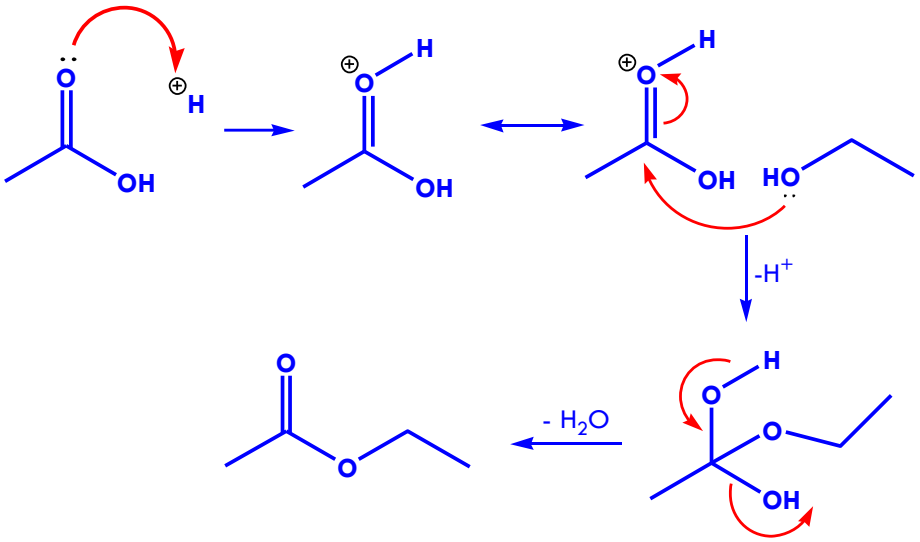

Pathway 2:

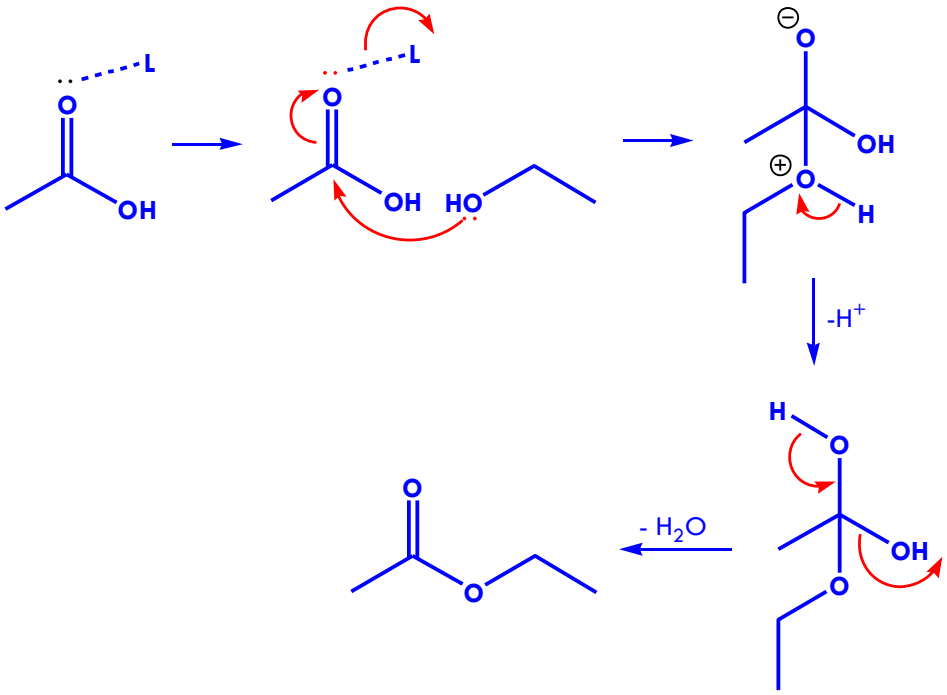

Figure 1.2 Reaction pathways for acetic acid esterification over acidic sites of solid acid catalysts.

1.2 Oxidation reactions

Oxidation of aromatic compounds such as styrene, toluene or benzyl alcohol to the carbonyl compound, benzaldehyde, is a valuable chemical process, since benzaldehyde is a versatile aromatic carbonyl compound used as a raw material in the perfumery, cosmetics and agrochemical industries. Oxidation of styrene and benzyl alcohol to benzaldehyde is normally

carried out in the presence of solvent, which leads to environmental concerns and wastage. Hence, exploration of solvent free oxidation is of paramount importance.

1.2.1 Manufacturing process and industrial use of benzaldehyde

Benzaldehyde (C_6H_5CHO) is an organic compound which consists of a benzene ring with a formyl substituent. It is the simplest aromatic aldehyde and one of the most industrially useful. As of 1999, 7000 tons of synthetic and 100 tons of natural benzaldehyde were produced annually [15]. Liquid phase chlorination and oxidation of toluene were the main routes, but numerous other methods were developed, such as the partial oxidation of benzyl alcohol, alkali hydrolysis of benzal chloride, and the carbonylation of benzene [16].

Industrially, benzaldehyde is used as a precursor to the manufacture of other organic compounds which largely range from pharmaceutical compounds to plastic additives. The aniline dye, malachite green is prepared from benzaldehyde and dimethylaniline, whereas benzaldehyde is also a precursor to certain acridine dyes. Benzaldehyde is also converted into derivatives of cinnamaldehyde and styrene via aldol condensations. The synthesis of mandelic acid begins with the addition of hydrocyanic acid to benzaldehyde.

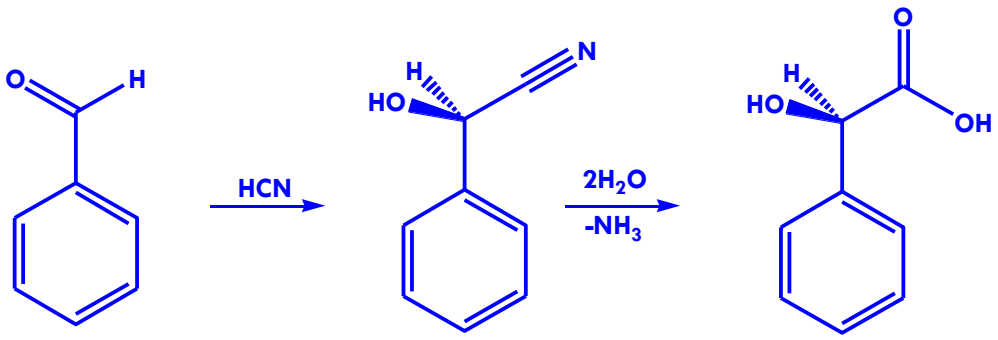

Figure 1.3 Scheme showing formation of mandelic acid from benzaldehyde.

1.2.2 Oxidation of styrene

In the oxidation of styrene, both homogeneous and heterogenous catalysts have been employed. Homogenous catalysts such as permanganates, chromates and hypochlorites that have been used for this reaction have limitations such as being toxic and hazardous if excess amounts are used [17]. In addition, these processes provide poor selectivity towards the desired product and the use of solvents. An improvement is obtained with the use of transition metal complex

systems. Although there is a vast improvement in the activity, a major disadvantage is the recycling of the complexes during product separation [18, 19]. As a result, extensive research has been undertaken using heterogenous catalysts such as metal oxides and solid acid catalysts [20-46]. The main products of this reaction are benzaldehyde and styrene oxide (Figure 1.4)

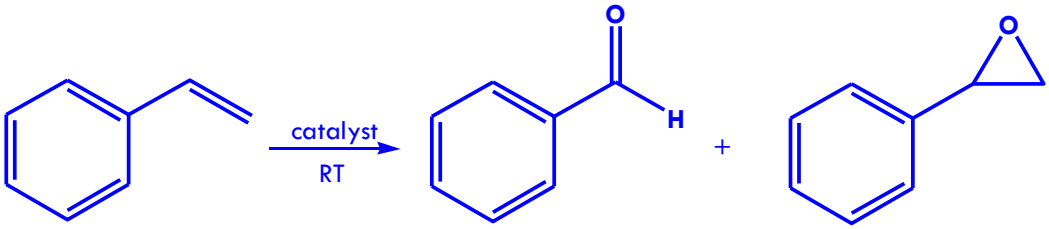

Figure 1.4 Scheme showing catalytic oxidation of styrene at room temperature.

Gichumbi *et al*. [20] synthesised and characterized piano-stool ruthenium complexes with N,N'-pyridine imine bidentate ligands for the oxidation of styrene. The complexation of Ru with bidentate ligand provides two polymorphs out of seven which showed good activity during oxidation. In a similar study, Zhang *et al*. [21] reported the synthesis and crystal structures of oxovanadium(V) complexes with hydrazone ligands. The crystal structures of the complexes which are stabilized by hydrogen bonds influence the catalytic performance for the oxidation of styrene.

Hulea *et al*. [22] investigated styrene oxidation using H_2O_2 as an oxidant over Ti incorporated into molecular sieves with MFI (TS-1), BEA (Ti-beta) and MCM-41 (TiMCM-41) topologies to assess the influence of the structural features of the catalyst, as well as the reaction conditions, which strongly affect the reaction yields with hydrogen peroxide. The main reactions in this study were the epoxidation of styrene, followed by the isomerization of styrene oxide into phenylacetaldehyde, as well as oxidative cleavage into benzaldehyde which was predominant on the Ti-beta and the TiMCM-41 catalysts. Copper(II) and oxovanadium(IV) Schiff base complexes were anchored onto a modified SBA-15 support and studied by Yang *et al*. [23] for styrene oxidation. Both the heterogenous copper and oxovanadium catalysts were more active than their homogenous counterparts with product selectivity varying with different oxidants. The supported oxovanadium complex showed a high yield of styrene oxide and was easily recoverable. In another study that assessed homogenous versus heterogenous catalysts, Silva *et al*. [24] investigated the use of homogenous Mn(III) salen complexes and compared them with the complexes encapsulated in NaX and NaY zeolites using TBHP as the source of

oxygen for styrene oxidation. The heterogenous system performed much better with no leaching of the complexes.

Zinc functionalized multi walled carbon nanotubes were prepared by Wan *et al*. [25] by impregnation and tested as a catalyst for styrene oxidation in the presence of hydrogen peroxide. The catalyst was efficient in the oxidation and a conversion of 94% was obtained with a selectivity of 90.6% towards styrene oxide. However, in a study conducted by Wang *et al*. [26], for a 44.7% conversion of styrene, the major product was benzaldehyde, a selectivity of 82.2% was obtained and a 17.7% selectivity towards styrene oxide. The catalyst used in this study was Ti-containing mesoporous silica. The size of the mesopores could be tuned when a nonionic surfactant P123 was used as a particle dispersing agent at room temperature. It was shown that the catalyst activity increased with a decrease in particle size.

Different types or morphologies of particles impacted on the styrene oxidation catalysis as shown by the study conducted by Chimentao *et al*. [27]. Silver nanoparticles, nanowires and nanopolyhedra, prepared using the polyol process, were supported on α-Al_2O_3. Here, phenylacetaldehyde and styrene oxide were the main products. It was also shown that the promotion of the catalysts with potassium and cesium improved the conversion and selectivity towards styrene oxide.

Titania and a mixed oxide of titania and silica were employed by Nie *et al*. [28] for the formation of benzaldehyde from styrene. They found that for the blank reaction at 100°C and 10 atm O_2, polystyrene was the major product. However, when the catalysts were used, benzaldehyde and formaldehyde were the major products, whereas minor quantities of phenylacetaldehyde, acetophenone, styrene oxide, benzoic acid and polymer were present in the product stream. They inferred that polymerization was the result of the formation of radicals but this was overcome by the addition of nitrobenzene which behaved as a radical inhibitor, hence an improvement in benzaldehyde selectivity. In a study that also involved titania, Lubis *et al*. [29] coated titania with carbon, subsequently treating it with a potassium hydroxide solution. It showed remarkable activity with the formation of benzaldehyde and phenylacetaldehyde as the major products.

Valand and co-workers [30] prepared a series of nano-mixed metal oxides of copper, nickel and cobalt by the ultrasonic cavitation-impregnation method and tested these materials in the

presence of TBHP and acetonitrile for the oxidation of styrene. In this study, the metal loadings, reaction temperature and reactant/oxidant ratio that were taken into account impacted directly on the selectivity toward the desired products, viz. benzaldehyde and styrene oxide. Mesoporous and macroporous materials, commonly used as efficient supports were employed by Luo and Lin [31] and Tanglumlert *et al*. [32] to prepare their catalysts for use in the oxidation of styrene. In the work done by Luo and Lin, Co functionalized MCM-41 was used, whereas in the case of Tanglumlert and colleagues, Fe and Ti functionalized SBA-1 were employed as catalysts. Here, the selectivity towards benzaldehyde and styrene oxide were 74% and 11%, respectively, for a conversion of 67% over the Fe catalyst at 80°C, while for the Ti catalyst, the selectivity towards benzaldehyde and styrene oxide were 50% and 48%, respectively for a conversion of 69%. In the former study by Luo and Lin, the solid catalysts showed good activity in the liquid phase oxidation of styrene and were stable towards leaching of the active Co species.

A series of spherical, vanadium-containing, mesoporous MCM-48 catalysts with different V/Si atomic ratios were synthesized by a direct hydrothermal method by Wang et al. [33] and were evaluated in the oxidation of styrene to benzaldehyde using H_2O_2 as oxidant. The prepared spherical V-MCM-48 showed higher catalytic activity in the catalytic conversion of styrene to benzaldehyde where it was inferred that V^{5+} species on the surface and produced from the oxidation of some V^{4+} in the framework act as active sites. Ramanathan and Sugunan [34] identified the spinel phase as the active phase for selectively forming benzaldehyde from styrene using gadolinium substituted nickel ferrite catalysts prepared by co-precipitation with hydrogen peroxide as the oxidant. The study included optimizing reaction conditions by considering reaction temperature, reaction time, reactant to oxidant ratio and solvent medium.

A further study used γ-alumina with different pore sizes which were impregnated with vanadium oxide. The catalytic effect was assessed in the styrene oxidation reaction by Ahmad *et al*. [35]. The secondary pores which had a pore diameter of ca. 50 nm improved the styrene oxidation rate after the conversion of styrene reached 30% compared to primary pores with diameter of 4 nm. In a study conducted by Zheng and co-workers [36], ultra-small Au nanoparticles (< 2 nm) supported on hollow silica nano-spheres were synthesized. The resulting solid catalysts showed good thermal stability and the small particle sizes were maintained, even at a temperature of 350°C and showed good catalytic activity in the oxidation of styrene using O_2 as oxidant at atmospheric pressure. The data gathered showed that the activity depended strongly on

the Au loading, an amount of 4 to 5 wt.% led to the highest activity. The solid catalyst was recycled for at least 8 reaction cycles without significant decrease in activity and selectivity.

1.2.2.1 Mechanistic pathways involved in oxidation of styrene

The mechanism proposed by Indira *et al*. [37] involving catalytic intermediate species is shown in Figure 1.5. Hydrogen peroxide is the oxidant with a Co complex as the catalyst. The free radical mechanism involves the interaction of H_2O_2 with Co^{2+} to form a hydroperoxy species in a pre-equilibrium step. This species, which is very unstable, then undergoes a one-electron reduction, losing a water molecule and rearranges to give the Co^{3+} peroxo species. In another pre-equilibrium step, the Co^{3+} peroxo species interacts with styrene to form a π-bonded transient species. The transfer of oxygen to the double bond in a rate determining step forms a metallo-epoxy intermediate species, which dissociates to form products, while regenerating the active species. The proposed mechanism for the oxidation of styrene in this study was found to be consistent with the observations made in kinetic and electronic spectroscopic studies of the reaction.

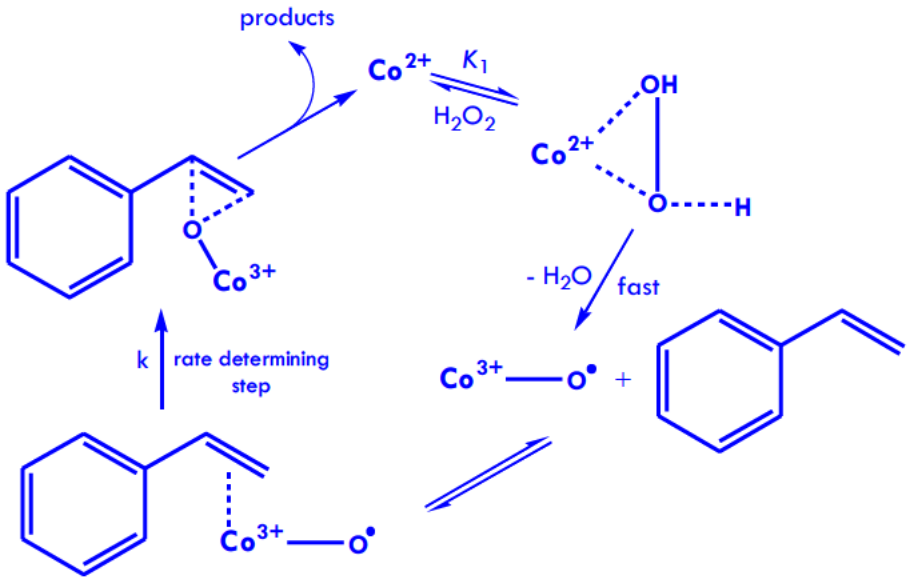

Figure 1.5 Scheme showing mechanistic pathways in the oxidation of styrene (adapted and redrawn from [37]).

In the study conducted by Valand and co-workers [30], on noting that the reactive sites favour the formation of benzaldehyde as a major product, seen very clearly in the experimental results, they proposed that the catalytic reaction follows a probable pathway similar to the Eley–Rideal mechanism. In styrene oxidation, the side chain can lead to various reaction products,

depending on the catalyst and reaction conditions. Two major reactions take place. They are the oxidative C=C cleavage into benzaldehyde and epoxidation. However, under the present catalysis conditions, they found that the major oxidation product obtained was benzaldehyde which was attributed to direct oxidative cleavage of C=C of styrene and fast conversion of styrene oxide to benzaldehyde. This was confirmed under the optimized reaction conditions by conducting a control experiment with styrene oxide as a substrate to confirm the reaction pathway (Figure 1.6).

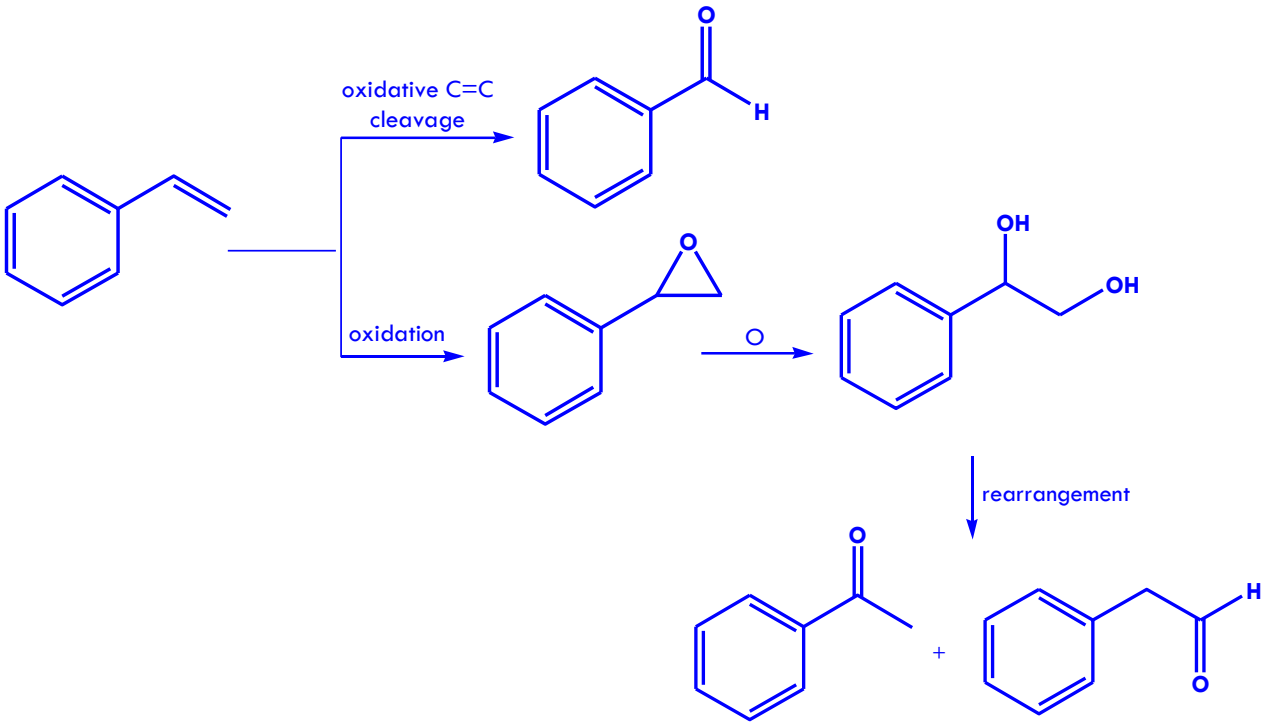

Figure 1.6 Proposed reaction scheme for styrene oxidation (adapted and redrawn from [30]).

1.2.3 Oxidation of benzyl alcohol

The conversion of benzyl alcohol to benzaldehyde which involves a one-step reaction (Figure 1.7) under eco-friendly conditions remains attractive and a challenge to both the academic sector and chemical industry due to importance of benzaldehyde in basic and applied research [38, 39].

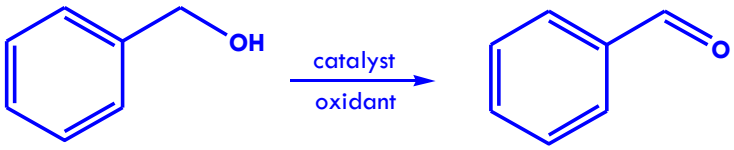

Figure 1.7 Scheme showing oxidation of benzyl alcohol to benzaldehyde.

Several catalytic materials have been developed to produce benzaldehyde from benzyl alcohol through homogeneous and heterogeneous oxidation catalysis, however the latter has shown to be more feasible. Weng *et al.* [40] studied the selective oxidation of benzyl alcohol with hydrogen peroxide over a reaction-controlled phase-transfer catalyst with hydrogen peroxide as the oxidant. In this system, the catalyst $[C_7H_7N(CH_3)_3]_3PMo_4O_{16}$ (BTPM) was easily recovered at the end of the reaction and it was ascertained that the counter-cation of the catalyst, reaction solvents, molar ratio of H_2O_2 to benzyl alcohol and pH value of system influenced the conversion and also determined the catalytic action of catalyst. Under the optimal conditions, the selectivity towards benzaldehyde was always 99%, and the conversion of benzyl alcohol reached a maximum of 93%. The catalysts were very stable as indicated by the catalyst recycle conducted.

A comparative study of the structural, optical and catalytic properties of $CoAl_2O_4$ nanoparticles for the selective oxidation of benzyl alcohol to benzaldehyde with hydrogen peroxide, was investigated by Ragupathi and co-workers [41]. $CoAl_2O_4$ prepared by the microwave method possessed a higher surface area and lower crystallite size than the one prepared by the conventional method, which resulted in an improved performance towards the selective oxidation of benzyl alcohol to benzaldehyde.

Guo and Li [42] investigated the selective oxidation of benzyl alcohol with aqueous hydrogen peroxide as oxidant, under solvent free conditions using tetra-alkyl pyridinium octamolybdate catalysts. The catalysts were efficient in the oxidation with a conversion consistently between 82 and 95% and selectivity towards benzaldehyde between 88 and 97%.

The study by Caravati *et al*. [43] involving the selective oxidation of benzyl alcohol to benzaldehyde with molecular oxygen in supercritical carbon dioxide over an alumina-supported palladium catalyst produced a selectivity towards benzaldehyde of 95%. The experiments conducted in a continuous flow fixed-bed reactor showed that the pressure influenced on the reaction rate and a significant increase of the rate (turnover frequency) from 900 h^{-1} to 1800 h^{-1} was observed when the pressure was increased from 140 to 150 bar.

In another study using palladium as the active metal in the catalyst, Savara *et al*. [44] elucidated the reaction mechanism involved in the oxidation of benzyl alcohol. Experiments were carried out in the liquid-phase in a batch reactor with *para*-xylene as the solvent and Pd nanoparticles

as the catalyst. The initial benzyl alcohol concentration, the oxygen partial pressure in the headspace and the reactor temperature were varied, and from trends in the concentration profiles and integrated production of each product, it was determined that two primary reaction paths existed, viz. an alkoxy pathway leading to toluene, benzaldehyde, and benzyl ether, and a carbonyloxyl pathway leading to benzoic acid, benzene, and benzyl benzoate.

The research group led by Hutchings also conducted a few experiments on benzyl alcohol oxidation [45, 46]. In one study, supported gold-palladium nanoparticles were used. It is well known that gold is active in oxidation processes, however in this study its efficiency was further enhanced by the addition of palladium. Here, the effect of the method of preparation of gold-palladium alloy nanoparticles supported on titania and its activity were assessed for the selective oxidation of benzyl alcohol. Of the impregnation and deposition-precipitation methods, the most active catalysts are prepared using the deposition-precipitation method. In the other study, gold nanoparticles supported on ceria foam were used as catalysts for benzyl alcohol oxidation. The foam was synthesized using *l*-asparagine to produce a cerium coordination polymer foam, which was calcined to give the oxide foam. Au nanoparticles were supported on the CeO_2 foams using a sol-immobilization method. The activity of the Au/foamCeO_2 under solvent-free conditions for benzyl alcohol oxidation was far superior to the standard Au/CeO_2 catalysts. The activity was dependent on the crystallization time of the precursor foam. A crystallization time of 4 h was found to produce the most active catalyst, which retained activity and a high selectivity towards benzaldehyde of ca. 96%.

A series of hydrotalcite (HT) and hydrotalcite-like compounds using Ni(II) as the bivalent cation were prepared by the co-precipitation method as supports for gold nanoparticles for the oxidation of benzyl alcohol by Guo *et al*. [47]. Good conversions and selectivity were obtained with visible light. On the basis of the results from the experiments carried out, a plausible reaction mechanism was proposed (Figure 1.8). Here, the catalyst surface is irradiated by visible light, exciting the gold nanoparticles on the surface of catalysts. The activated gold nanoparticles adsorb the H atoms of the OH group of the benzyl alcohol and form Au-H. The O atoms of the OH group in the benzyl alcohol molecules are adsorbed by the Al^{3+} of the hydrotalcite and simultaneously, the Ni^{2+} adsorbs the dissociated O atoms from O_2 which made the O atom adsorb the α-H of the benzyl alcohol. The α-H is then separated from the benzyl alcohol molecules, subsequently forming OH with the O atom on Ni^{2+}. The H atom adsorbed on the gold particles is removed and combines with the OH adsorbed by Al^{3+} to form water.

Thereafter, the OH on the Ni^{2+} surface is transferred to the surface of Al^{3+} and the O atom of the benzyl alcohol molecules adsorbed by Al^{3+} is removed, generating the final product, benzaldehyde.

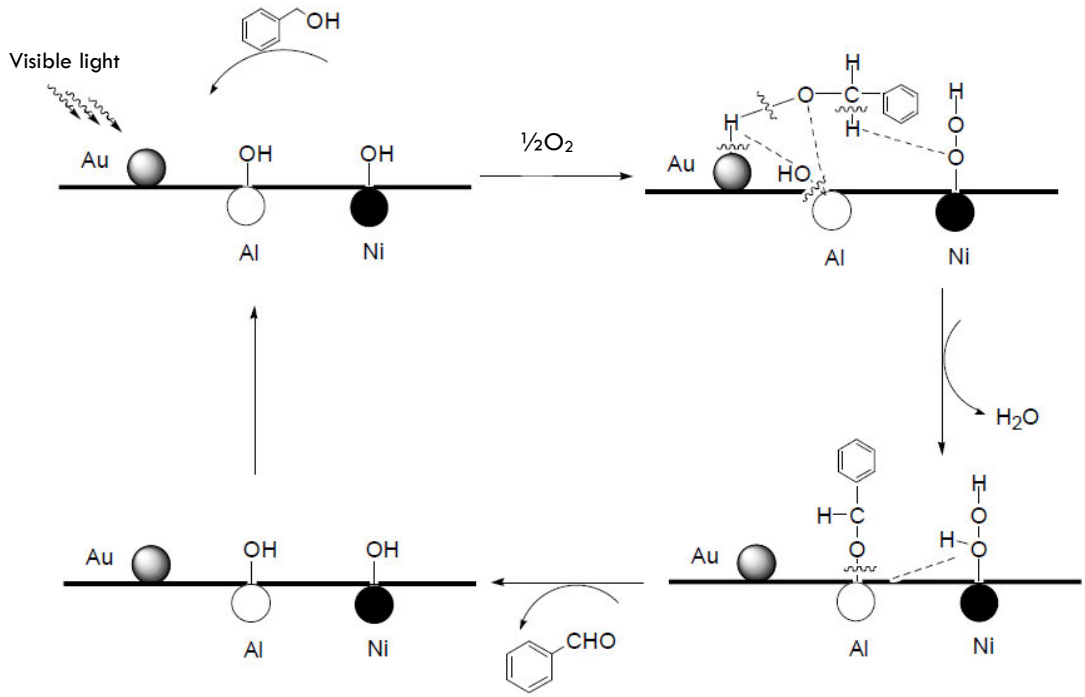

Figure 1.8 Scheme showing the mechanism for the photocatalytic aerobic oxidations of benzyl alcohol [47].

A photocatalyst, TiO_2/Cu(II) was used by Marotta *et al*. [48] for the selective oxidation of benzyl alcohol to benzaldehyde in water. A simplified pictorial scheme of the mechanism for the selective photo-oxidation of benzyl alcohol to benzaldehyde by TiO_2 photo-catalysis is shown in Figure 1.9. The best result found, in terms of yield, was of 35% for benzaldehyde with respect to the initial benzyl alcohol concentration. By-products, present at trace level, were 2-hydroxy-benzyl-alcohol, 4-hydroxy-benzylalcohol, 2-hydroxy-benzaldehyde and 4-hydroxy-benzaldehyde. On the basis of the formation of these species, HO radicals were thought to be responsible.

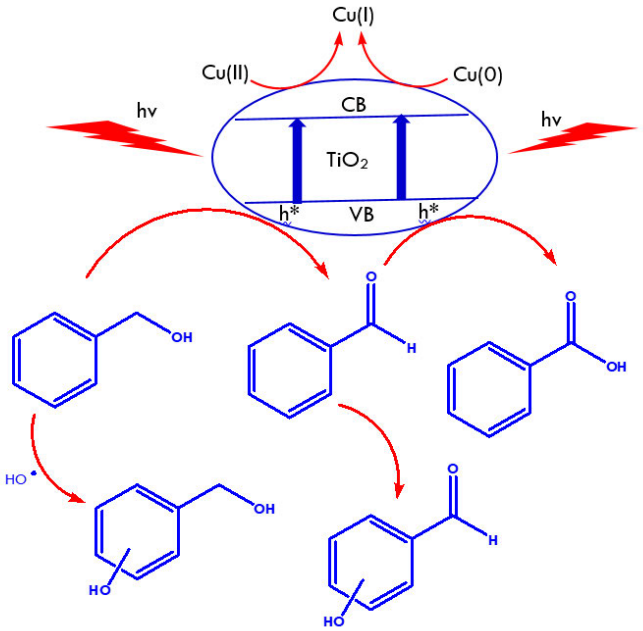

Figure 1.9 Scheme showing mechanism of selective oxidation of benzyl alcohol by TiO_2/Cu(II)/UV (adapted and redrawn from [48]).

In a study by Bijudas [49], who investigated the selective oxidation of benzyl alcohol by using acidified dichromate in aqueous acetic acid medium, suggested that the overall mechanism most probably involves the formation of a chromate ester in a fast pre-equilibrium step, followed by disproportionation of the ester in a subsequent slow step via a cyclic concerted symmetrical transition state, leading to the product (Figure 1.10).

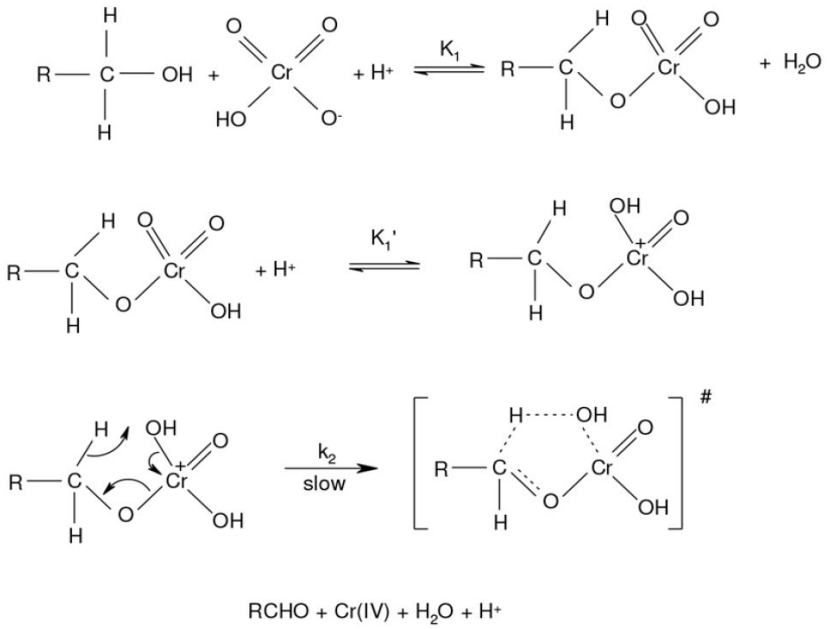

Figure 1.10 Scheme showing mechanism involving a hydride ion transfer through an ester intermediate [49].

The esterification reaction that produces ethyl acetate, together with the oxidation of styrene and benzyl alcohol to benzaldehyde, discussed thus far, are important means of ester and aldehyde production. However, many catalytic routes that are employed to facilitate these reactions have drawbacks, the most obvious being the harm caused to the environment. It is with this in mind, that extensive research is invested in developing materials that are efficient and eco-friendly. Amongst the wide range of solid acid catalysts, heteropolyacids (HPAs) and related polyoxometalate compounds have been used quite extensively over the years in various industrial applications for the synthesis of bulk and fine chemicals along with value added chemical intermediates [50-56]. HPAs have advantages that make them economically and environmentally attractive such as their strong Brønsted acidity which nearly approaches the superacid region. They are also strongly oxidizing, enabling fast reversible multi-electron redox transformations, in most cases at room temperature. In heterogeneous catalysis, the protons of HPAs are often exchanged with metals or metals are incorporated into its structure that eventually leads to an improvement in the surface area, thermal stability, mechanical strength and the available active sites. As a result the active metal and the HPA are considered as integral parts of the catalytic system.

1.3 Heteropolyacids

Heteropolyacids (HPAs) or polyoxometalates (POMs) are group of solid acids made up from the combination of hydrogen and oxygen atoms with certain metals as well as non-metals. The combinations of addenda atoms and various types of hetero atoms gives rise to a variety of heteropolyacids. One of the best known group of heteropolyacids is the Keggin ion based HPA, mainly due to its stability and easy availability. The general formula of heteropolyacids is written as follows:

$$[X_xM_mO_y]^{(-q)}$$

where X = the hetero atom (B, Al, Si, Ge, P, As, Fe, Mn, Co, Cu and Zn), M = addenda atoms (Mo, W, V, Ta, Nb, Os) that are attached to the hetero atoms via oxygen atoms and -q = charge ranging from -3 to -28. (Figure 1.11).

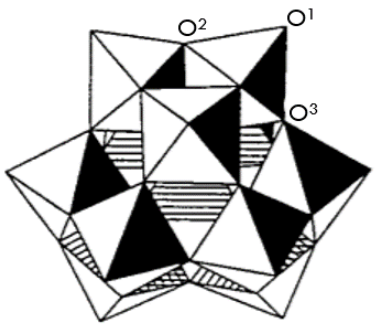

Figure 1.11 The Keggin structure of the $XM_{12}O_{40}^{x-8}$ anion (R-isomer): terminal (O^1), edge-bridging (O^2), and corner bridging (O^3) oxygen atoms (Adapted from [50]).

The Keggin ion structure is mainly composed of one heteroatom surrounded by four oxygen atoms to form a tetrahedron. The heteroatom is centrally located and caged by 12 octahedral MO_6 units linked to one another by the adjacent oxygen atoms. There are a total of 24 bridging oxygen atoms linked to 12 addenda atoms. The metal centres in 12 octahedra are arranged on a sphere almost equidistant from each other in four M_3O_{13} units giving the complete structure an overall symmetry of a tetrahedral nature. Keggin anions have three types of outer oxygen atoms as potential protonation centres, the terminal oxygen as in M=O and two edge bridging, corner sharing, M-O-M (Figure 1.11). In the free Keggin anion in the gas phase, the M-Oe-M oxygen is thought to be the predominant protonation site. Solid HPA protons take part in the formation of the HPA crystal structure, linking the neighbouring heteropolyanion. In this, the more accessible terminal oxygens can be protonated. Thus, from single-crystal X-ray and neutron diffraction data, the crystal structure of HPA such as phosphotungstic acid (PTA) hexahydrate is formed by packing the heteropolyanion into a body-centred cubic structure. The bulk proton sites in PTA hexahydrate are represented as diaquahydrogen ions, $H_5O_2^+$ (Figure 1.12), each of which links four neighbouring heteropolyanions by forming hydrogen bonds with the terminal W=O oxygens.

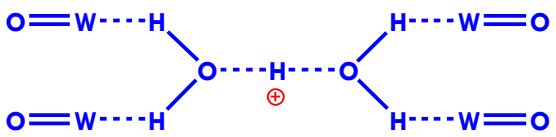

Figure 1.12 The schematic structure of bulk proton sites in $H_3PW_{12}O_{40}.6H_2O$.

From X-ray data, the proton positions are localized on the basis of hydrogen-bonding and the known geometry of the water molecule. Evidence of the predominant protonation of the terminal oxygens in solid PTA has been obtained by ^{17}O NMR by comparing solution and solid-state spectra. The resonance for the terminal oxygen in solid PTA exhibits a large 60 ppm up field shift compared to the aqueous solution spectrum, whereas the bridging oxygen resonances have practically the same positions in both spectra, since in aqueous solution, PTA is completely de-protonated, and the terminal oxygens are identified as the predominant protonation sites in solid HPA.

The structure of proton sites in the dehydrated PTA is shown in Figure 1.13. This structure is assumed to be directly formed from the proton structure of the PTA hydrate upon dehydration. Stoichiometrically, each proton is shared by four, equivalent terminal oxygens belonging to four different heteropolyanions. The same structure was assigned for the structurally similar HPA salts, viz. $Cs_3PW_{12}O_{40}$, in which the Cs^+ ions each have four, equivalent terminal oxygens as the closest neighbours. One of the advantages of using HPA as catalysts is that their properties can be controlled in a systematic way by replacing protons or by substituting metal atoms in the framework [57-61].

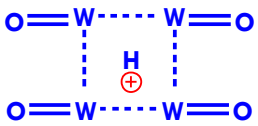

Figure 1.13 The schematic structure of bulk proton sites in $H_3PW_{12}O_{40}$ catalyst.

1.3.1 Heteropolyacid catalysts in esterification catalysis

Heteropolyacid catalysts are used in a variety of important commercial processes, one such process being the oxidation of ethylene to acetic acid catalyzed by Pd-HPAs in Japan producing 100000 tons per year. Various other reactions using HPAs include the oxidation of lower alkanes, methanol oxidation, cyclohexanol dehydrogenation, esterification of acetic acid, the conversion of cellulose to sugar alcohol, selective hydro-isomerization of *n*-pentane to isopentane, skeletal isomerisation of 1-butene, alkylation of biphenyl, alkylation-acylation and tetrahydro-pyranylation of aromatic compounds, NO_x storage and reduction and in the synthesis of zero sulphur diesel [62-88].

Sepulveda *et al.* [89] employed tungstophosphoric acid (HPA) catalysts supported over SiO_2, ZrO_2 and carbon in its repeated use in the liquid phase reaction of esterification of acetic acid with butanol. The results revealed that the silica- and zirconia-supported HPA had an intrinsic activity per unit protonic acid site greater than that of an Amberlyst W35 resin. Carbon-supported HPA catalysts had a slightly lower activity but they showed a sustained conversion level upon reuse. Tests showed that both butanol and water leached HPA from the silica- and zirconia-supported catalysts and that the effect was minimal in the case of the carbon catalysts.

Esterification of acetic acid with *sec*-butanol using supported dodecatungstophosphoric acid, $H_3PW_{12}O_{40}$ (DTP) on acid modified Montmorillonite clay (AT-Mont) matrix was carried out by Bhorodwaj and Dutta [90]. A series of catalysts having 5, 10, 20 and 30% loading of DTP on the clay were synthesized and evaluated as catalysts with the 20% catalyst showing the highest catalytic activity with about 80% conversion and a selectivity of nearly 100% towards sec-butyl acetate. The high catalytic activity was attributed to a high dispersion of the DTP on the clay, providing more surface area and active sites than pure HPA. The variation of different reaction parameters, such as reaction temperature, reaction time, mole ratio of acid and alcohol and catalyst amount impacted on the activity.

A series of highly active, selective, and stable silver-exchanged phosphotungstic acid catalysts were prepared, characterized, and assessed for the glycerol esterification reaction with acetic acid to produce valuable biofuel additives by Zhu *et al*. [91]. The structures, morphologies, acidities, and water tolerance of these samples were determined by FTIR, Raman, XRD, SEM-EDX, FT-IR of pyridine adsorption, and H_2O-TPD. Several known acidic catalysts were also used in the esterification reaction for comparison purposes. Among all the catalysts, the silver-exchanged phosphotungstic acid showed high activity, with 97% conversion within 15 min of reaction time and good stability.

Keggin heteropolyacids were immobilized on functionalized silica as their onium (*γ*-propyl-*N*-pyridinium, *γ*-propyl-*N*-methyl and *γ*-propyl-*N*-butyl-imidazolium) salts by Kovalchuk *et al*. [92] and used in the esterification of acetic acid and ethanol. These solids showed good catalytic performance and relative high structural stability, and among the heteropolyacids studied, $H_4SiW_{12}O_{40}$ was the most active and promising for catalyst design. Zhao *et al*. [93] synthesized a heteropolyacid catalyst using a surfactant, cetyltrimethyl ammonium, and used

it as a water-tolerant heterogeneous catalyst in an esterification reaction. They reported a high conversion of 95% and an excellent yield of 92%, attributed due to the acidic properties and structure of the HPA. This micellar polyoxometalate catalyst was also stable during the reaction and was recycled by a simple separation process.

Coupling HPAs with ionic liquids are thought to improve catalytic acivity. A range of mesoporous and macroporous materials were used as supports for HPAs and employed in esterification reactions. Wu *et al*. [94] synthesised lacunary polyoxometalates incorporated into hexagonal mesoporous silica matrix materials. Characterization results show that the materials possessed an ordered pore structure and high specific surface areas ranging from 626-878 m^2 g^{-1} with a mesopore diameter of about 3.8 nm. Excellent catalytic performance is observed and a good reusability of the catalysts for the esterification of *n*-butanol with acetic acid is obtained.

Dufaud and co-workers [95] developed a method of synthesizing stable and reactive modified mesoporous hybrid materials with intact heteropolyacid (HPA) Keggin units by a one-pot method using a mixture of structure directing agents. They found that sequential calcination steps were key to obtaining stable HPA containing materials. All materials were characterized by various physical and spectroscopic methods to verify the type of materials synthesised. These materials were effective in the esterification reaction compared to a relevant homogeneous acid. Wu *et al*. [96] synthesized Keggin-structured HPAs anchored on amino-functionalized MCM-41 and the materials were compared with HPAs directly supported on MCM-41 synthesised by impregnation for evaluation in the esterification of *n*-butanol with acetic acid. HPAs anchored on amino-functionalized MCM-41 gave very stable and substantially higher activity than the ones supported on HPA catalysts. The low activity demonstrated by the impregnated catalysts were attributed to the leaching of HPA active sites. In a study conducted by Leng *et al*. [97], a number of solid organic heteropolyacid (HPA) salts were prepared by combining Keggin heteropolyanions with ionic liquid-forming cations, functionalized by propane sulfonate and their catalytic activities were assessed in esterification reactions by testing the influence of organic cations, function of heteropolyanions, scope of reactions, optimization of reaction conditions and catalytic reusability. The obtained catalysts produced high yield and selectivity towards target esters and were easily recyclable. The authors inferred that the highly efficient nature of these catalysts is due to the pseudo-liquid behavior of HPA salts that allows the propane sulfonate acidic species in the bulk to behave as active centers for esterification.

1.3.2 Heteropolyacid catalysts in benzaldehyde synthesis

Hu *et al*. [98] reported the selective oxidation of styrene to benzaldehyde over Schiff base-modified ordered mesoporous silica materials impregnated with the transition metal-monosubstituted Keggin-type polyoxometalates. The excellent catalytic performances of these catalysts were attributed mainly to the relatively easy electron-donating ability of the Schiff base ligand, which facilitates the electron transfer rate of the Keggin-type unit. Additionally, the ordered mesostructure of the material also plays an important role in obtaining high reactivity and selectivity towards the styrene oxidation reaction. In a study undertaken by Patel *et al*. [99], a Keggin-type cesium salt of a mono Mn(II)-substituted phosphotungstate ($Cs_5[PMnW_{11}O_{39}]$) was synthesized and characterized in solution as well as in the solid state by spectroscopic, magnetic and electrochemical techniques. It was observed that the complex crystallized in the tetragonal phase and X-ray analysis showed two types of disorder in which the Mn and W atoms are distributed over the 12 positions. In the non-aqueous oxidation of styrene using molecular oxygen, the complex gave greater than 99.0% selectivity towards benzaldehyde and was recyclable.

Lanthanide-containing Keggin-type polyoxometalates (LnPOMs), $[Ln(PW_{11}O_{39})_2]^{11-}$, where Ln = Eu^{3+} and Sm^{3+}, were incorporated for the first time into porous chromium terephthalate MIL-101(Cr) *via* an impregnation method by Granadeiro *et al*. [100] to be used as heterogeneous catalysts in the oxidation of styrene using hydrogen peroxide as the oxidant and acetonitrile as the solvent. Their catalytic activity was also compared with the homogeneous LnPOMs catalysts in order to evaluate the effect of the incorporation on the catalytic activity. The composite materials exhibit higher catalytic activities toward the oxidation of styrene than the corresponding isolated LnPOMs with complete conversion of the substrate after 4 h and 5 h for the samarium and europium composites, respectively.

The kinetics and phase transfer effects using a series of ruthenium substituted polyoxotungstates, used to catalyze the cleavage oxidation of styrene, were studied by Xinrong *et al*. [101]. Under the experimental conditions investigated, benzaldehyde and benzoic acid were the main reaction products and kinetic studies showed that the reactions giving these products were the result of consecutive reactions consisting of the initial oxidation of styrene into benzaldehyde and the subsequent oxidation of benzaldehyde to benzoic acid. The first

oxidation step has been shown to be first order with respect to substrate and its activation energy was similar to that catalyzed by different polyanions.

Benzaldehyde is also produced by the catalytic oxidation of benzyl alcohol. Assady *et al*. [102] immobilized $[PW_{11}ZnO_{39}]^{5-}$ on activated carbon used them in the oxidation of various alcohols, including benzyl alcohol, with hydrogen peroxide. The catalysts were very efficient for small-scale synthesis because of easy separation from the reaction mixture, they were relatively cheap, showed high activity, selectivity and stability, as well as good retention of activity in subsequent catalytic cycles. Park *et al*. [103] measured the reduction potentials of $H_3PMo_xW_{12-x}O_{40}$ Keggin HPA and $H_6P_2Mo_xW_{18-x}O_{62}$ Wells-Dawson HPA catalysts and correlated the values to the redox property, i.e. reduction potential and absorption edge energy, in the vapour-phase oxidation of benzyl alcohol. In this study, yield for benzaldehyde increased with increasing reduction potential and with decreasing absorption edge energy of the HPA catalyst, regardless of the identity of HPA catalyst.

Rao *et al*. [104] and Jing and co-workers [105] used vanadium based HPAs to investigate benzaldehyde synthesis from benzyl alcohol. In the former study, a series of 12-molybdophosphoric acid (MPA) supported on V_2O_5 dispersed γ-Al_2O_3 catalysts with different vanadia loadings were prepared by impregnation. The catalysts exhibited high catalytic activity with the conversion of benzyl alcohol depending on the vanadia content. The catalyst with a 15 wt% V_2O_5 loading showed optimum activity, attributing the high oxidation activity of this catalysts to the synergistic effect between MPA and V_2O_5. In the other study, a series of polyoxometalate (POM)-based amphiphilic catalysts were prepared via functionalization of the V-containing Keggin POM, $H_4PMo_{11}VO_{40}$, by cationic surfactants with different carbon-chain lengths. Among the catalysts investigated, the amphiphilic $(ODA)_4PMo_{11}VO_{40}$ showed the highest catalytic efficiency for the selective oxidation of benzyl alcohol with a maximum conversion of 61% with a selectivity of 99% towards benzaldehyde under the optimized reaction conditions. The catalyst also offered excellent reusability, confirmed by the recycling experiments conducted with the used catalyst.

1.4 Aims and objectives

Metal exchanged heteropolyacid catalysts have been investigated in various organic reactions due their tunable properties that directly affect the catalytic performance. In this study, various heteropolyacids and modified heteropolyacids were used for a number of organic reactions. The aims and objectives of this study include:

- The preparation of series of heteropolyacids using well known methods. Modifying the heteropolyacids by simple ion exchange with various metals taking into account the required metal loading in the various heteropolyacids to ensure the retention of the primary structure of Keggin ion of heteropolyacid.
- To determine the physicochemical functionalities of catalysts using a range of spectroscopic and adsorption techniques such as infrared spectroscopy, pyridine infrared adsorption studies, X-ray diffraction, surface studies and catalyst composition.
- To test all catalyst formulations in organic reactions such as esterification and selective oxidation.

1.5 Structure of thesis

The thesis consists of six chapters:

- Chapter 1 is based on the introduction and literature review, together with the aims and objectives of the study.
- Chapter 2 provides a mini review on the Knoevenagel condensation reaction over metal containing heteropolyacid catalysts.
- Chapter 3 describes the synergistic role of Brønsted and Lewis acidity in alkali metal exchanged heteropolyacid catalysts for esterification of acetic acid at room temperature.
- Chapter 4 investigates the role of alkali metal exchanged phosphomolybdic acid catalysts in the solvent free oxidation of styrene to benzaldehyde at room temperature.
- Chapter 5 assesses the solvent free oxidation of benzyl alcohol to benzaldehyde over copper and zinc modified phosphomolybdic acid catalysts at room temperature.
- Chapter 6 provides the concluding remarks for the entire study.

References

[1] J.R. Sowa Jr., *Catalysis of Organic Reactions*, CRC Press, 2005, Ch. 29, 251-260.

[2] I. Mochida, Y. Anju, A. Kato, T. Seiyama, *J Catal*, **21(3)** (1971) 263-269.

[3] M. Shirai, N. Ichikuni, K. Asakura, Y. Iwasawa, *Catal Today*, **8(1)** (1990) 57-66.

[4] M. Mazzotti, B. Neri, D. Gelosa, A. Kruglov, M. Morbidelli, *Ind Eng Chem Res*, **36(1)** (1997) 3-10.

[5] S.I. Kirbaslar, Z.B. Baykal, U. Dramur, *Turk J Eng Environ Sci*, **25** (2001) 569-577.

[6] H.M. Anasthas, V.G.Gaikar, *Reac Funct Poly*, **47(1) (2001)** 23-35.

[7] B.S. Furniss, A.J. Hannaford, P.W.G. Smith, A.R. Tatchell, *Vogel's: Textbook of practical organic chemistry*, Longman Group UK, 5th Edition, 1999.

[8] R. Koster, B. van der Linden, E. Poels, A. Bliek, *J Catal*, **204(2)** (2001) 333-338.

[9] M. Furuta, M.C. Kung, H.H. Kung, *Appl Catal A: Gen*, **201(1)** (2000) L9-L11.

[10] C. Chilev, E. Simeonov, *J Chem Tech Metall*, **52(3)** (2017) 463-474.

[11] K. Konakom, A. Saengchan, P. Kittisupakorn, I.M. Mujtaba, *Proceedings of the World Congress on Engineering and Computer Science 2010 Vol II*, San Francisco, USA.

[12] O. Chidi, O.I. Peter, *J Phys Chem Biophys*, **6(3)** (2016) 219-222.

[13] Y. Hua, F. Xiaozhen, Z. Shaoqing, *J Chem Pharm Res*, **7(10) (**2015) 445-448.

[14] K. Inui, T. Kurabayashi, S. Sato, *J Catal*, **212** (2002) 207–215.

[15] M.L. Passos, C.P. Ribeiro, F.L. Boca Raton, *Innovation in food engineering:new techniques and products*, CRC Press, 2010.

[16] F. Brühne, E. Wright, *"Benzaldehyde" in Ullmann's Encyclopedia of Industrial Chemistry*, Wiley-VCH, Weinheim, 2002.

[17] J.T. Lutz, *in Technology*, ed. M. Kirk-Othmer, D. Grayson, G.J. Eckroth, C.I. Bushey, Wiley, New York, 3rd edn., 1980, 251.

[18] S.L. Regen, C. Koteel, *J Am Chem Soc*, **99** (1977) 3837-3838.

[19] Z. Zhang , Y.Z. Wu , Z. Min, F.C. Yan, *Syn React Inorg Metal-Org Nano-Metal Chem*, **38** (2008) 352-355.

[20] J.M. Gichumbi, H.B. Friedrich, B. Omondi, *J Organometal Chem*, **808** (2016) 87-96.

[21] Y. Zhang, T. Yang, B.Y. Zheng, M.Y. Liu, N. Xing, *Polyhedron*, **121** (2017) 123-129.

[22] V. Hulea, E. Dumitriu, *Appl Catal A: Gen*, **277** (2004) 99-106.

[23] Y. Yang, Y. Zhang, S. Hao, J. Guan, H. Ding, F. Shang, P. Qiu, Q. Kan, *Appl Catal A: Gen*, **381** (2010) 274-281.

[24] M. Silva, C. Freire, B.D. Castro, J.L. Figueiredo, *J Mol Catal A: Chem*, **258** (2006) 327-333.

[25] Y. Wan, Q. Liang, Z. Li, S. Xu, X. Hub, Q. Liu, D. Lu, *J Mol Catal A: Chem*, **402** (2015) 29-36.

[26] J. Wang, J. Lu, J. Yang, R. Chen, Y. Zhang, D. Yin, J. Wang, *Appl Surf Sci*, **283** (2013) 794-801.

[27] R.J. Chimentao, I. Kirm, F. Medina, X. Rodrıguez, Y. Cesteros, P. Salagre, J.E. Sueiras, J.L.G. Fierro, *Appl Surf Sci*, **252** (2005) 793-800.

[28] L. Nie, K.K. Xin, W.S. Li, X.P. Zhou, *Catal Commun*, **8** (2007) 488-492.

[29] S. Lubis, L. Yuliati, S.L. Lee, I. Sumpono, H. Nur, *Chem Eng J*, **209** (2012) 486-493.

[30] J. Valand, H. Parekh, H.B. Friedrich, *Catal Commun*, **40** (2013) 149-153.

[31] Y. Luo, J. Lin, *Micro Meso Mater*, **86** (2005) 23-30.

[32] W. Tanglumlert, T. Imae, T.J. White, S. Wongkasemjit, *Catal Commun*, **10** (2009) 1070-1073.

[33] H. Wang, W. Qian, J. Chen, Y. Wu, X. Xu, J. Wang, Y. Kong, *RSC Adv*, **4** (2014) 50832-50839.

[34] R. Ramanathan, S. Sugunan, *Catal Commun*, **8** (2007) 1521-1526.

[35] A.L. Ahmad, C.P. Leo, S.R.A. Shukor, *J Porous Mater*, **16** (2009) 33-40.

[36] Y. Zheng, X. Zhang, Y. Yao, X. Chen, Q. Yang, *RSC Adv*, **5** (2015) 105747-105752.

[37] V. Indira, S.B. Halligudi, S. Gopinathan, C. Gopinathan, *React Kinet Catal Lett*, **73** (2001) 99-107.

[38] G. Franz, R.A. Sheldon, *Ullmann's Encyclopedia of Industrial Chemistry*, 5th Ed. VCH Weinheim: Germany, **1991,** p. 261.

[39] Q.H. Xia, H.Q. Ge, C.P. Ye, Z.M. Liu, K.X. Su, *Chem Rev*, **105** (2005) 1603-1662.

[40] Z. Weng, G. Liao, J. Wang, X. Jian, *Catal Commun*, **8(10)** 2007 1493-1496.

[41] C. Ragupathi, J. J. Vijaya, S. Narayanan, S.K. Jesudoss, L.J. Kennedy, *Ceramics Inter*, **41(2)** (2015) 2069-2080.

[42] M.-L. Guo, H.- Z. Li, *Green Chem*, **9** (2007) 421-423.

[43] M. Caravati, J.D. Grunwaldt, A. Baiker, *Phys Chem Chem Phys*, **7(2)** (2005) 278-285.

[44] A. Savara, C.E. Chan-Thaw, I. Rossetti, A. Villa, L. Prati, *ChemCatChem*, 6 (2014) 3464-3473.

[45] P.J. Miedziak, Q. He, J.K. Edwards, S.H. Taylor, D.W. Knight, B. Tarbit, C.J. Kiely, G.J. Hutchings, *Catal Today*, **163(1)** (2011) 47-54.

[46] M. Alhumaimess, Z. Lin, W. Weng, N. Dimitratos, N. Dummer, S.H. Taylor, J.K. Bartley, C.J. Kiely, G.J. Hutchings, . *ChemSusChem*, **5(1)** (2012) 125-131.

[47] D. Guo, Y. Wang, P. Zhao, M. Bai, H. Xin, Z. Guo, J. Li, *Catalysts*, **6** (2016) 64-77.

[48] R. Marotta, I. Di Somma, D. Spasiano, R. Andreozzi, V. Caprio, *Chem Eng J*, **172** (2011) 243-249.

[49] K. Bijudas, *Orient J Chem*, **30(3)** (2014) 1391-1396.

[50] I.V. Kozhevnikov, *Chem Rev*, **98** (1998) 171-198.

[51] I.V. Kozhevnikov, *Catal Rev Sci Eng*, **37** (1995) 311-352.

[52] N. Mizuno, M. Misono, *Chem Rev*, **98** (1998) 199-218.

[53] L.E. Briand, G.T. Baronetti, H.J. Thomas, *Appl Catal A: Gen*, **256** (2003) 37-50.

[54] M.N. Timofeeva, *Appl Catal A: Gen*, **256** (2003) 19-35.

[55] M. Misono, *Catal Rev Sci Eng*, **29** (1987) 269-321.

[56] C.L. Hill, C.M.P. McCartha, *Coordination Chem Rev*, **143** (1995) 407-455.

[57] I.K. Song, M.A. Barteau, *J Mol Catal A: Gen*, **182-183** (2002)185-193.

[58] I.K. Song, M.A. Barteau, *J Mol Catal A: Gen*, **212** (2004) 229-236.

[59] M.H. Youn, D.R. Park, J.C. Jung, H. Kim, M.A. Barteau, I.K. Song, *Korean J Chem Eng*, **24** (2007) 51-54.

[60] M.T. Pope, *Heteropoly, isopoly oxometalates*, Springer-Verlag, New York, 1983.

[61] W. Chu, X. Yang, Y. Shan, X. Ye, Y. Wu, *Catal Lett*, **42** (1996) 201-208.

[62] S.M. Kumbar, S.B. Halligudi, *Catal Comm*, **8** (2007) 800-806.

[63] A. Llanos, L. Melo, F. Avendano, A. Montes, J.L. Brito, *Catal Today*, **133-135** (2008) 20-27.

[64] S. Thomas, K. Vaezzadeh, V. Pitchon, *Top Catal*, **30-31** (2004) 207-213.

[65] S.A. Popova, A.L. Tarasov, L.M. Kustov, I.Y. Chukicheva, A.V. Kuchin, *Russian J Phy Chem A*, **87** (2013) 342-344.

[66] S. Benadji, P. Eloy, A. Leonard, B.L. Su, C. Rabia, E.M. Gaigneaux, *Micro Meso Mater*, **154** (2012) 153-163

[67] Y. Kamiya, Y. Ooka, C. Obara, R. Ohnishi, T. Fujita, Y. Kurata, K. Tsuji, T. Nakajyo, T. Okuhara, *J Mol Catal A: Chem*, **262** (2007) 77-85.

[68] L.A.M. Cardoso, W.A. Jr, A.R.E. Gonzaga, L.M.G. Aguiar, H.M.C. Andrade, *J Mol Catal A: Chem* **209** (2004) 189-197.

[69] H. Hamad, M. Soulard, B. Lebeau, J. Patarin, T. Hamieh, J. Toufaily, H. Mahzoul, *J Mol Catal A: Chem*, **278** (2007) 53-63.

[70] N. Mizuno, D.J. Suh, W. Han, T. Kudo, *J Mol Catal A: Chem*, **114** (1996) 309-317.

[71] D.R. Park, H. Kim, J.C. Jung, S.H. Lee, J. Lee, I.K. Song, *React Kinet Catal Lett,* **93** (2008) 43-49.

[72] R. Palkovits, K. Tajvidi, A.M. Ruppert, J. Procelewska, *Chem Comm,* **47** (2011) 576-578.

[73] V. Palermo, G.P. Romanelli, P.G. Vazquez, *J Mol Catal A: Chem*, **373** (2013) 142-150.

[74] A. Engin, H. Haluk, K. Gurkan, *Green Chem*, **5** (2003) 460-466.

[75] C.F. Oliveira, L.M. Dezaneti, F.A.C. Garcia, J.L. Macedo, J.A. Dias, S.C.L. Dias, K.S.P. Alvim, *Appl Catal A: Gen,* **372** (2010) 153-161.

[76] A. Angelis, P. Pollesel, D. Molinari, W.N. Parker Jr, A. Frattini, F. Cavani, S. Martins, C. Perego, *Pure Appl Chem*, **79** (2007) 1887-1894.

[77] G.D. Yadav, G George, *Catal Today*, **141** (2009) 130-137.

[78] M. Hinoa, K. Aratab, *Green Chem,* **3** (2001) 170-172.

[79] A. Miyaji, T. Echizen, K. Nagata, Y. Yoshinaga, T. Okuhara, *J Mol Catal A: Chem*, **201** (2003) 145-153.

[80] E.L Salinas, J.G.H. Corteaz, M.A.C Jaacome, J. Navarrete, M.E. Llanos, A. Vaazquez, H. Armendariz, T. Loapez, *Appl. Catal. A: Gen* 175 (1998) 43-53.

[81] A.I. Tropecelo, M.H. Casimiro, I.M. Fonseca, A.M. Ramos, J. Vital, J.E. Castanheiro, *Appl Catal A: Gen,* **390** (2010) 183-189.

[82] B.M. Devassy, G.V. Shanbhag, S.B. Halligudi, *J Mol.Catal A: Chem*, **247** (2006) 162-170.

[83] N. Bhatt, A. Patel, *J Mol Catal A: Chem,* **238** (2005) 223-228.

[84] G. Kamalakar, K. Komura, Y. Sugi, *Appl Catal A: Gen*, **261** (2004) 163–170.

[85] L.M.G. Sainero, S. Damyanova, J.L.G. Fierro, *Appl Catal A: Gen*, **208** (2001) 63-75.

[86] G. Kamalakar, K. Komura, Y. Sugi, *Catal Lett,* **108** (2006) 31-35.

[87] K. Rajasekar, A. Pandurangan, *Catal Commun,* **8** (2007) 635-643.

[88] V Brahmkhatri, A. Patel, *Appl Catal A: Gen,* **403** (2011) 161-172.

[89] J.H. Sepulveda, J.C. Yori, C.R. Vera, *Appl Catal A: Gen,* **288** (2005) 18-24.

[90] S.K. Bhorodwaj, D.K. Dutta, *Appl Catal A: Gen,* **378** (2010) 221-226.

[91] S. Zhu, X. Gao, F. Dong, Y. Zhu, H. Zheng, Y. Li, *J Catal,* **306** (2013) 155-163.

[92] T.V. Kovalchuk, J.N. Kochkin, H. Sfihi, V.N. Zaitsev, J. Fraissard, *J Catal,* **263** (2009) 247-257.

[93] J. Zhao, H. Guan, W. Shi, M. Cheng, X. Wang, S. Li, *Catal Commun,* **20** (2012) 103-106.

[94] N. Wu, B. Li, W. Ma, C. Han, *Micro Meso Mater,* **186** (2014) 155-162.

[95] V. Dufaud, F. Lefebvre, G. P. Niccolai, M. Aouine, *J Mater Chem,* **19** (2009) 1142-1150.

[96] S. Wu, J. Wang, W. Zhang, X. Ren, *Catal Lett,* **125** (2008) 308-314.

[97] Y. Leng, J. Wang, D. Zhu, Y. Wu, P. Zhao, *J Mol Catal A: Chem,* **313** (2009) 1-6.

[98] J. Hu, K. Li, W. Li, F. Ma, Y. Guo, *Appl Catal A: Gen,* **364** (2009) 211-220.

[99] K. Patel, P. Shringarpure, A. Patel, *Trans Metal Chem,* **36** (2010) 171-177.

[100] C.M. Granadeiro, P. Silva, V.K. Saini, F.A.A. Paz, J. Pires, L.C. Silva, S.S. Balul, *Catal Today,* **218-219** (2013) 35-42.

[101] L. Xinrong, X. Jinyu, L. Huizhang, Y. B. Jin, S. X. Gaoyang, *J Mol Catal A: Chem,* **61** (2000) 163-169.

[102] E. Assady, B. Yadollahi, M.R. Farsani, M. Moghadam, *Appl Organometal Chem,* **29** (2015) 561-565.

[103] D.R. Park, J.H. Song, S.H. Lee, S.H. Song, H. Kim, J.C. Jung, I.K. Song, *Appl Catal A: Gen,* **349** (2008) 222-228.

[104] P.S.N. Rao, K.T.V. Rao, P.S.S. Prasad, N. Lingaiah, *Chin J Catal,* **32** (2011) 1719-1726.

[105] L. Jing, J. Shi, F. Zhang, Y. Zhong, W. Zhu, *Ind Eng Chem Res,* **52** (2013) 10095-10104.

CHAPTER TWO

REVIEW ON THE KNOEVENAGEL CONDENSATION REACTION OVER METAL CONTAINING HETEROPOLYACID CATALYSTS

Abstract

The Knoevenagel condensation reaction is an important C-C bond formation reaction that has been studied extensively over the past few decades. In the present review, the Knoevenagel reaction to produce olefins over a range of heterogenous catalysts, with special emphasis on eco-friendly metal containing heteropolyacids is discussed. The metal containing heteropolyacid catalysts were synthesized by ion-exchange and in all cases, the signature Keggin-like structure of the material was always maintained after incorporation of the metal. This was confirmed by various physical and chemical characterization techniques. The catalytic performance directly correlated with the acidity of the materials and was largely dependent on the type of metal which replaced the protons of the heteropolyacid.

Keywords: Knoevenagel condensation reaction, eco-friendly, acidity, metal containing heteropolyacids

2.1 Background of the Knoevenagel condensation reaction

The Knoevenagel condensation reaction is an organic reaction named after Emil Knoevenagel. It is a modification of the aldol condensation and takes place through a nucleophilic addition of an active hydrogen compound to a carbonyl group followed by a dehydration reaction in which a molecule of water is eliminated. The product is often a *α,β*-unsaturated ketone or a conjugated enone [1]. A general reaction is shown below:

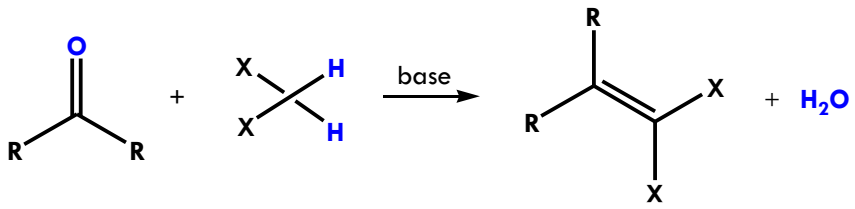

Figure 2.1 A general Knoevenagel condensation reaction.

In the reaction shown in Figure 2.1, the carbonyl group is an aldehyde or a ketone and the catalyst is usually a weakly basic amine. The active hydrogen component can have the form, X-CH_2-X or X-CHR-X, e.g. diethyl malonate, ethyl acetoacetate or malonic acid, or cyanoacetic acid and X-CHR_1R_2, e.g. nitromethane [2]. Here, X is an electron withdrawing functional group, powerful enough to facilitate deprotonation to the enolate ion, in the presence of a mild base. If a strong base is used in this reaction, self-condensation of the aldehyde or ketone might be induced.

2.2 Importance of the Knoevenagel reaction

In the last few decades, the Knoevenagel condensation reaction has emerged as one of the most studied reactions catalyzed by various systems for the synthesis of olefins. Apart from the synthesis of simple alkenes, this reaction has been modified to produce various important precursors for the chemical and pharmaceutical industry. One such modification is the Doebner modification in which acrolein can react with malonic acid in the presence of a base, in this case pyridine to produce a *trans*-diene, shown in Figure 2.2:

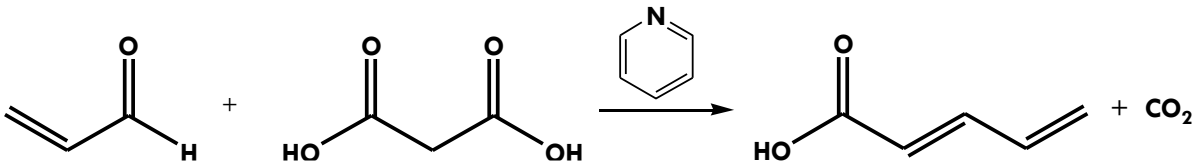

Figure 2.2 The Doebner modification of the Knoevenagel reaction.

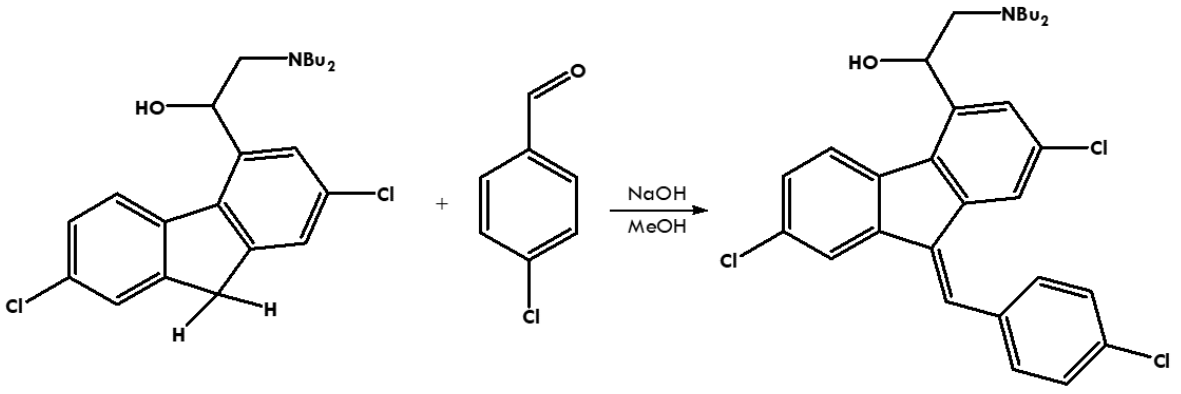

Figure 2.3 Synthesis of lumefantrine via Knoevenagel condensation.

The Knoevenagel condensation reaction is also demonstrated in the reaction of 2-methoxy benzaldehyde with thiobarbituric acid in ethanol using piperidine as a base to produce an

enone which is a charge transfer complex molecule and is a key step in the commercial production of the antimalarial drug, lumefantrine, a component of Coartem [3] (Figure 2.3). The initial reaction product is a 50:50 mixture of *E* and *Z* isomers, however the more stable *Z*-isomer is eventually obtained due to equilibration of the isomers around the hydroxyl precursor.

The Hantzsch pyridine synthesis, the Gewald reaction and the Feist–Benary furan synthesis all contain a Knoevenagel reaction step. In the Hantzsch pyridine synthesis, the reaction proceeds between formaldehyde, 2 equivalents ethyl acetoacetate and a nitrogen donor such as ammonium acetate or ammonia. The initial reaction product is a dihydropyridine, which is oxidized to pyridine and is an important class of calcium channel blockers, which are used in the manufacture of nifedipine, amlodipine or nimodipine (Figure 2.4). This reaction has also been investigated in a one-pot synthesis and proceeds in water as solvent with direct aromatization by ferric chloride, manganese dioxide or potassium permanganate [4].

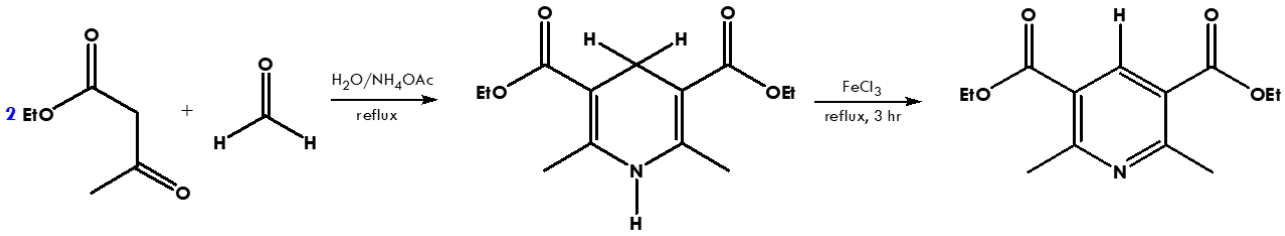

Figure 2.4 One-pot Hantzsch pyridine synthesis [4].

In the Gewald reaction, the condensation of a ketone or an aldehyde with an α-cyanoester in the presence of elemental sulfur and base takes place to give a poly-substituted 2-amino-thiophene as shown in Figure 2.5.

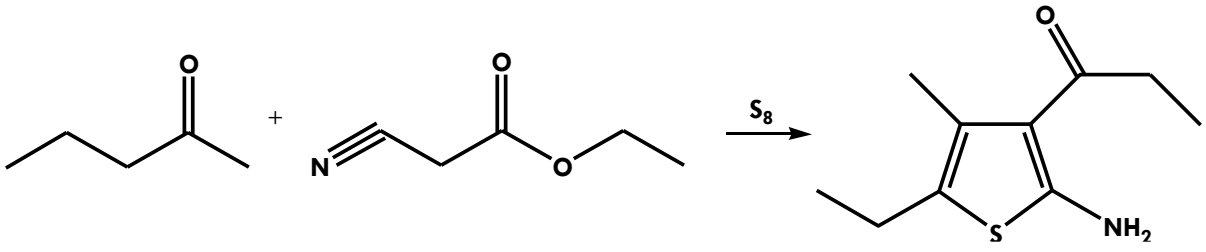

Figure 2.5 The Gewald reaction [5].

In one variation of the Gewald reaction, a 3-acetyl-2-aminothiophene is synthesized starting from a dithiane, an adduct of sulfur and acetone if R=CH_3 or acetaldehyde if R=H and the sodium salt of cyanoacetone [6] (Figure 2.6):

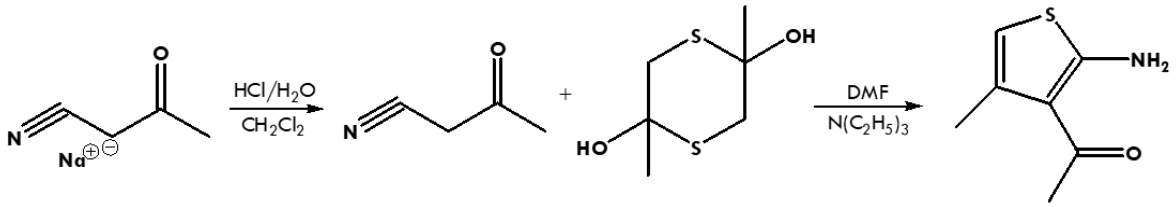

Figure 2.6 Variation of the Gewald reaction [6].

In the Feist-Benary synthesis, an organic reaction takes place between α-halogen ketones and β-dicarbonyl compounds, catalysed by amines such as ammonia or pyridine to produce furan compounds [7]. The first step in the ring synthesis is related to the Knoevenagel condensation while in the second step, the enolate displaces an alkylhalogen in a nucleophilic aliphatic substitution (Figure 2.7).

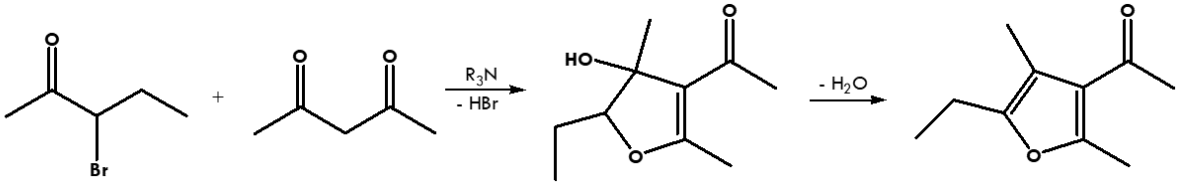

Figure 2.7 The Feist-Benary synthesis [7].

2.3 The Knoevenagel reaction over solid catalysts

The Knoevenagel reaction was generally carried out under homogenous conditions using amines as the catalyst in the presence of a base. A major disadvantage of this approach is the separation of the product which renders the process very expensive, since it requires inorganic acids and large amounts of volatile organic solvents for the isolation of the product. As a result, there has been increasing emphasis on the need to design solid acid catalysts that are environmentally friendly due to the enactment of stringent environment protection laws.

The salts of amines, Lewis acids such as $CuCl_2$, $ZnCl_2$ and SmI_2 and the ZnY zeolites are some of the catalysts that have been employed in the Knoevenagel condensation reaction [8-11], together with a host of other materials containing both acidic and basic sites have been reported

in literature [12-17]. Activated hydrotalcites were also used for the condensation reactions producing excellent yields, however, the reactions were carried out using toluene and DMF as solvents [18]. Joshi *et al.* [19] studied the effect of incorporating alkali metals in NaX- type zeolites in influencing the activity in the Knoevenagel condensation reaction. They found that an increase in the cation diameter improved activity by 50 %.

In a number of studies conducted by Corma and co-workers, carried out in heterogeneous medium, using base catalysts such as aluminiphosphate oxynitrides, zeolites, sepiolites and hydrotalcites, produced promising results. However, all the catalytic reactions required the presence of solvents [20–23]. To avoid the use of organic solvents, water was investigated as a desirable solvent with mixed results [24]. It was later agreed that most desirable is conducting such a reaction to produce excellent yields under solvent free conditions. This was emphatically emphasized by both Metzger [25] and Tanaka and Toda [26].

Pillai *et al*. [27, 28] studied the Knoevenagel reaction using cobalt, iridium and platinum hydroxyapatites. Hydroxyapatites (HAp) are bifunctional materials that contain both acidic and basic sites in their crystal lattice. Their results showed that the IrHAp catalyzed reactions gave higher yields than PtHAp catalyzed reactions, but both IrHAp and PtHAp catalysed reactions were very efficient in the Knoevenagel reaction without the use of a solvent, with the overall production of excellent yields. The cobalt hydroxyapatite also produced reasonable yields, but not as efficiently as the precious group metals. Table 2.1 provides a summary of the research carried out in this field.

Recently, much attention has been focused on easily reusable solid acid catalysts such as heteropolyacids (HPAs). HPAs are discrete transition metal oxide cluster anions and comprise a class of inorganic complexes of unrivalled versatility and structural variation in both symmetry and size, with applications in many fields of science [29]. Varying the acidity of HPAs is one of the areas that has been exploited for the Knoevenagel reaction and this is achieved by exchanging protons with the appropriate metal, providing unique structural as well as chemical properties.

Viswanadham *et al*. [30, 31] investigate the use of vanadium and copper exchanged HPAs for the Knoevenagel reaction under solvent free conditions. In the case of the vanadium based catalysts, the activity was dependent on the acidity of the materials which was a direct

consequence of the V/P ratio. A similar situation existed for the copper exchanged HPA. A mechanism of this reaction over acidic sites of the copper catalyst during condensation was also proposed (Figure 2.8).

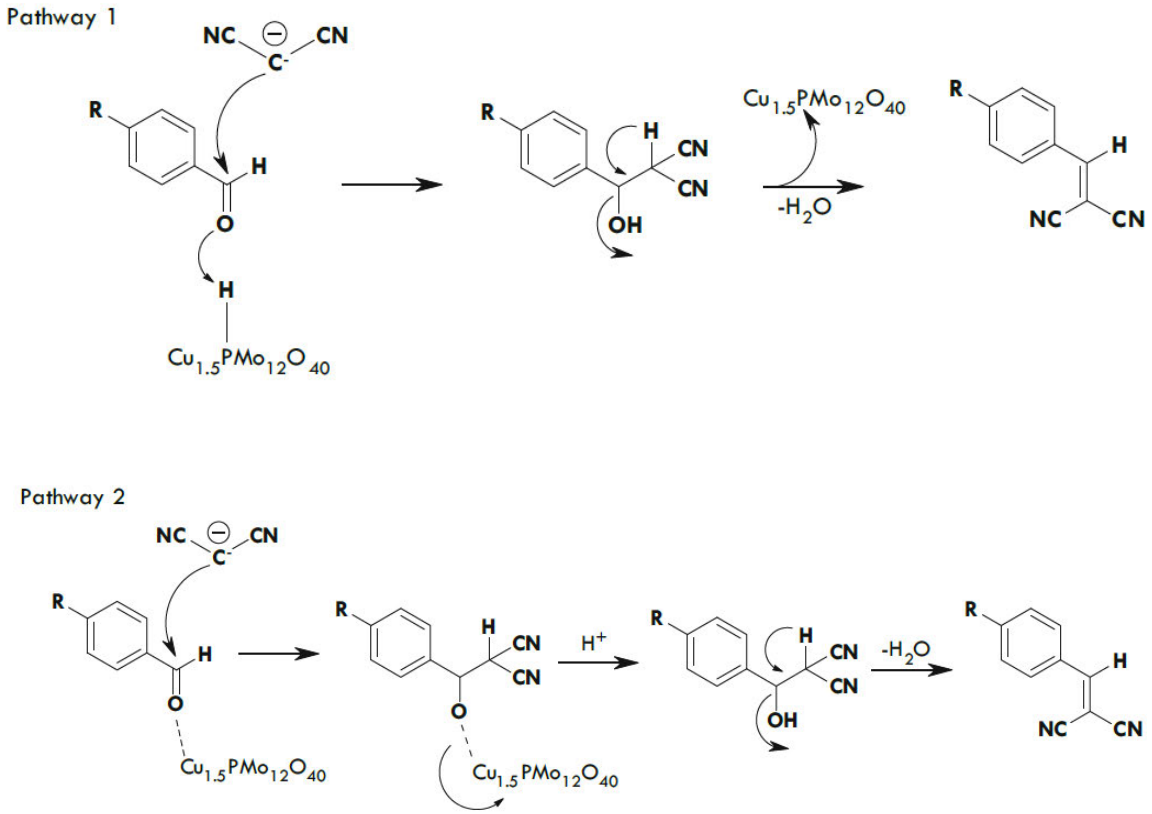

Figure 2.8 Proposed reaction mechanism for the Knoevenagel condensation over Cu–PMA catalysts [31].

Table 2.1 Comparison of different types of catalysts used in the Knoevenagel condensation.

Catalyst	Reaction conditions	Conversion (%)	Advantages	Disadvantages	Reference
LiOH	1 /1 /2/26/10	90	Achieving higher yields at room temperature in short reaction time intervals	Base and solvent is used in the reaction and acid is required for neutralization and huge amount of acid and solvent is required in pilot plant.	32
$GaCl_3$	2/2.5/0/RT/2	96.7	Achieving higher yields at room temperature in short reaction time intervals	Lack of catalyst reusability	33

Phosphane	5/6.5/0/80/240	98	Achieving higher yields at higher reaction time intervals	Phosphane is toxic and recycling is critical	34
Fe_3O_4@SiO_2	0.1/0.1/0.4/75/15	100	Best yields	Solvent used	35
$InBr_3$	0.6/0.66/0.6/60/480	3	Very poor yields	Solvent used and lack of reusability	36
P4VP/Al_2O_3-SiO_2	2/2/10/100/30	98	Better yields	Solvent used and no recycling	37
copper metal powder	0.12/0.1/1/56/120	99	Better yields	Solvent used and no recycling	38
TEA:piperidine	4.7/4.7/5/ 120/180	90	Good yields	Solvent used in huge amounts	39
polyurethane	1/1.1/1/50/840	98	Good yields	Long reaction time, solvent used.	40
Ethylenediammonium Diacetate	2/2/30/RT/60	87	Higher yields	Solvent used	41
Amine-functionalized MOF	1/1/6/80/ 270	51	Lower yields	Solvent used	42
$NiFe_2O_4$	1/1.2/4/RT/300	98	Good yields	Solvent used	43
amine-functionalized mesoporous zirconia	10/10/50/RT/1440	99	Long reaction times achieved better yields	Solvent used	44
Ionic Liquid	5/5/0/RT/10	96	Good yields	No recycling	45
KOH/SnO_2	2/2/1/RT/15	97	Good yields	Solvent used	46
PTA	10/10/10/100/15	91	Better yields	Solvent used	47
V-PMA	10/10/0/70/10	96	Good yields	No solvent and easy recycling and eco-friendly	30
Cu-PMA	10/10/0/70/15	95	Good yields	No solvent and easy recycling and eco-friendly	31

Reaction conditions: aldehyde (mmol) /active methylene compound (mmol) /solvent (mL)/reaction temperature (°C)/reaction time (min)

2.4 Conclusion

Base catalysts such as KOH and amines and organic TEA:piperidine-like materials are efficient in promoting the Knoevenagel condensation reaction resulting in acceptable yields, however the isolation of product is difficult and expensive. Metal salts also result in the reaction producing good yields, but solvents are used which render purification of solvent after isolation

of product expensive and the use of solvents is regarded as having a negative impact on the environment. It is possible to employ solid acid catalysts under solvent free conditions for this reaction. It was shown that solid acid catalysts such as heteropolyacids are acceptable at all levels for this reaction. They can be modified to improve activity, are eco-friendly and can operate under solvent free conditions.

References

[1] G. Jones, *Org React,* (1967) 204-599.

[2] J. March , *Advanced Organic Chemistry: Reactions, Mechanisms, and Structure 3rd ed.*, New York: Wiley 1985.

[3] U. Beutler, P.C. Fuenfschilling, A. Steinkemper, *Org Process Res Dev,* **11(3)** (2007) 341-345.

[4] J.J. Xia, G.W.Wang, *Synthesis,* **14** (2005) 2379-2383.

[5] R.W. Sabnis, *Sulfur Rep,* **16** (1994) 1-17.

[6] G.A. Eller, W. Holzer, *Molecules,* **11** (2006) 371-376.

[7] M.A. Calter, R.M. Phillips, C. Flaschenriem, *J Amer Chem Soc,* **127** (42) (2005) 14566-14567.

[8] O. Attanasi, P. Fillippone, A. Mei, *Syn Commun,* **13** (1983) 1203-1208.

[9] P. Shanthan Rao, R.V. Venkatratnam, *Tetrahedron Lett,* **32** (1991) 5821-5822.

[10] W. Bao, Y. Zhang, J. Wang, *Syn Commun,* **26** (1996) 3025-3028.

[11] S. Saravanamurugan, *Appl Catal A: Gen,* **298** (2006) 8-15.

[12] F.T. Boullet, A. Focucad, *Tetrahedron Lett,* **23** (1982) 4927-4928.

[13] D.J. Macquarrie, J.H. Clark, A. Lambert, J.E. Gmode, A. Priest, *React Funct Polym,* 35 (1997) 153-158.

[14] D. Brunel, *Micro Meso Mater,* **27** (1993) 329-344.

[15] R.W. Hein, M.J. Astle, J.R. Shelton, *J Org Chem,* **26** (1961) 4874-4878.

[16] H. Moison, F.T. Boullet, A. Focaud, *Tetrahedron,* **43** (1987) 537-542.

[17] F. Bigi, L. Chesini, R. Maggi, G. Sartori, *J Org Chem,* **64** (1999) 1033-1035.

[18] M. Lakshmi Kantam, B.M. Choudary, C.V. Reddy, K.K. Rao, F. Figueras, *Chem Commun,* (1998) 1033-1034.

[19] U.D. Joshi, P.N. Joshi, S.S. Tamhankar, V.V. Joshi, C.V. Rode, V.P. Shiralkar, *Appl Catal A Gen,* **239** (2003) 209-220.

[20] M.J. Climent, A. Corma, V. Forens, A. Frau, R.G. Lopez, S. Iborra, J. Primo, *J*

Catal, **163** (1996) 392-398.

[21] A. Corma, V. Fornes, R.M.M. Aranda, H. Garcia, J. Primo, *Appl Catal*, **59** (1990) 237-248.

[22] A. Corma, R.M.M. Aranda, F. Sanchez, M. Guinst, J. Barrault, C. Bouchoule, D. Duprez, R. Maurel, C. Montassier, *Stud Surf Sci Catal*, **62** (1991) 503.

[23] A. Corma, R.M.M. Aranda, *Appl Catal A: Gen*, **105** (1993) 271-279.

[24] H.A. Oskooie, M.M. Heravi, F. Derikvand, M. Khorasani, *Syn Commun*, **36** (2006) 2819-2823.

[25] J.O. Metzger, *Angew Chem Inter Ed*, **37** (1998) 2975-2978.

[26] K. Tanaka, F. Toda, *Chem Rev*, **100** (2000) 1025-1074.

[27] M.K. Pillai, S. Singh, S.B. Jonnalagadda, *Syn Commun*, **40** (2010) 3710–3715.

[28] M.K. Pillai, S. Singh, S.B. Jonnalagadda, *Kinet Catal*, **52** (2011) 536-539.

[29] M.T. Pope, *Inorganic Chemistry Concepts Vol. 8: Heteropoly and Isopoly Oxometalates*, Springer, Berlin, 1983.

[30] B. Viswanadham, P. Jhansi, K.V.R. Chary, H.B. Friedrich, S. Singh, *Catal Lett*, **146** (2016) 364-372.

[31] B. Viswanadham, J. Pedada, H.B. Friedrich, S. Singh, *Catal Lett*, **146** (2016) 1470-1477.

[32] M.A. Pasha, K. Manjula, *J Sau Chem Soc*, **15** (2011) 283-286.

[33] L. Muralidhar, C.R. Girija, *J Sau Chem Soc*, **18** (2014) 541-544.

[34] J.S. Yadav, B.V.S. Reddy, A.K. Basa, B. Visali, A.V. Narsaiah, K. Nagaiah, *Eur J Org Chem*, (2004) 546-551.

[35] J.B.M.R. Filho, G.P. Pires, J.M.G.O. Ferreira, E.E.S. Teotonio, J.A. Vale, *Catal Lett*, **147** (2017) 167-180.

[36] Y. Ogiwara, K. Takahashi, T. Kitazawa, N. Sakai, *J Org Chem*, **80** (2015) 3101-3110.

[37] M. Kolahdoozan, R.J. Kalbasi, Z.S. Shahzeidi, F. Zamani, *J Chem*, **2013** (2013) 496837.

[38] E.M. Schneider, M. Zeltner, N. Kranzlin, R.N. Grass, W.J. Stark, *Chem Commun*, **51** (2015) 10695-10698.

[39] H.S. Pawar, A.S. Wagh, A.M. Lali, *New J Chem*, **40** (2016) 4962-4968.

[40] S.K. Dey, N.S. Amadeu, C. Janiak, *Chem Commun*, **52** (2016) 7834-7837.

[41] C. Su, Z.C. Chen, Q.G. Zheng, *Synth*, **4** (2003) 555-559.

[42] A. Taher, D.J. Lee, B.K. Lee, I.M. Lee, *Synlett*, **27** (2016) A-E.

[43] Q. Li, X. Wang, Y. Yu, Y. Chen, L. Dai, *Tetrahedron*, **72** (2016) 8358-8363.

[44] K.M. Parida, S. Mallick, P.C. Sahoo, S.K. Rana, *Appl Catal A: Gen,* **381** (2010) 226-232.

[45] B.C. Ranu, R. Jana, *Eur J Org Chem,* (2006) 3767-3770.

[46] J. Xie, L. Chen, C.T. Au, S.F. Yin, *Catal Commun*, **66** (2015) 30-33.

[47] H.A. Oskooie, M.M. Heravi, F. Derikvand, M. Khorasani, F.F. Bamoharram, *Syn Commun*, **36** (2006) 2819-2823.

CHAPTER THREE

SYNERGISTIC ROLE OF BRØNSTED AND LEWIS ACIDITY IN ALKALI METAL EXCHANGED HETEROPOLYACID CATALYSTS FOR ESTERIFICATION OF ACETIC ACID AT ROOM TEMPERATURE

Abstract

A series of Cs exchanged phosphotungstic acid (PTA) catalysts were synthesized by the ion exchanged method and were characterized by X-ray diffraction, FT-IR spectroscopy, pyridine adsorbed FT-IR spectroscopy, SEM, BF-TEM, ICP-OES and BET surface area analysis. For comparison purposes, K exchanged PTA, Cs and K exchanged phosphomolybdic acid (PMA) catalysts were also prepared. XRD diffractograms showed that the crystallites of the Keggin ion are maintained, while FT-IR spectra also revealed the characteristic bands of the Keggin ion at all metal loadings of all the catalysts. From pyridine adsorbed FT-IR spectroscopy, it was observed that the Brønsted and Lewis acidity were significantly maintained at lower metal loadings, whereas STEM analysis showed a uniform distribution of the elements which correlated well with the theoretical atomic values of the loaded metals for all the catalysts, which were verified by ICP results. The efficiency of various metal exchanged heteropolyacid catalysts was assessed for the esterification reaction using various substrates and the Cs exchanged phosphotungstic acid catalysts showed superior activity compared to the other catalysts. In particular, the Cs exchanged phosphotungstic acid with a 1 wt.% loading showed the highest activity and was most tolerant to the presence of water that was produced in the reaction. The catalytic activity correlates well with the Brønsted and Lewis acidity, as well as Keggin ion density of the catalysts.

Keywords: esterification; Brønsted and Lewis acidity; Cs-PTA; Keggin ion; room temperature

3.1 Introduction

Keggin type polyoxometalates, especially heteropolyacids (HPAs) are well known solid acid catalysts containing tunable Brønsted acidity and redox properties for various kinds of

reactions such as alkylation, esterification, dehydration, condensation and oxidation [1-12]. Among these reaction processes, esterification is an important chemical route whose products have potential applications in paints and perfumes and can be used as solvents in column chromatography and extractions in industrial as well as academic laboratories [12,13].

Ethyl acetate, one of the valuable chemical produced by esterification, is synthesized via the Fischer process. Sulfuric acid is used as the catalyst and the reaction produces a 65% yield at room temperature. However, the corrosive nature of sulfuric acid, in the long term, leads to reactor damage. In addition, the large scale production of ethyl acetate using large amounts of sulfuric acid results in coke formation. Another disadvantage is the relative ease of dehydrogenation of alcohol to produce the aldehyde as an interfering side reaction. Product isolation which requires more volatile organic solvents is also a major concern. Apart from sulfuric acid, phosphoric acid, surfactant-combined catalysts, choline chloride, and Brønsted acidic ionic liquid catalysts were also studied for the esterification reaction at room temperature [14-16]. However, these materials are also not eco-friendly, are toxic, and isolation of the product is difficult. Therefore, developing a catalyst which allows for easy isolation of product and is eco-friendly, to uphold the call for green chemical processes, is always a challenge. It has been shown that catalytic materials can be produced without the use of hazardous materials which are harmful to the environment.

In various studies, Fardood and co-workers [17-21] produced efficient catalytic materials from natural resources. In one study, magnesium ferrite nanoparticles were synthesized using tragacanth gum as a bio-template, with magnesium and iron nitrate as the metal source by the novel sol–gel method without adding external surfactant [19]. In another study, zinc oxide nanoparticles were also prepared by a similar method, instead Arabic gum was used as the bio-template [20]. In both the studies, the materials were efficient in the photodegradation of dyes.

The esterification reaction between acetic acid and an alcohol proceeds via Brønsted (B) and Lewis (L) acidic sites and the rate of reaction can be tuned by altering the Brønsted and Lewis acid sites of the catalyst. Solid acid catalysts seem to be ideal systems, since their acidity can be tuned to promote an eco-friendly esterification synthesis and also allows for catalyst recyclability. HPAs have strong Brønsted and Lewis acidity, however their major drawback is their solubility in organic reaction medium which requires an additional solvent for separation,

resulting in an expensive process for ester synthesis. This drawback can be alleviated by modifying HPA by exchanging its protons with a metal. Also, the exchange of protons with a metal is one of the ways of tuning the nature of acidity of the catalysts. Examples of these modified HPAs are phosphotungstic acid (PTA) and phosphomolybdic acid (PMA).

Eom *et al*. [22] showed that Cs exchanged phosphotungstic acid showed better activity than the commercially available $NiMo/Al_2O_3$ catalyst in the hydrocracking of extra-heavy oil, attributing the superior performance to the presence of Cs in the phosphotungstic acid, which stabilized the Keggin structure even at high calcination temperatures and also provides increased surface acid density necessary for higher activity. The versatile nature of HPAs is well known and studies with wide applications were reported, such as for the Beckmann rearrangement reaction, acylation, ether formation and carbonylation [23-35]. Shiju *et al*. [23] investigated the potential of Cs exchanged phosphotungstic acid catalysts for the liquid-phase Beckmann rearrangement of oximes to produce amides and lactam. It was observed that Cs with a 2.5wt% content was the most selective for the formation of Ɛ-caprolactam from cyclohexanone oxime among all the catalysts studied, whereas Srikanth *et al*. [24], in a totally different type of study, used Cs exchanged heteropolyacid catalysts functionalized with differing Sn content to study glycerol carbonylation in the presence of urea to produce glycerol carbonate, resulting in a 91 % glycerol conversion with 83% glycerol carbonate selectivity at 140°C.

In this study, the effect of Cs exchanged PTA catalysts with respect to the role of acidity as well as the impact of the Keggin ion density during the esterification reaction at room temperature was investigated. For comparative purposes, PMA catalysts were also studied.

3.2 Experimental

3.2.1 Catalyst synthesis

A series of Cs exchanged phosphotungstic acid catalysts with various Cs amounts ranging from 0.5 to 3wt.% loadings were synthesised by the ion exchanged method according to a previously reported method [8]. In a typical synthesis, for a 1 wt.% Cs loading, 0.326 g of Cs_2CO_3 (Sigma Aldrich, SA) was dissolved in 10 mL of double distilled water. This solution was added drop

wise to a solution of 5.76 g of $H_3PW_{12}O_{40}$ (Sigma Aldrich, SA) made up in 15 mL of double distilled water. The resulting mixture was centrifuged to remove the precipitate which was then washed repeatedly with double distilled water. The solid was dried at 200°C for 10 h. The prepared catalysts, $Cs_{0.5}PW_{12}O_{40}$, $Cs_{1.0}PW_{12}O_{40}$, $Cs_{2.0}PW_{12}O_{40}$ and $Cs_{3.0}PW_{12}O_{40}$ were denoted as 0.5CsPTA, 1CsPTA, 2CsPTA and 3CsPTA, respectively. In similar method, a 1 wt.% K exchanged phosphotungstic acid catalyst, denoted 1KPTA and 1 wt.% K and Cs exchanged phosphomolybdic acid catalysts, denoted 1KPMA and 1CsPMA, respectively, were synthesized.

3.2.2 Catalyst characterization

Powder X-ray diffraction patterns of selected catalysts were obtained using a Bruker D8 Advance diffractometer, equipped a Cu Ka radiation source (1.5406 Å) at 40 kV and 30 mA. The measurements were recorded in steps of 0.045° with a count time of 0.5 s in the range of 5 to 40°.

The surface area was determined using N_2 adsorption isotherms at -196°C by the multipoint BET method taking 0.162 nm^2 as its cross-sectional area. Prior to these experiments, the materials were degassed under helium flow overnight at 200°C using a Micrometrics Flow Prep 060 and all experiments were carried out at a relative pressure range (p/p°) of 0.05 to 0.9.

Infrared (IR) spectra were recorded on a Perkin Elmer Precisely equipped with a Universal ATR sampling accessory using a diamond crystal. The powdered material was placed on the crystal and a force of 120 psi was applied to ensure proper contact between the material and the crystal. The spectra were analyzed using Spectrum 100 software. Ex situ pyridine adsorbed FT-IR experiments were carried out on a Perkin Elmer ATR spectrometer at room temperature. Prior to analysis, pyridine adsorption experiments were carried out by placing a drop of pyridine on a small amount of the catalyst, followed by drying under air flow for 1 h to remove the reversibly adsorbed pyridine.

Chemical analysis of elements in the materials was examined by STEM analysis and by inductively coupled plasma-optical emission spectroscopy (ICP-OES). The surface morphology of the materials was obtained using scanning electron microscopy (SEM) utilizing

a Leo 1450 Scanning Electron Microscope. Prior to SEM analysis, the samples were mounted on aluminium stubs using double sided carbon tape and subsequently gold spluttered using the Polaron E5100 coating unit. ICP analysis was conducted using a Perkin Elmer Optical Emission Spectrometer Optima 5300 DV.

^{31}P NMR spectra of catalyst were recorded on a Bruker Advance 400 MHz spectrometer and chemical shifts were reported relative to 85% H_3PO_4 in D_2O used as an external standard at 298 K.

3.2.3 Catalytic testing

Eco-friendly esterification of acetic acid with ethanol was carried out in a 10 mL round bottom flask at room temperature. In a typical experiment, 10 mmol of acetic acid, 20 mmol of ethanol and 0.1 g of the catalyst were placed in the flask, under stirring (Scheme 1). The reaction was monitored using a Perkin Elmer Auto system gas chromatograph with a flame ionization detector (GC-FID). The catalyst was then recycled and used for the same reaction.

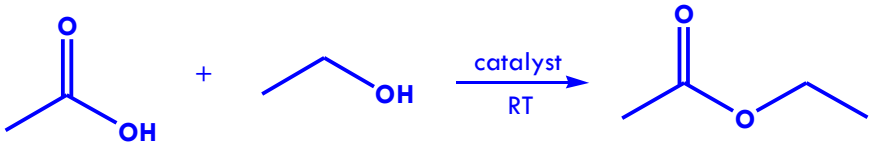

Figure 3.1 Scheme showing sterification of acetic acid to ethyl acetate over a Cs exchanged phosphotungstic acid catalyst.

3.3 Results and discussion

3.3.1 Elemental composition and surface studies

The ICP results and the BET surface area of the Cs exchanged PTA catalysts are shown in Table 3.1. The results indicate that the nominal Cs content correlates well with values obtained from ICP analysis. There was a slight decrease in the Cs content of the regenerated catalyst indicating that leaching was negligible.

Table 3.1 BET surface area, Keggin ion density and K and Cs content of HPA catalysts

Catalyst	BET surface area (m^2/g)	Cs/K content theoretical per Keggin ion (atomic %)	[a]Cs/K content practical per Keggin ion (atomic %)	Keggin anion density (HPA/nm^2)
PTA	4.5	--	--	4.5
1CsPTA	7.6	1	1.2	2.6
2CsPTA	120	2	2.2	0.16
3CsPTA	141	3	3.0	0.13
1KPTA	15	--	--	1.4
PMA	2.7	--	--	1.2
1KPMA	66	1	1.0	0.5
1CsPMA	25	1	0.9	0.12

[a]Cs/K content obtained from STEM analysis

The surface areas of the catalysts show that PTA has lower surface area compared to Cs exchanged PTA catalysts because of its highly crystalline nature, correlating well with XRD results. The Keggin ion density of pure PTA and Cs exchanged PTA were calculated according to the equation reported by Viswanadham *et al*. [5]. These results show that catalysts with higher Keggin ion density values have lower BET surface areas due to a more crystalline nature.

3.3.2 Powder X-ray diffraction

The XRD patterns of phosphotungstic acid (PTA) and Cs exchanged PTA catalysts are shown in Figure 3.2. The pure PTA shows reflections at 2θ values of 10.6º, 26.4º and 35.9º, representing the primary structure of Keggin ion. There is no change in the diffraction patterns of the Cs exchanged PTA catalysts, suggesting that the Keggin ion of the heteropolyacid is maintained with Cs incorporation. However, there is a slight shift of the characteristic reflection at 26.4° to 26.0 and 26.2° for the 0.5CsPTA and 1CsPTA catalysts, respectively. In general, the pure PTA is more crystalline than the Cs exchanged PTA catalysts.

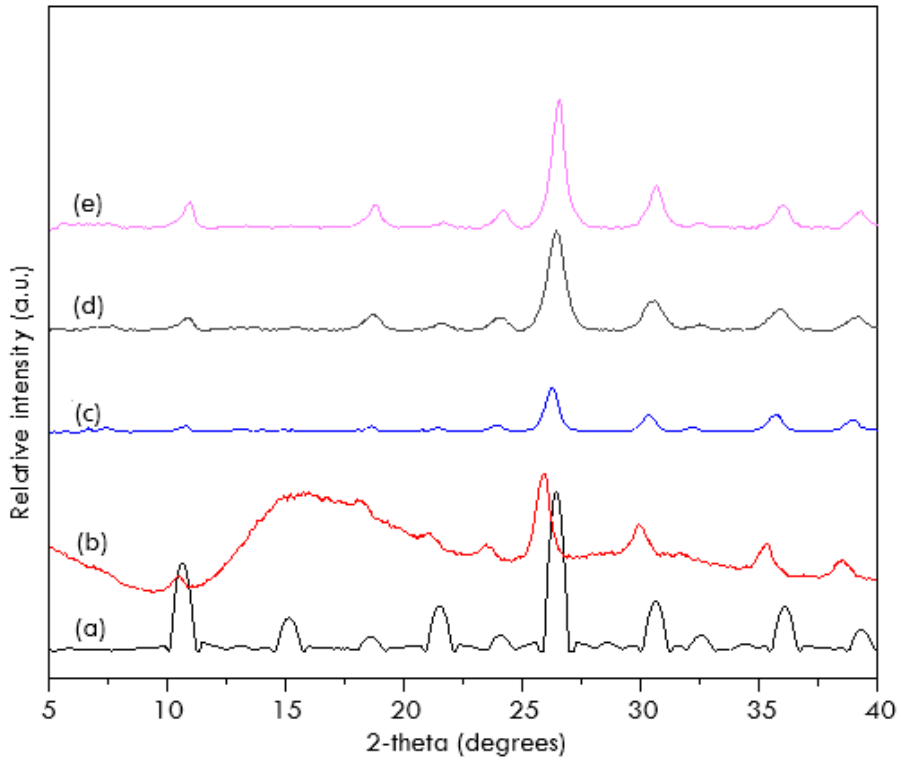

Figure 3.2 X-diffraction profiles of (a) PTA, (b) 0.5CsPTA, (c) 1CsPTA, (d) 2CsPTA and (e) 3CsPTA catalysts

3.3.3 Infrared spectroscopy

The infrared spectra of the PTA and the Cs exchanged PTA catalysts are shown in Figure 3.3. PTA exhibits four well defined characteristic IR bands at 1074, 976, 904 and 768 cm^{-1} attributed to P-O, W-O, W-O_b-W and W-O_c-W vibrations of the Keggin ion, respectively [2,3]. These characteristic bands are retained for the Cs exchanged PTA catalysts except for a slight difference in wave number of the W-O_b-W IR band, further confirming that the Keggin ion structure is not interrupted in the Cs exchanged catalysts. A similar pattern was observed for the K exchanged PTA catalyst and the K and Cs exchanged phosphomolybdic acid (PMA) catalysts (Figure 3.4).

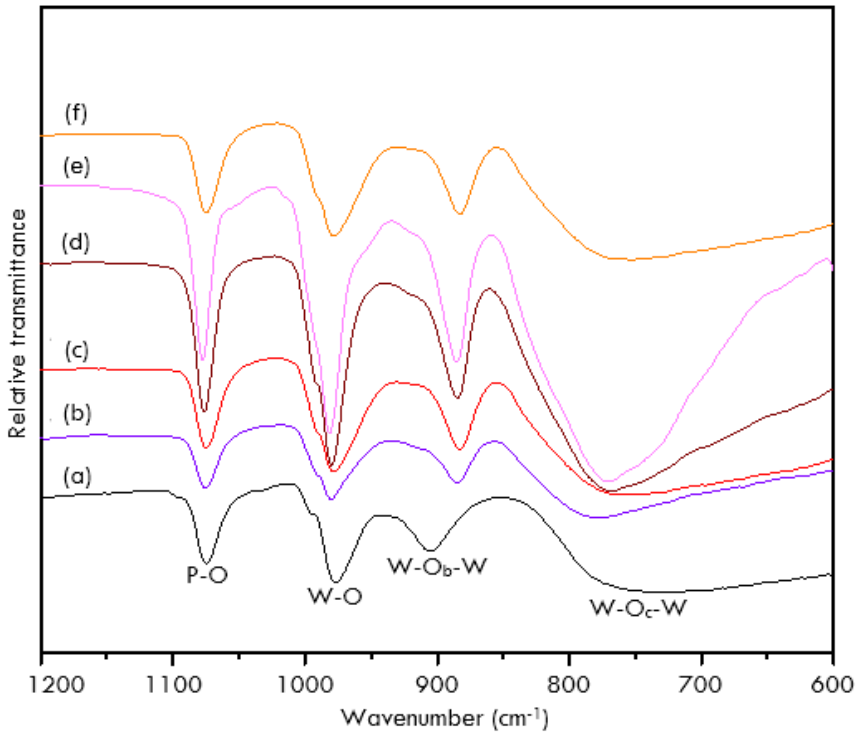

Figure 3.3 FT-IR spectra (a) PTA, (b) 0.5CsPTA, (c) 1CsPTA (d) 2CsPTA, (e) 3CsPTA and (f) regenerated 1CsPTA catalysts.

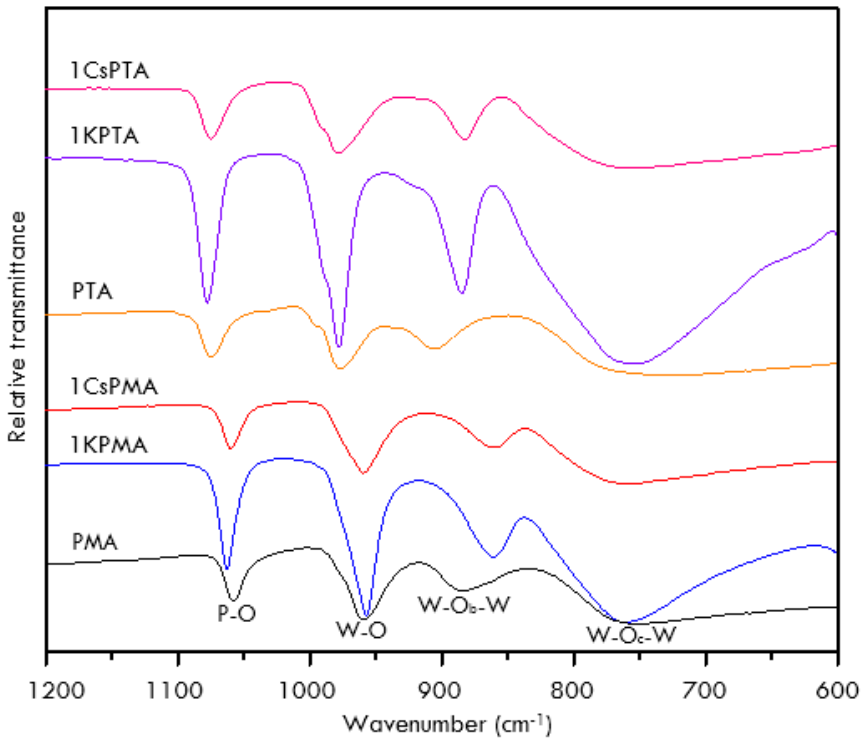

Figure 3.4 FT-IR spectra of 1 wt.% K and Cs exchanged heteropolyacid catalysts.

The Brønsted (B) and Lewis (L) acidic sites of the pure PTA and the Cs exchanged catalysts were investigated by ex situ pyridine adsorbed FT-IR spectroscopy (Figure 3.5(A)). The bands located at 1535, 1486, 1438 cm^{-1} are due to B, B+L and L acidity of the catalysts, respectively.

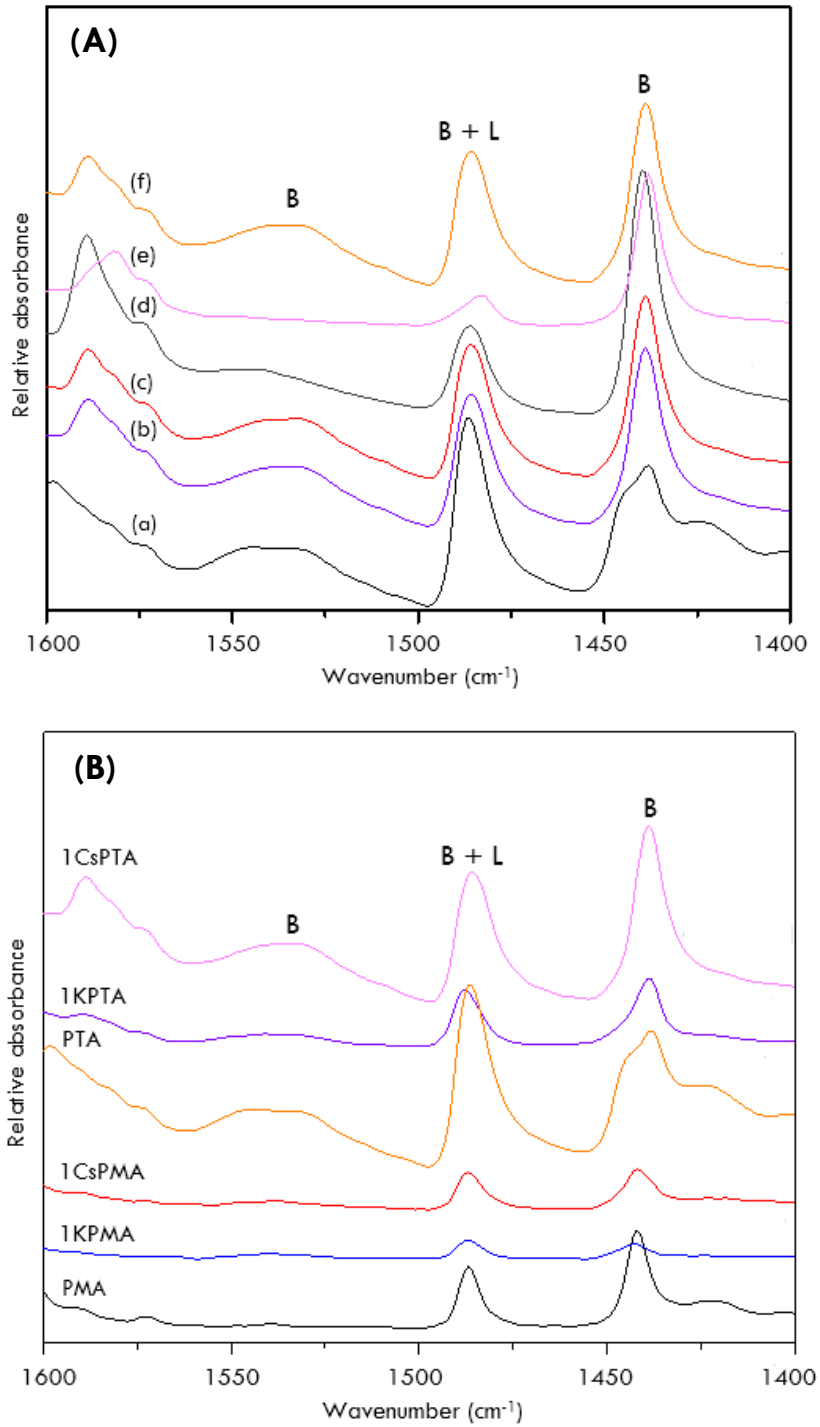

Figure 3.5 Py-FTIR spectra of (a) PTA, (b) 0.5CsPTA, (c) 1CsPTA, (d) 2CsPTA, (e) 3CsPTA and (f) regenerated 1CsPTA catalysts (A) and K and Cs exchanged heteropolyacid catalysts (B).

The results show that the strength of the acidity is quite prominent for the pure PTA and at low loadings of Cs due to a combination of strong B and L sites. The acidic strength diminishes gradually as the content of Cs is increased.

Comparing the Cs exchanged PTA catalysts with other alkali metal exchanged heteropolyacid catalysts, the pure PTA has more B/L acidic sites compared to the pure PMA catalyst due to PTA having stronger B acidity than the PMA catalyst. Cs exchanged PTA catalysts displayed a higher B/L ratio than the K exchanged PTA catalyst (Figure 3.5(B)).

3.3.4 ^{31}P NMR spectroscopy

The ^{31}P NMR spectra of pure PTA and Cs exchanged PTA catalysts were recorded and the results are shown in Figure C3.1 (Appendix C). The spectra show that PTA has a single peak at -15.2 ppm, whereas the Cs exchanged PTA catalysts with lower Cs loadings (0.5 and 1 wt.%) show two peaks, at -15.3 and -15.1 ppm. However, at higher Cs loadings the above peaks are not observed. These results show the slightly soluble nature of the Keggin ion of PTA at lower Cs loadings. This is also strong evidence that at higher Cs loadings, the catalyst is more water tolerant than the Cs exchanged catalysts with lower loadings. A similar behaviour is observed with the Cs exchanged PMA and the K exchanged PTA and PMA catalysts.

3.3.5 Electron microscopy

The morphology of PTA and the synthesised CsPTA catalysts were studied and the images are shown in Figure C3.2 (Appendix C). After the exchange of protons with Cs in PTA, the catalysts showed a more defined spherical morphology. BF-STEM analysis of the fresh and regenerated catalyst was carried out to map the relative spatial distribution of the elements present in the synthesised catalysts and to approximate the Cs content present in the Keggin ion of the PTA catalysts (Table 3.1, Figure 3.6 and Figure C3.3, Appendix C). There was a correlation of the theoretical Cs loading with that obtained from BF-STEM analysis.

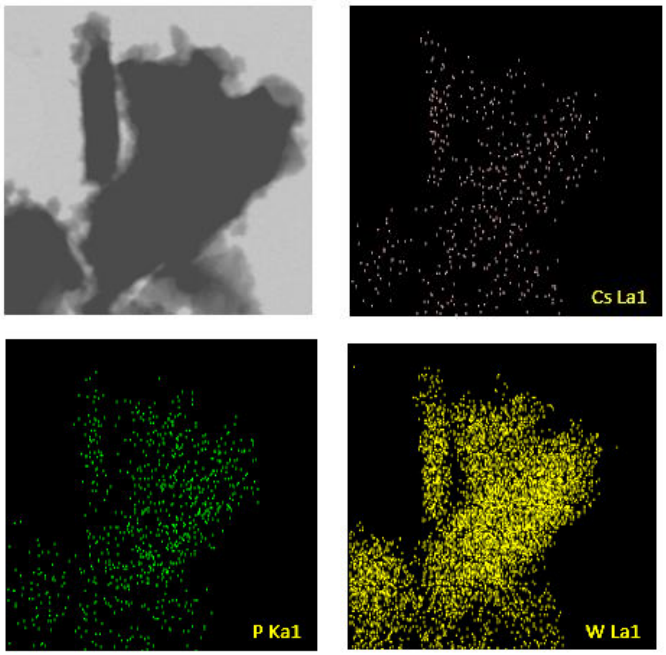

Figure 3.6 BF-STEM analysis of the 1CsPTA catalyst.

3.3.6 Catalytic esterification reaction studies

Blank studies, carried out under conditions similar to the catalytic reactions showed a 2% yield towards ethyl acetate. Results of the catalytic synthesis of ethyl acetate over Cs exchanged PTA catalysts under atmospheric pressure and at room temperature are given in Table 3.2.

Table 3.2 Catalytic results over Cs exchanged phosphotungstic acid catalysts[a]

Catalyst	Conversion (%)	Ethyl acetate yield (%)	TON
Blank	2	2	---
PTA	78	78	128
0.5CsPTA	74	74	121
1CsPTA	72	72	118
2CsPTA	40	40	66
3CsPTA	5	5	8
1KPTA	61	61	100
PMA	57	57	93
1KPMA	46	46	75
1CsPMA	53	53	87

[a]Reaction conditions: 10 mmol (acetic acid), 20 mmol (ethanol), catalyst = 0.1 g, Reaction temperature = RT; TON= number of moles of product/number of moles of catalyst

The bare phosphotungstic acid catalyst gave a 78% yield, whereas the Cs exchanged PTA catalysts with 0.5 and 1 wt.% loadings gave yields of 74 and 72 %, respectively. The slight decrease in the yield for the Cs exchanged PTA catalysts when compared to the bulk PTA catalyst was attributed to a decrease in acidity of these catalysts due to the exchange of the acidic protons in the PTA with Cs. However, the major advantage of incorporating Cs is to obtain a more heterogeneous catalyst. The significant drop in ethyl acetate yield at higher Cs loadings is mainly due to a significant decrease in the Brønsted acidity of the catalysts.

The catalytic performance is also explained in terms of Keggin ion density and it is observed that a higher density of the Keggin ion results in improved catalytic activity. This is reflected in the lower Cs exchanged catalysts which have higher Keggin ion densities, leading to higher activity towards ethyl acetate. The reaction was also performed over phosphomolybdic acid (PMA) and metal exchanged PMA catalysts (Table 2). Result show that the Cs exchanged heteropolyacid catalysts performed better than the K exchanged catalysts, attributed to a greater acidic nature of the Cs exchanged catalysts (Figure 3.4).

Further studies were conducted using different mole ratios of reactants over the 1CsPTA catalyst and these results are tabulated in Table 3.3. It can be seen that a 1:2 mole ratio of acetic acid to ethanol gives the best activity towards ethyl acetate, compared to a decrease in the mole ratios, where ethanol is in excess resulting in dilution of the feedstock which impacts the activity considerably.

Table 3.3 Catalytic results of various mole ratios of reactants over the1CsPTA catalyst[a]

Mole ratio (acetic acid/ethanol)	Acetic acid conversion (%)	Ethyl acetate yield (%)
1:1	60	60
1:2	72	72
1:3	63	63
1:4	59	59
1:8	57	57
1:10	55	55

[a]Reaction conditions: 10 mmol (acetic acid), 10-40 mmol (ethanol), catalyst = 0.1 g, Reaction temperature = RT

Varying the amounts of the catalyst also has an influence on the formation of ethyl acetate (Table 3.4). The ethyl acetate yield was 55% when 0.05 g of catalyst was used. This yield increased significantly to about 72% on doubling the amount of catalyst. However, there was no significant increase in the yields with further increase in the amount of catalyst. The time on stream studies show an increase in acetic acid conversion with increase in time which reaches its maximum of 84% after 48 h at room temperature (Table 3.5).

Table 3.4 Catalytic results of various amounts of CsPTA-1 catalysts[a]

Catalyst amount (g)	Acetic acid conversion (%)	Ethyl acetate yield (%)
0.05	55	55
0.1	72	72
0.2	73	73
0.3	75	75

[a]Reaction conditions: 10 mmol (Acetic acid), 20 mmol (ethanol), Catalyst= 0.1 g, Reaction temperature = RT

Table 3.5 Catalytic results of TOS over 1CsPTA catalyst[a]

Reaction time (h)	Acetic acid conversion (%)	Ethyl acetate yield (%)
6	21	21
12	39	39
18	58	58
24	72	72
30	74	74
40	79	79
48	84	84
50	84	84
55	84	84
60	84	84
65	84	84
70	84	84

[a]Reaction conditions: 10 mmol (acetic acid), 20 mmol (ethanol), catalyst = 0.1 g, Reaction temperature = RT

The esterification of acetic acid reaction with other alcohols was also studied and the results are tabulated in Table 3.6. These findings indicate that increasing the carbon chain length of the alcohol leads to a decrease in the yield of the ester.

Table 3.6 Catalytic results of esterification with various alcohols over CsPTA-1 catalysts[a]

Alcohol	Acetic acid conversion (%)	Ester yield (%)
methanol	76	76
ethanol	72	72
butanol	65	65
hexanol	52	52
benzyl alcohol	63	63

[a]Reaction conditions: 10 mmol (acetic acid), 20 mmol (alcohol), catalyst = 0.1 g, Reaction temperature = RT

We also studied recycling of the optimized catalyst under the same reaction conditions and the results are shown in Figure 3.7.

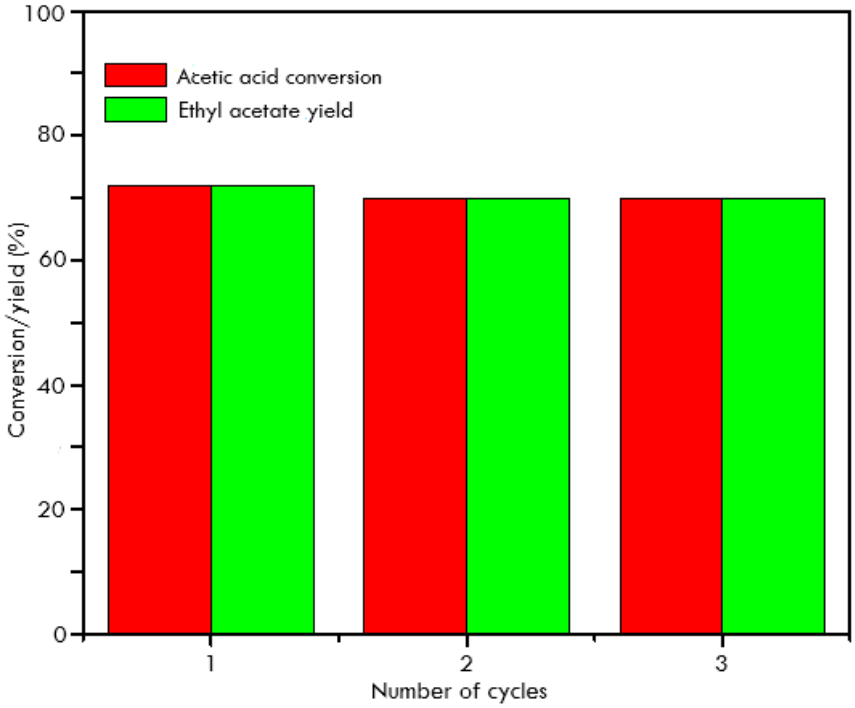

Figure 3.7 Catalytic results over recycled 1CsPTA catalyst.

Before the recycling reactions, the white solid catalyst was separated from the reaction mixture, then dried and calcined at 200ºC for 12 h. Thereafter, the calcined catalyst was characterized by FT-IR and Py-FTIR spectroscopy to identify the structural and acidity functionalities of recycled catalyst. The FT-IR spectra (Figure 3.2) show no changes in the Keggin ion structure of the recycled 1CsPTA catalyst, while the Py-FTIR spectra exhibits very minimal change in acidity of the material (Figure 3.3). The catalytic results (Figure 3.7)

indicate only a slight drop in the conversion towards ethyl acetate synthesis after 3 cycles, likely due to mechanical loss of the catalyst.

3.4 Conclusion

Pyridine-FTIR showed that the incorporation of an alkali metal into the HPAs decreased the acidity and this directly influenced the efficiency of the esterification reaction. XRD and IR results confirmed the retention of the Keggin ion structure of the HPA after exchange of the protons with the metal. The Cs exchanged HPA catalysts were tolerant to the presence of water produced during esterification compared to both the pure PTA and PMA catalysts as shown by ^{31}P NMR spectroscopy. In general, the Cs exchanged PTA catalysts showed better performance in ethyl acetate formation than the other catalysts and this is related to these catalysts possessing more Brønsted and Lewis acid sites. The 1CsPTA maintained its structure, acidity and performance when subjected to recycling.

References

[1] I.V. Kozhevnikov, Chem. Rev. 98**,** 171(1998)

[2] N. Mizuno, M. Misono, Chem. Rev. 98, 199 (1998)

[3] B. Viswanadham, P. Jhansi, K.V.R. Chary, H.B. Friedrich, S. Singh, Catal. Lett. 146, 364 (2016)

[4] B. Viswanadham, J. Pedada, H.B. Friedrich, S. Singh, Catal. Lett. 146, 1470 (2016)

[5] B. Viswanadham, V.P. Kumar, K.V.R. Chary, Catal. Lett. 144, 744 (2014)

[6] B. Viswanadham, A. Srikanth, K.V.R. Chary, J. Chem. Sci. 126, 445 (2014)

[7] B. Viswanadham, A. Srikanth, V.P. Kumar, K.V.R. Chary, J. Nanosci. Nanotech. 15, 5391 (2015)

[8] V. Balaga, J. Pedada, H.B. Friedrich, S. Singh, J. Mol. Catal. A: Chem. 425, 116 (2016)

[9] W. Shi, J. Zhao, X. Yuan, S. Wang, X. Wang, M. Huo, Chem. Eng. Technol. 35**,** 347 (2012)

[10] M.N. Timofeeva, Appl. Catal. A: Gen. 256, 19 (2003)

[11] T. Okuhara, Chem. Rev. 102, 3641 (2002)

[12] M. Tao, L. Xue, Z. Sun, S. Wang, X. Wang, J. Shi, Sci. Report 5**,** 13764 (2015)

[13] M. Misono, Catal. Today 144**,** 285 (2009)

[14] J. Cao, B. Qi, J. Liu, Y. Shang, H. Liu, W. Wang, J. Lu, Z. Chen, H. Zhang, X. Zhou, RSC. Adv. 6, 21612 (2016)

[15] L. Gang, L. Xinzong, W. Eli, New. J. Chem. 31**,** 348 (2007)

[16] D. Jiang, Y.Y. Wang, L.Y. Dai, React. Kinet. Catal. Lett. 93, 257 (2008)

[17] S.T. Fardood, A. Ramazani, S. Moradi, Chem. J. Mold. 12, 115 (2017)

[18] S.T. Fardood, A. Ramazani, S. Moradi, J. Sol-Gel. Sci. Technol. 82, 432 (2017)

[19] S.T. Fardood, Z. Golfar, A. Ramazani, J. Mater. Sci: Mater. Electron. 28, 17002 (2017)

[20] S.T. Fardood, A. Ramazani, S. Moradi, P.A. Asiabi, J. Mater. Sci: Mater. Electron. 28, 13596 (2017)

[21] A. Ramazani, P.A. Asiabi, H. Aghahosseini, F. Gouranlou, Curr. Org. Chem. 21, 908 (2017)

[22] H.J. Eom, D.W. Lee, S. Kim, S.H. Chung, Y.G. Hur, K.Y. Lee, Fuel 126**,** 263 (2014)

[23] N.R. Shiju, H.M. Williams, D.R. Brown, Appl. Catal. B: Env. 90**,** 451 (2009)

[24] A. Srikanth, B. Viswanadham, V.P. Kumar, N.R. Anipindi, K.V.R. Chary, Appl. Petrochem. Res. 6, 145 (2016)

[25] T. Okuhara, H. Watanabe, T. Nishimura, K. Inumaru, M. Misono, Chem. Mater. 12**,** 2230 (2000)

[26] J. Kaur, I.V. Kozhevnikov, Chem. Comm. 2508 (2002)

[27] M. Srinivas, G. Raveendra, G. Parameswaram, P.S.S. Prasad, N. Lingaiah, J. Mol. Catal. A: Chem. 413**,** 7 (2016)

[28] J.A. Dias, E. Caliman, S.C.L. Dias, Micro. Meso. Mater. 76, 221 (2004)

[29] Y. Izumi, M. Ogawa, K. Urabe, Appl. Catal. A: Gen. 132, 127 (1995)

[30] L. Pesaresi, D.R. Brown, A.F. Lee, J.M. Montero, H. Williams, K. Wilson Appl. Catal. A: Gen 360, 50 (2009)

[31] S.S. Kale, U. Armbruster, R. Eckelt, U. Bentrup, S.B. Umbarkar, M.K. Dongare, A. Martin, Appl. Catal. A: Gen. 527, 9 (2016)

[32] K. Narasimharao, D.R. Brown, A.F. Lee, A.D. Newman, P.F. Siril, S.J. Tavener, K. Wilson, J. Catal. 248, 226 (2007)

[33] H.W. Park, S. Park, D.R. Park, J.H. Choi, I.K. Song, Catal. Comm. 12, 1 (2010)

[34] L. Matachowski, A. Zieba, M. Zembala, A. Drelinkiewicz, Catal. Lett. 133, 49 (2009)

[35] N. Essayem, G. Coudurier, M. Fournier, J.C. Vedrine, Catal. Lett. 34, 223 (1995)

CHAPTER FOUR

THE ROLE OF ALKALI METAL EXCHANGED PHOSPHOMOLYBDIC ACID CATALYSTS IN THE SOLVENT FREE OXIDATION OF STYRENE TO BENZALDEHYDE AT ROOM TEMPERATURE

Abstract

A series of alkali metal exchanged phosphomolybdic acid catalysts were synthesized by ion exchange, characterized by various physico-chemical techniques and used in the solvent free oxidation of styrene to benzaldehyde. XRD and infrared results showed that the primary structure of the Keggin ion usually present in phosphomolybdic acid is retained after metal exchange. HR-TEM analysis show a well-constructed spherical morphology of the materials with a lower degree of crystalinity. Type IV isotherms with mesoporous structure are observed from nitrogen adsorption-desorption isotherm studies and ex situ pyridine adsorption experiments reveal that Brønsted acidic sites increased after metal exchange. The K exchanged phosphomolybdic acid catalysts were most efficient in the conversion of styrene to benzaldehyde and the order of reactivity of the alkali metal exchanged phosphomolybdic acid catalysts was K > Rb > Cs. Insight into the reaction pathway by investigating the oxidation styrene oxide was obtained. The results show that phenyl acetaldehyde together with benzaldehyde are produced, providing some evidence that styrene oxidation proceeds via C=C cleavage to selectively produce benzaldehyde. The catalyst was easily recovered and was reused for up to three cycles showing stable activity.

Keywords: oxidation, styrene, benzaldehyde, alkali metal-PMA, acidity

4.1 Introduction

Solvent free oxidation of styrene to the benzaldehyde and styrene oxide has shown great importance in basic and applied research due to its extensive applications in industrial chemical processes and also in academia. Benzaldehyde is the versatile aromatic carbonyl compound used in perfumery, cosmetics and agrochemical industries, while styrene oxide is used a starting material in the manufacture of epoxy resin, absorbents and flavoring agents [1, 2]. The oxidation of styrene was initially carried out using homogeneous catalysts containing components such as permanganates, chromates and hypochlorites. In addition to these formulations being toxic, poor selectivity was obtained in all reactions and the inherent use of solvents is a disadvantage with regards to environmental concerns [3].

Transition metal complexes have been used as catalysts. Although reasonable activities were obtained, a major drawback was recyclability and problems associated with separation of the product stream [4, 5]. As a result, extensive research into more viable and environmentally friendly catalysts for these type of reactions has been undertaken. Among these are the metal oxide systems, metal complex systems and solid acid catalysts [5-13].

Solid heteropolyacid (HPA) catalysts are recognized one of the more efficient catalytic systems for styrene oxidation, due to their tunable acidic and oxidation functionalities and they are also environmentally friendly and recyclable [14-29]. It has also been established that metal containing heteropolyacids produce excellent results for the oxidation of styrene [6-13]. The research has been focused on metals such as Mn, Co and Ni. On further investigation, it has been found that the catalytic properties can be greatly tuned by considering the use of alkali metals and recently there has been a growing interest in the study of alkali metals such K, Rb and Cs containing materials as catalysts in various catalytic transformations [30-44]. Pure heteropolyacid catalysts shows low yields of benzaldehyde during styrene oxidation, probably due to its low surface area. However when protons are exchanged with alkali metal species such as K, Rb and Cs into the Keggin ion of heteropolyacids, an improvement in the surface area is achieved, also altering the acidity is accomplished to the benefit of the oxidation reaction.

Recently, the oxidation of toluene over Cs exchanged phosphomolybdic acid (PMA) catalysts was reported. In this study, it was clear that the acidity and mesoporous nature of catalysts influenced the activity as well as the selectivity [21] (Appendix B). The oxidation of styrene was studied using oxidants such as air, H_2O_2 and TBHP [5-13]. Of the oxidants employed, TBHP showed the highest selectivity towards the desired product although there was moderate conversion of the substrate [45].

In the present work, the liquid phase solvent free oxidation of styrene to benzaldehyde was studied over alkali metal exchanged heteropolyacid catalysts to assess the effect of the different alkali metals.

4.2 Experimental

4.2.1 Catalyst synthesis

A series of alkali metal exchanged phosphomolybdic acid catalysts with different metal loadings, ranging from 1 to 3 wt% were synthesized by ion exchange according to a method reported previously [21]. In a typical synthesis, for a 1 wt% K loading, 0.138 g of K_2CO_3 (Sigma Aldrich, SA) was dissolved in 10 mL of double distilled water. This solution was added drop wise to a solution of 3.65 g of $H_3PMo_{12}O_{40}$ (Sigma Aldrich, SA) made up in 15 mL of double distilled water. The resulting mixture was centrifuged to remove the precipitate which was then washed repeatedly with double distilled water. The solid was dried at 200°C for 10 h. This catalyst with the theoretical formula, $K_{1.0}PMo_{12}O_{40}$, was denoted as 1KPMA. The other catalysts were prepared using the method described and were denoted in a similar manner to 1KPMA.

4.2.2 Catalyst characterization

Powder X-ray diffraction patterns of samples were obtained with a Bruker D8 Advance diffractometer, using a Cu Ka radiation source (1.5406Å) at 40 kV and 30 mA. The measurements were recorded in steps of 0.045° with a count time of 0.5 s in the range of 5-40°.

The surface area of catalysts was estimated using N_2 adsorption isotherms at -196°C by the multipoint BET method taking 0.162 nm^2 as its cross-sectional area. The pore size distribution was measured by N_2 adsorption-desorption isotherms using a Micrometrics ASAP 2020 multi-point BET surface area analyzer. Prior to N_2 gas sorption experiments, the materials were degassed under helium flow overnight at 200°C using a Micrometrics Flow Prep 060 to remove adsorbed moisture or impurities from surface of the catalyst. The experiments were carried over a p/p_o pressure range of 0.05 to 0.9 by using nitrogen adsorption-desorption method. The surface area was calculated from adsorption isotherm points at relative nitrogen pressures (p/p_o) between 0.05 and 0.3, while the pore size was calculated by BJH method.

Infrared (IR) spectra were recorded on a Perkin Elmer Precisely equipped with a Universal ATR sampling accessory using a diamond crystal. All spectra generated were analyzed using Spectrum 100 software. Ex-situ pyridine adsorbed infrared experiments were carried out by placing a drop of pyridine on a small amount of the catalyst, followed by evacuation in air for 1 h to remove the reversibly adsorbed pyridine and the spectra were recorded on a PerkinElmer ATR spectrometer at room temperature..

The surface morphology of the materials was obtained using scanning electron microscopy (SEM), utilizing a Leo 1450 Scanning Electron Microscope. Prior to SEM analysis, the samples were mounted on aluminium stubs using double sided carbon tape and subsequently gold spluttered using the Polaron E5100 coating unit.

Transmission electron microscopy (TEM) images were obtained on a Jeol JEM-1010 electron microscope. The images were captured and analyzed using iTEM software. Distribution and chemical analysis of elements in the materials was examined by STEM analysis.

4.2.3 Catalytic testing

Solvent free styrene oxidation experiments were conducted in a 50 mL round bottom flask at room temperature. In a typical run, 10 mmol of styrene, 10 mmol of the oxidant and 0.1g of the catalyst were placed in the flask, under stirring at room temperature and the reaction was constantly

monitored by GC. The overall reaction is shown in Figure 4.1. At the end of the reaction, the catalyst was removed, dried in an oven set at 200°C and used for the same reaction.

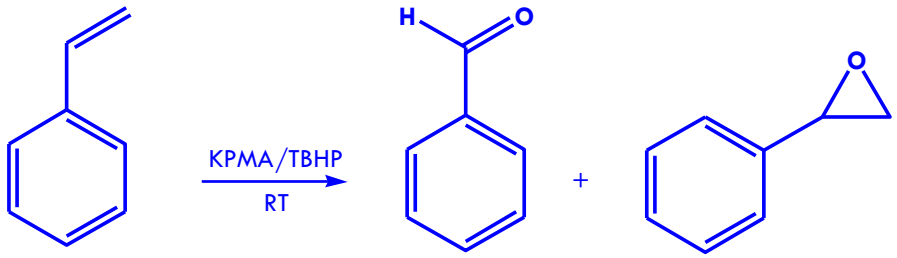

Figure 4.1 Reaction scheme showing oxidation of styrene over a potassium metal exchanged heteropolyacid catalyst.

4.3 Results and discussion

4.3.1 Catalyst characterization

4.3.1.1 X-ray diffraction

X-ray diffraction patterns of the pure PMA and the K exchanged PMA catalysts are shown in Figure 4.2. Pure PMA shows the triclinic structure, whereas the cubic structure of the Keggin ion is observed for the K exchanged materials [21]. Sharp diffraction patterns were observed in the K exchanged PMA catalysts compared to pure PMA, revealing a more crystalline nature of the Keggin ion [21].

The XRD diffractograms of the 2 wt% loadings of K, Rb and Cs exchanged PMA catalysts, together with the pure PMA are shown in Figure 4.3. Similar profiles exhibited by the Rb and Cs exchanged catalysts to the K are observed and there is every indication that the Keggin ion is present.

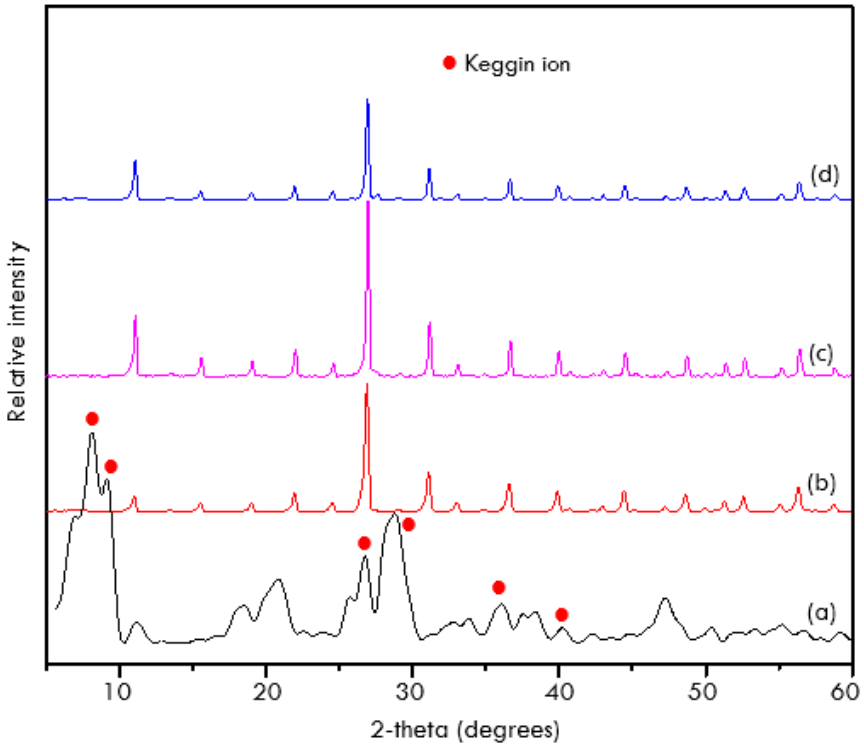

Figure 4.2 X-ray diffraction patterns of (a) PMA, (b) 1KPMA, (c) 2KPMA and (d) 3KPMA catalysts.

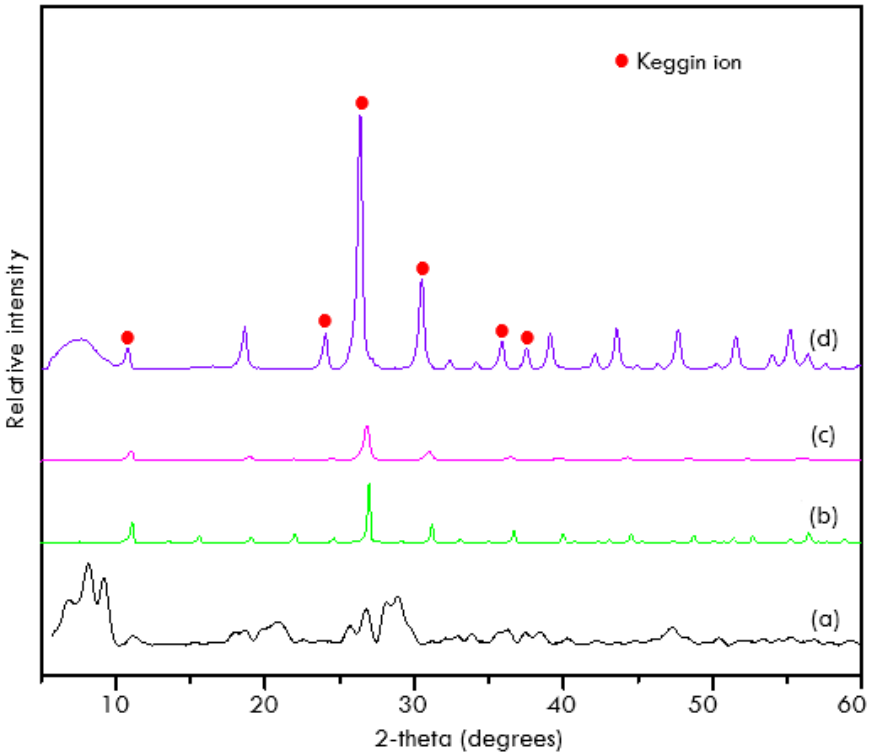

Figure 4.3 X-ray diffraction patterns of (a) PMA, (b) 2KPMA, (c) 2RbPMA and (d) 2CsPMA catalysts

4.3.1.2 Infrared spectroscopy

Infrared spectra of pure PMA and the modified KPMA catalysts show four well defined characteristic IR bands in the 500-1200 cm^{-1} region (Figure 4.4). These IR bands, in the case of pure PMA at 760, 889, 961 and 1058 cm^{-1} are assigned to Mo-O_c-Mo, Mo-O_t-Mo, Mo=O and P-O bands, respectively [21]. In the modified catalysts, slight shifts in these bands are observed, probably implying exchange of the proton by the metal [21]. This was also true for the Rb and Cs exchanged catalysts as shown in Figure C4.1, Appendix C.

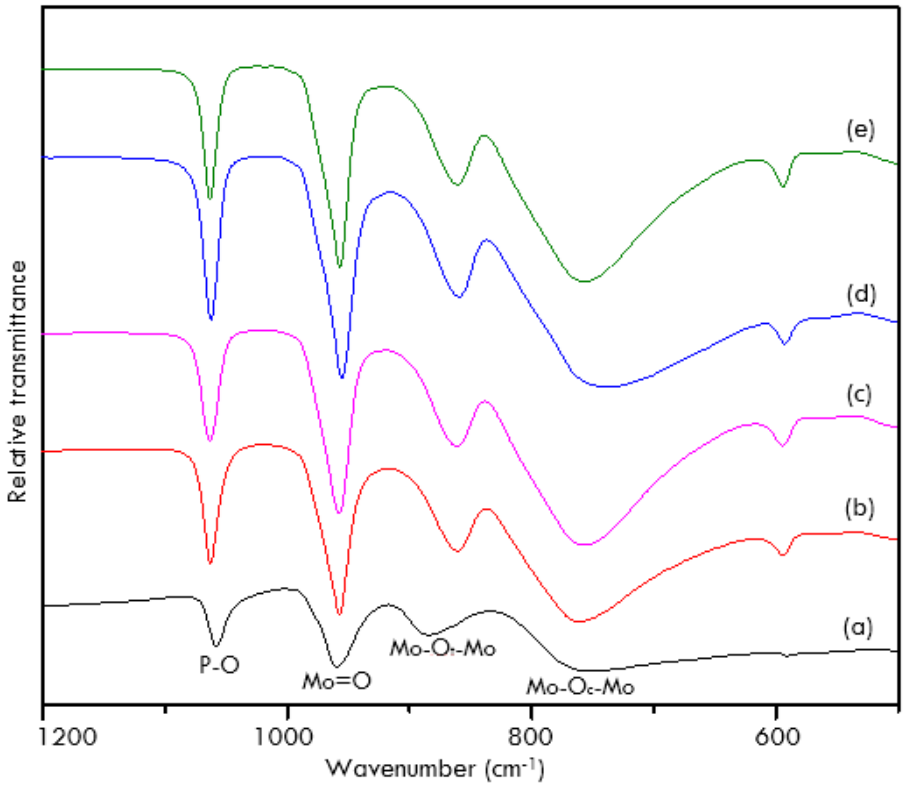

Figure 4.4 IR spectra of (a) PMA, (b) 1KPMA, (c) 2KPMA, (d) 3KPMA and (e) regenerated 2KPMA catalysts.

The nature of acidic sites were examined by ex-situ pyridine adsorbed IR spectroscopy (1600-1400 cm^{-1}). The spectra of the parent PMA and K exchanged PMA catalysts are shown Figure 4.5. The bands at 1539, 1487 and 1442 cm^{-1} are attributed to Brønsted (B), Brønsted and Lewis (B + L) and Lewis (L) acidic sites, respectively [21]. The parent PMA contained more L acid sites that B acid sites. The Brønsted acidity increased when metal was incorporated and B acidity increase

further with an increase in K loadings, but reached a maximum for the 2KPMA, thereafter showed a slight decrease for 3KPMA where Lewis acidity was dominant. The acidity of the Rb and Cs exchanged PMA-2 catalysts was also determined and compared with 2KPMA (Figure C4.2, Appendix C). 2KPMA contained more B acidic sites than both the 2RbPMA and 2CsPMA catalysts.

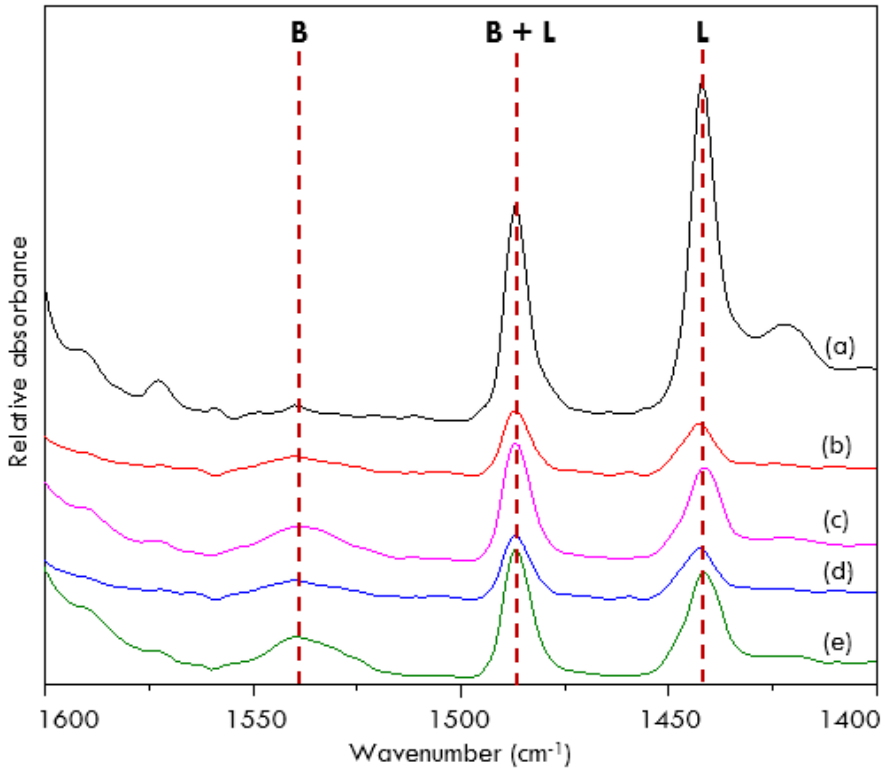

Figure 4.5 Pyridine infrared spectra of (a) PMA, (b) 1KPMA, (c) 2KPMA, (d) 3KPMA and (e) regenerated 2KPMA catalysts.

4.3.1.3 Surface studies

Surface properties of the catalysts such as surface area, pore volume and pore size of parent PMA and K-PMA catalysts were determined. The BET surface area of the catalysts increased with an increase in the metal loadings. However, this trend changed for all the catalysts with a loading of 3 wt% which showed a decrease in the surface area (Table 4.1). From the adsorption isotherms for PMA and the K exchanged catalysts, type IV isotherms with hysteresis loops were obtained which

indicated presence of mesoporous materials (Figure C4.3, Appendix C). The high surface area 2KPMA which implies a lower Keggin anion density and this is reflected by lower crystalinity of the Keggin ion units obtained compared to other loadings. This result correlates well with the X-ray diffraction studies.

Table 4.1 Elemental content and surface study data of PMA and metal exchanged catalysts.

Catalyst	Surface area (m^2/g)	Pore volume (cm^3/g)	Pore diameter (Å)	Metal content Calc. (wt%)	Metal content Expt. (wt%)[a]	Metal content Expt. (wt%)[b]	Keggin ion density (HPA/nm^2)
PMA	2.7	0.01	128	0	--	--	1.20
KPMA-1	66	0.02	81	1.0	1.1	0.9	0.0489
KPMA-2	133	0.05	46	2.0	2.0	1.8	0.0238
KPMA-3	101	0.03	43	3.0	3.0	2.7	0.0307
RbPMA-1	28	0.04	89	1.0	--	0.92	0.1126
RbPMA-2	181	0.07	40	2.0	1.9	1.89	0.0166
RbPMA-3	115	0.09	60	3.0	2.8	2.8	0.0252
CsPMA-1	25	0.03	80	1.0	0.9	0.95	0.1231
CsPMA-2	146	0.14	40	2.0	2.1	1.92	0.0197
CsPMA-3	80	0.08	50	3.0	2.9	3.0	0.0338

[a] Metal content obtained from STEM analysis. [b] Metal content obtained from flame photometry and ICP analysis

Comparing the isotherms of PMA and 2KPMA with its Rb and Cs counterparts (Figure 4.6, Table 4.1), it can be seen clearly that all the materials possess mesoporous character in keeping with their type IV isotherms.

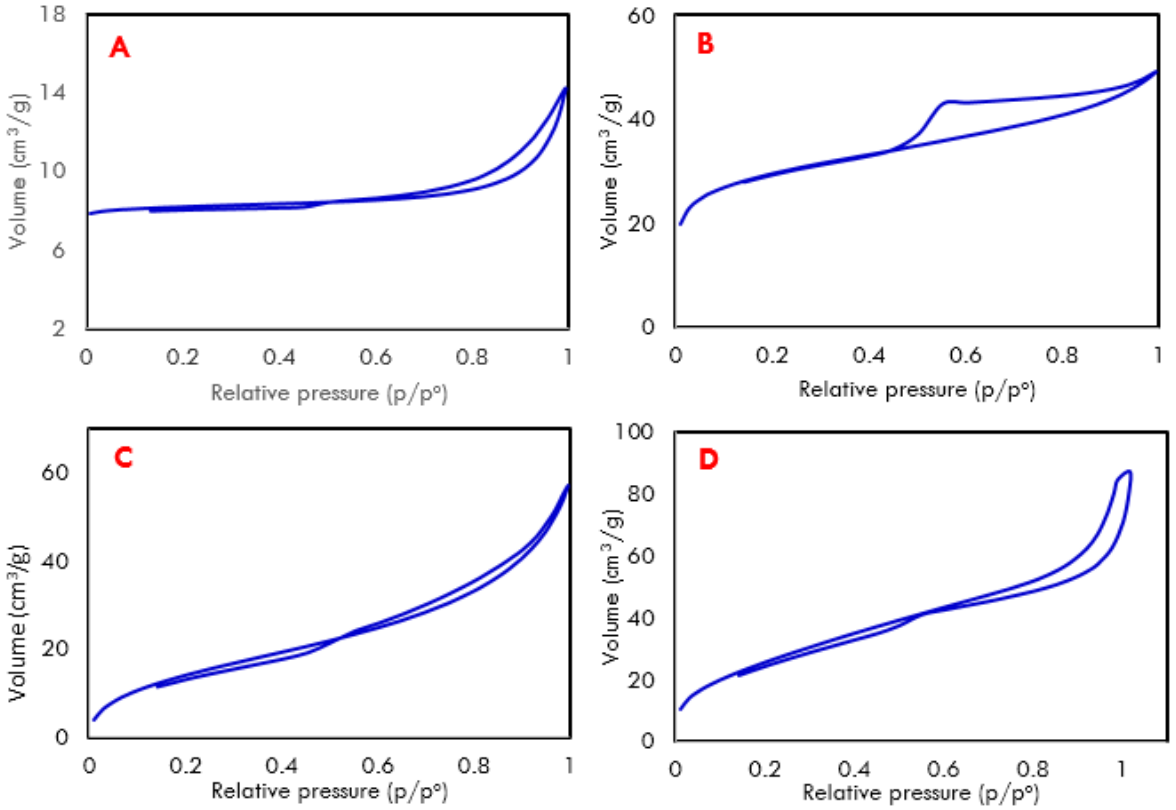

Figure 4.6 N_2 isotherms of (A) PMA, (B) 2KPMA, (C) 2RbPMA and (D) 2CsPMA catalysts.

4.3.1.4 Electron microscopy

The surface morphology of PMA and metal exchanged PMA catalysts are shown in Figure 4.7. The PMA shows bulk like morphology, whereas the metal exchanged catalysts exhibited a well-defined spherical morphology. From HR-TEM images, the metal exchanged catalysts display well defined particles with sizes ranging from 300 to 450 Å, whereas for the PMA, particles varied between 18000 to 20000 Å.

BF-STEM analysis of the metal exchanged PMA catalysts was carried out to map the structure and relative spatial distribution of the elements. Examples of some of these analyses for the K exchanged catalysts are shown in Figure 4.8. In general, the metal content in the Keggin anion matches theoretical loadings (Table 4.1). These results are reinforced with data obtained by flame photometry and ICP analysis.

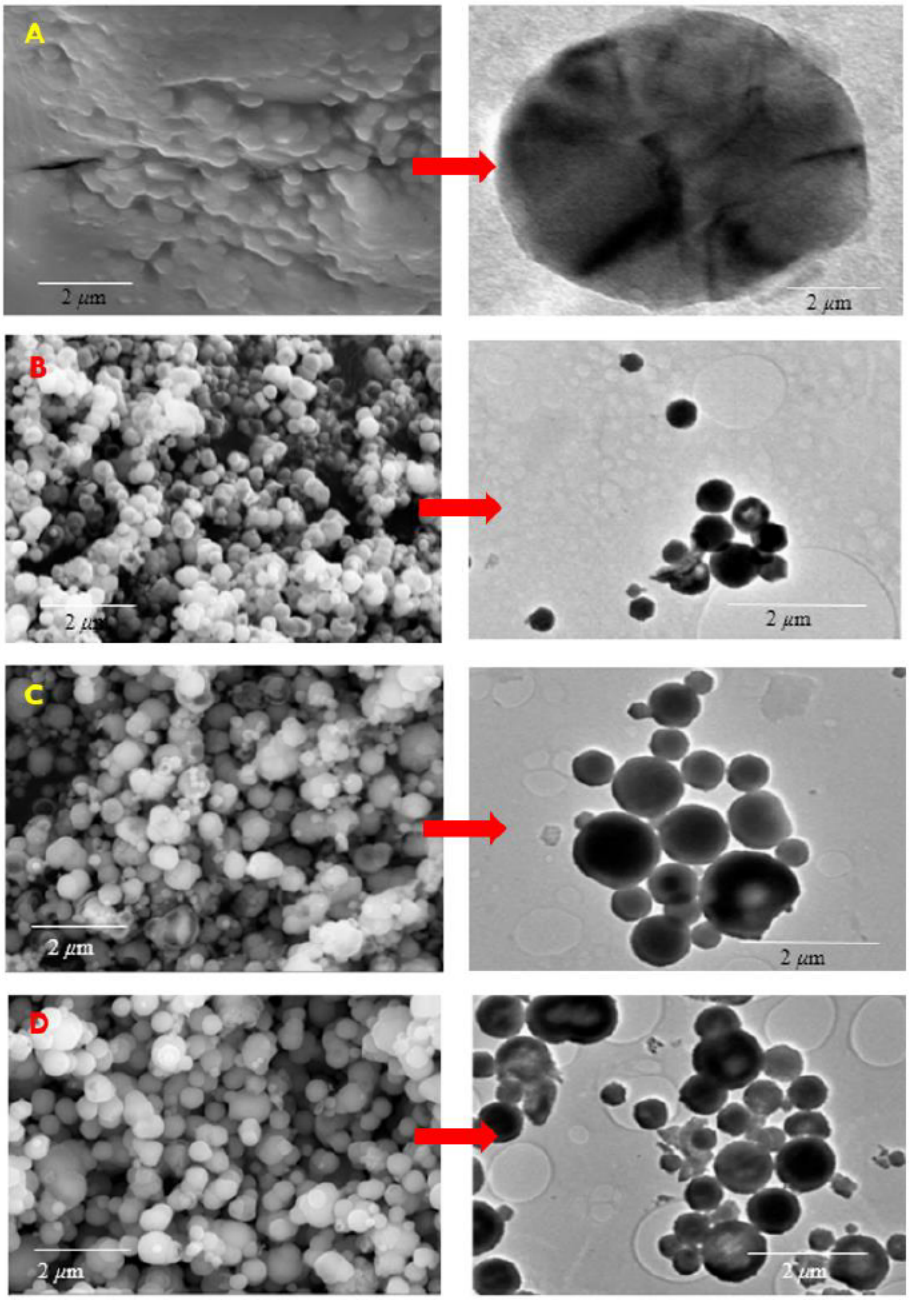

Figure 4.7 SEM and HR-TEM images of (A) PMA, (B) 2KPMA, (C) 2RbPMA and (D) 2CsPMA, respectively.

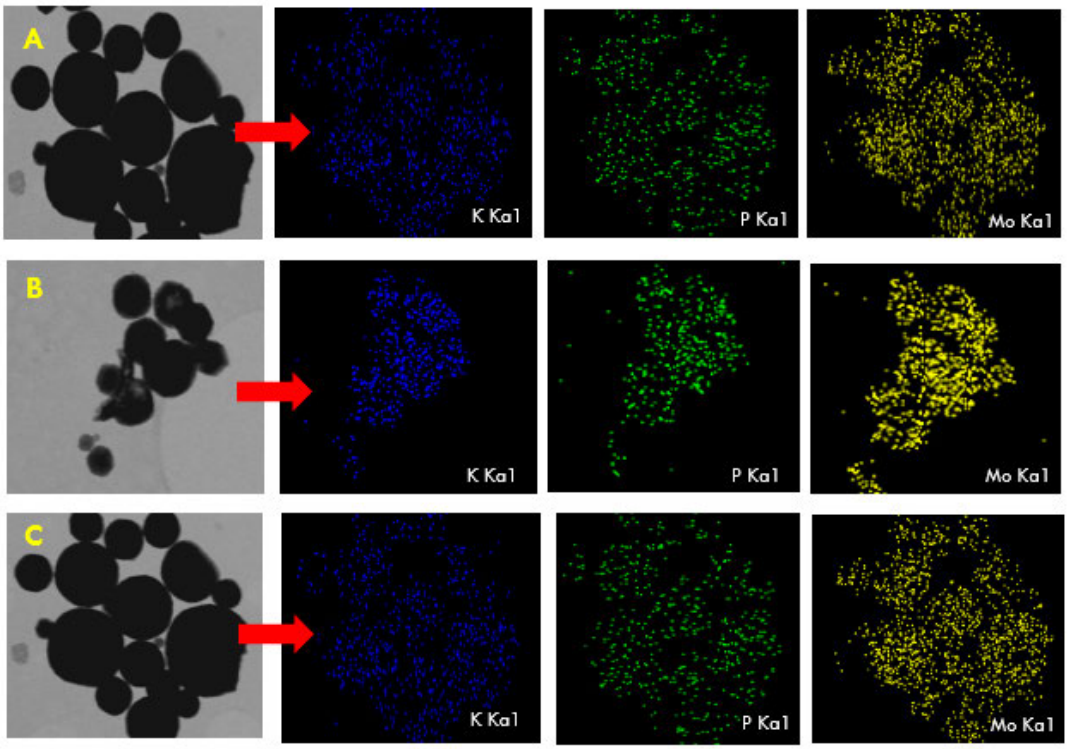

Figure 4.8 BF-STEM analysis of (A) 1KPMA, (B) 2KPMA and (C) 3KPMA catalysts.

4.3.2 Catalytic activity studies

A detail study was performed on the oxidation of styrene to benzaldehyde to optimize the conditions at room temperature with various reaction parameters, such as, mole ratio of styrene to TBHP, amount of catalyst, various oxidants, reaction temperature, time on stream and recycling. Initially, blank reactions showed a 2 % conversion with a 73% and 18 % selectivity towards benzaldehyde and styrene oxide, respectively, recorded at room temperature for 24 h. The pure phosphomolybdic acid showed a 4.5 % conversion, with similar selectivity as the blank. Among the potassium exchanged catalysts, 2KPMA showed highest activity with an 80% selectivity towards benzaldehyde, probably attributed availability of active sites because of its large surface area and the surface acidity of the catalyst (Table 4.2). The results correlated well with the nature of acidic sites of the catalyst, in this case, Brønsted acidic sites [21]. From the pyridine infrared studies, 2KPMA had the highest surface Brønsted acidic sites than the other K exchanged PMA

and PMA, itself. It is also possible that the mesoporous nature of the 2KPMA catalyst influences activity, since it has higher pore volume and surface area.

Table 4.2 Catalytic results over alkali metal exchanged phosphomolybdic acid catalysts[a].

Catalyst	Conversion (%)	Selectivity (%)			TON[c]
		benzaldehyde	styrene oxide	others[b]	
Blank	2.0	73	18	9	--
PMA	4.5	79	16	5	7.6
1KPMA	6.7	79	16	5	11.3
2KPMA	8.5	80	16	4	14.5
3KPMA	7.0	80	16	4	12.0
1RbPMA	6.2	79	15	6	10.5
2RbPMA	7.4	82	14	4	13.0
3RbPMA	6.3	80	15	5	10.8
1CsPMA	5.8	79	14	7	9.9
2CsPMA	6.5	80	15	5	11.1
3CsPMA	5.9	78	16	6	9.8

[a]Reaction conditions: styrene (10 mmol), TBHP (10 mmol), catalyst = 0.1 g, reaction temperature = RT, reaction time = 24 h; [b]Others = 1-phenylethane -1,2-diol, phenyl acetaldehyde; [c]TON = number of moles of product/number of moles of catalyst; reactions done in triplicate.

Styrene oxidation over the Rb and Cs exchanged PMA catalysts under similar reaction conditions indicate that the 2 wt% catalysts showed a similar activity trend to the 2KPMA catalyst, but not as efficient. The order of reactivity of styrene oxidation follows the order, K > Rb > Cs, probably due to K being more efficient in generating TBHP radicals than Rb or Cs in the other catalysts.

Styrene oxidation was then conducted over the 2KPMA catalyst by varying the TBHP concentration. The results are tabulated in Table C4.1, Appendix C. These findings show that the activity increased initially with oxidant concentration. Thereafter, only a slight increase in the activity was observed, but the selectivity decreased marginally leading to the undesired diol. The catalytic reaction was also investigated using different amounts of the 2KPMA catalyst (Table C4.2, Appendix C). The styrene conversion increases with an increase in the catalyst amount, however, the selectivity towards benzaldehyde decreased significantly due to over oxidation of benzaldehyde to benzoic acid. It was also found that a lower concentration of reactant used gave

higher activity and selectivity (Table C4.3, Appendix C). Of the various oxidants studied, TBHP is the only active oxidant at room temperature, producing a conversion of 8.5% and an 80% selectivity towards benzaldehyde. H_2O_2 and air showed no activity at room temperature (Figure C4.4, Appendix C).

A comparative study of the oxidation of styrene to other aromatic compounds such as benzyl alcohol and toluene was conducted at room temperature over the 2KPMA catalyst (Table 4.3). Benzyl alcohol is more reactive than styrene and toluene. It is also highly selective towards benzaldehyde, probably due to the carbinol group being more reactive towards carbonyl compound than olefins and alkanes. A similar activity pattern was obtained with the 2RbPMA and 2CsPMA catalysts.

Table 4.3 Catalytic results over KPMA-2 catalysts at room temperature.

Substrate	Conversion (%)	Selectivity (%)		
		benzaldehyde	styrene oxide	others[b]
toluene	1.2	99	0	1
styrene	8.5	80	16	4
benzyl alcohol	19.7	97	0	3

[a]Reaction conditions: substrate (10 mmol), TBHP (10 mmol), catalyst = 0.1 g, reaction time = 24 h;

[b]others = 1-phenylethane -1,2-diol, phenyl acetaldehyde, benzoic acid; reactions done in triplicate.

Time on stream studies was carried out to determine the influence of reaction time on conversion and selectivity over the 2KPMA catalyst (Figure 4.9). Initially, the selectivity towards benzaldehyde and styrene oxide was 77% and 28%, respectively. Over time, the selectivity towards benzaldehyde increased while there was a decrease in styrene oxide selectivity, indicating that the formation of benzaldehyde occurs via styrene oxide. This result supports the assumption that there are most probably two pathways for benzaldehyde formation, one is C=C cleavage and the other is the cleavage of styrene oxide to produce benzaldehyde. To further gather evidence, the oxidation styrene oxide was studied under present conditions. These results show that phenyl acetaldehyde together with benzaldehyde is are produced (Table 4.4), providing some evidence that styrene oxidation proceeds via C=C cleavage to selectively produce benzaldehyde.

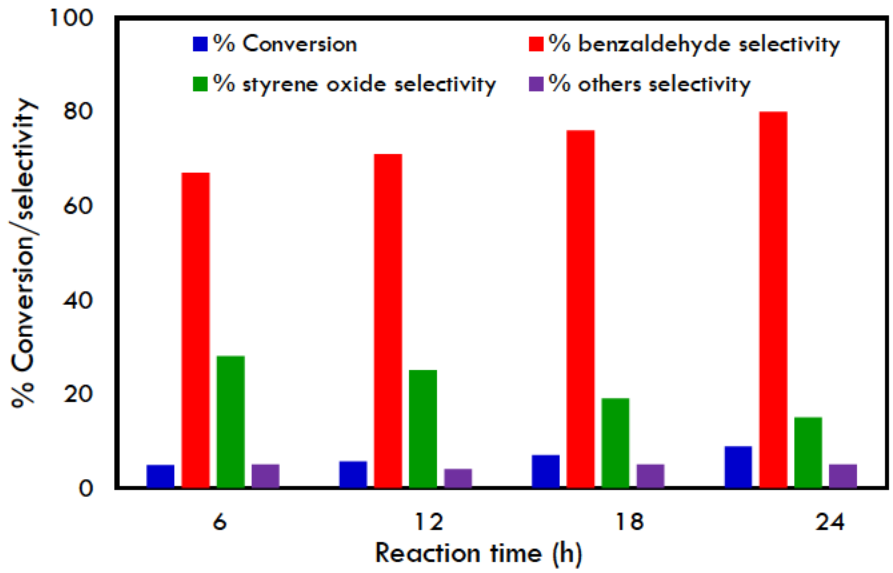

Figure 4.9 Time on stream results for the oxidation of styrene over 2KPMA at room temperature.

Table 4.4 Styrene oxide oxidation over 2KPMA catalyst.

Reaction time (h)	Conversion (%)	Selectivity (%)		
		phenyl acetaldehyde	benzaldehyde	[a]others
1	97	71	22	7
2	97.3	69	23	8
3	97.9	68	24	8
4	98	67	25	8
5	98.1	66	26	8

[a]Reaction conditions: styrene oxide (10 mmol), TBHP (10 mmol), catalyst = 0.1 g, reaction temperature = RT; [a]others = 1-phenylethane -1,2-diol, benzoic acid; reactions done in triplicate.

Recycling experiments were carried out to investigate the stability of the 2KPMA catalyst (Figure C4.5, Appendix C). The catalyst was separated from aqueous layer, filtered and washed several times with organic solvent dichloromethane to remove any organic moiety on the surface of the catalyst and dried in an oven over night. It was then characterized by infrared spectroscopy (Figures 4.3 and 4.4) to observe any structural changes and any changes in the surface acidity. There was minimal change in structural and acidic properties of the catalysts. Although there was minimal change in the conversion, changes in the selectivity were evident. This could be due to the loss of metal after each cycle as corroborated by ICP analysis.

4.4 Conclusion

Eco-friendly heterogeneous metal exchanged phosphomolybdic acid catalysts were efficient for the solvent free oxidation of styrene to benzaldehyde. The 2KPMA catalyst performed much better than its Rb and Cs counterparts in terms of selectivity towards benzaldehyde. The catalytic activity correlated well with the physical and chemical properties of the catalyst. The metal exchanged catalysts with a 2wt% loading showed the highest surface areas ranging between 130-180 m^2/g, all of them exhibiting Type IV isotherms, clearly demonstrating their mesoporous nature. XRD patterns and infrared spectroscopy showed that the primary structure of the Keggin ion remains intact after incorporation of the metal, while pyridine adsorbed spectroscopy shows the existence of Brønsted as well as Lewis acid sites on the surface. The surface of all the catalysts possessed a uniform spherical morphology and from BF STEM analysis, an even distribution of metals in the catalysts were observed. The regenerated catalyst showed minimal change in structural and acidic properties, reflected in the catalytic results done up to 3 cycles.

References

[1] Gerhartz W (1985) Ullmann's Encyclopedia of Industrial Chemistry. VCH Weinheim, Germany.

[2] Fey F, Fischer H, Bachmann S, Albert K, Bolm C (2010) J Org Chem 66:8154-8159.

[3] Lutz JT, Othmer MK, Grayson D, Eckroth GJ, Bushey CI (1980) Encyclopedia of Chemical Technology. Wiley, New York.

[4] Regen SL, Koteel C (1977) J Am Chem Soc 99:3837-3838.

[5] Zhang Z, Wu YZ, Min Z, Yan FC (2008) Syn React Inorg Metal-Org Nano-Metal Chem 38:352-355.

[6] Soyeb P, Anjali P (2013) Ind Eng Chem Res 52:11913-11919.

[7] Soyeb P, Anjali P (2014) Catal Sci Technol 4:648-656.

[8] Hu J, Li K, Li W, Ma F, Guo Y (2009) Appl Catal A: Gen 364:211-220.

[9] Rao AS, Anjali P, Das SK (2014) J Chem Sci 126:1641-1645.

[10] Tang J, Yang XL, Zhang XW, Wang M, Wu C.D (2010) Dalton Trans 39:3396-3399.

[11] Armatas GS, Bilis G, Louloudi M (2011) J Mater Chem 21:2997-3005.

[12] Fu J, Sun H, Xu Y, Wang C, Zhu D, Sun Q, Liu H (2012) Cryst Eng Comm 14:5148-5150.

[13] Patel A, Patel K (2014) Inorg Chimi Acta 419:130-134.

[14] Kozhevnikov IV (1998) Chem Rev 98:171-198.

[15] Mizuno N, Misono M (1998) Chem Rev 98:199-218.

[16] Viswanadham B, Jhansi P, Chary KVR, Friedrich HB, Singh S (2016) Catal Lett 146:364-372.

[17] Viswanadham B, Pedada J, Friedrich HB, Singh S (2016) Catal Lett 146:1470-1477.

[18] Viswanadham B, Kumar VP, Chary KVR (2014) Catal Lett 144:744-755.

[19] Viswanadham B, Srikanth A, Chary KVR (2014) J Chem Sci 126:445-454.

[20] Viswanadham B, Srikanth A, Kumar VP, Chary KVR (2015) J Nanosci Nanotech 15:5391-5402.

[21] Balaga V, Pedada J, Friedrich HB, Singh S, (2016) J Mol Catal A: Chem 425:116-123.

[22] Yamaguchi S, Sumimoto S, Ichihashi Y, Nishiyama S, Tsuruya S (2005) Ind Eng Chem 44:1-7.

[23] Wang G, Han Y, Wang F, Chu Y, Chen X (2015) Reac Kinet Mech Catal 115:679-690.

[24] Marosi L, Cox G, Tenten A, Hibst H (2000) J Catal 194:140-145.

[25] Long Z, Zhou Y, Chen G, Ge W, Wang J (2014) Sci Report 4:3651-3658.

[26] Fumin Z, Maiping G, Hanqing G, Jun W (2007) Chin J Chem Eng 15:895-898.

[27] Sharma P, Patel A (2009) Ind J Chem 48A:964-968.

[28] Song IK, Lee JK, Park GI, Lee WY (1997) Stud Surf Sci Catal 110:1183-1192.

[29] Misono M, (2001) Chem Commun 13:1141-1152.

[30] Hamid SBA, Daud NA, Suppiah DD, Yehya WA, Sudarsanam P, Bhargava SK (2016) Polyhedron 120:154-161.

[31] Srikanth A, Viswanadham B, Kumar VP, Anipindi NR, Chary KVR (2016) Appl Petrochem Res 6:145-153.

[32] Eom HJ, Lee DW, Kim S, Chung SH, Hur YG, Lee KY (2014) Fuel 126:263-272.

[33] Shiju NR, Williams HM, Brown DR (2009) Appl Catal B: Env 90:451-457.

[34] Okuhara T, Watanabe H, Nishimura T, Inumaru K, Misono M (2000) Chem Mater 12: 2230-2238.

[35] Kaur J, Kozhevnikov IV (2002) Chem Comm 2508-2509.

[36] Srinivas M, Raveendra G, Parameswaram G, Prasad PSS, Lingaiah N (2016) J Mol Catal A: Chem 413:7-14.

[37] Dias JA, Caliman E, Dias SCL (2004) Micro Meso Mater 76:221-232.

[38] Izumi Y, Ogawa M, Urabe K (1995) Appl Catal A: Gen 132:127-140.

[39] Pesaresi L, Brown DR, Lee AF, Montero JM, Williams H, Wilson K (2009) Appl Catal A: Gen 360:50-58.

[40] Kale SS, Armbruster U, Eckelt R, Bentrup U, Umbarkar SB, Dongare MK, Martin A (2016) Appl Catal A:Gen 527:9-18.

[41] Narasimharao K, Brown DR, Lee AF, Newman AD, Siril PF, Tavener SJ, Wilson K (2007) J Catal 248:226-234.

[42] Park HW, Park S, Park DR, Choi JH, Song IK (2010) Catal Comm 12:1-4.

[43] Matachowski L, Zieba A, Zembala M, Drelinkiewicz A (2009) Catal Lett 133:49-62.

[44] Essayem N, Coudurier G, Fournier M, Vedrine JC (1995) Catal Lett 34:223-235.

[45] Valand J, Parekh H, Friedrich HB (2013) Catal Comm 40:149-153.

CHAPTER FIVE

SOLVENT FREE OXIDATION OF BENZYL ALCOHOL TO BENZALDEHYDE OVER COPPER AND ZINC MODIFIED PHOSPHOMOLYBDIC ACID CATALYSTS AT ROOM TEMPERATURE

Abstract

Copper and zinc exchanged heteropolyacid catalysts were synthesized by the ion exchange method and were characterized by various techniques such as X-ray diffraction, infrared spectroscopy, pyridine adsorbed infrared spectroscopy, BET surface studies, ^{31}P NMR spectroscopy and inductively coupled plasma-optical emission spectroscopy to investigate its physico-chemical properties. XRD diffractograms showed that crystallites of the Keggin ion of the heteropolyacid was present and was retained after metal modification as observed from infrared spectroscopy. From pyridine adsorbed infrared, the Brønsted/Lewis acid site ratio increased in the metal exchanged phosphomolybdic acid catalysts, whereas there was a decrease in the ratio for the modified phosphotungstic acid catalysts. ^{31}P NMR spectra results showed that the metal was successfully exchanged with protons and was not incorporated in the primary structure of heteropolyacid catalyst, thus maintaining the Keggin ion. ICP analysis indicated a correlation of the theoretical metal content with the experimental loadings of the catalysts. In the oxidation of benzyl alcohol over metal exchanged catalysts, the Zn exchanged phosphomolybdic acid catalysts showed higher oxidation activity and correlated well with the acidity of the catalysts.

Keywords: PMA, PTA, benzyl alcohol, benzaldehyde, TBHP

5.1 Introduction

The conversion of benzyl alcohol to benzaldehyde under eco-friendly conditions remains attractive and a challenge to both the academic sector and chemical industry due to importance of benzaldehyde in basic and applied research [1-2]. Benzaldehyde is a versatile aromatic

carbonyl compound that is used in the perfumery, cosmetics and agrochemical industries [3-4]. Several catalytic materials have been developed to produce benzaldehyde from benzyl alcohol through homogeneous and heterogeneous oxidation catalysis [5-24]. In homogeneous catalysis [5-6], difficulty in retrieving the catalyst is encountered and large amounts of solvents are required which is expensive and not eco-friendly. As a result, solvent free heterogeneous catalysts have received more attention because of easy recovery and recyclability. Among the various materials studied, solid acid catalytic materials such heteropolyacids have gained popularity due to its bifunctional acidic and redox character [7-21]. In addition, a major advantage is that its acid-base and redox propertied can tuned by simple exchange of protons with metal.

Zn and Cu exchanged heteropolyacid catalysts were studied for several reactions such as the Knoevenagel condensation reaction, oxidation reactions and acid catalyzed organic transformations [25-29]. Khabazzadeh *et al*. [25] developed $Cu_{1\cdot5}PMo_{12}O_{40}$ and $Cu_{1\cdot5}PW_{12}O_{40}$ reusable and efficient catalysts for the preparation of 1-amidoalkyl-2-naphthols, while Patil *et al*. [26] studied the low temperature activation of methane over a Zn exchanged heteropolyacid resulting in the selective formation of methanol and acetic acid during reaction. Jagadeeswaraiah *et al*. [27] showed that the addition of Zn^{2+} ions into the secondary structure of heteropolyacid was efficient during glycerol carbonate synthesis from glycerol and urea. Rao *et al*. [28] showed that niobia supported on Zn exchanged phosphotungstic acid catalysts exhibited good activity during the conversion of furfuryl alcohol to butyl levulinate and related this to the acidic sites of catalysts. Viswanadham *et al*. [29] reported on Cu exchanged heteropolyacid catalysts and showed that increasing the Brønsted and Lewis acidity results in higher activity during Knoevenagel condensation reaction.

The objective of this investigation is to develop several Cu and Zn exchanged heteropolyacid catalysts for the oxidation of benzyl alcohol and to understand the influence of various reaction parameters such as reaction temperature, catalyst loading, mole ratio of reactant to oxidant, various oxidants, time-on-stream and regeneration studies for this reaction.

5.2 Experimental

5.2.1 Catalyst synthesis

$H_3PMo_{12}O_{40}$ and $H_3PW_{12}O_{40}$, zinc sulphate hydrate, copper sulphate hydrate and barium hydroxide were procured from Sigma-Aldrich (RSA). The Zn and Cu exchanged catalysts were synthesized according to a method described previously [29]. In typical synthesis, 0.18 g of barium hydroxide was added to an aqueous mixture of 2.0 g of phosphomolybdic acid in 5 mL distilled water. Thereafter, 0.16 g of $CuSO_4.5H_2O$ was added to replace barium with copper by precipitating the barium as $BaSO_4$. The $Cu_{1.5}PMo_{12}O_{40}$ solid was recovered by centrifugation and dried 100°C for 10 h in an oven. The catalyst was denoted as Cu-PMA. Similarly, the other catalysts, viz. $Cu_{1.5}PW_{12}O_{40}$, $Zn_{1.5}PMo_{12}O_{40}$ and $Zn_{1.5}PW_{12}O_{40}$, denoted as Cu-PTA, Zn-PMA and Zn-PTA, respectively, were synthesized.

5.2.2 Catalyst characterization

Powder X-ray diffraction patterns of selected catalysts were obtained using a Bruker D8 Advance diffractometer, equipped with a Cu Kα radiation source (λ = 1.5406Å) at 40 kV and 30 mA. The measurements were recorded in steps of 0.045° with a count time of 0.5 s in the range of 5 to 40°. The surface area was determined using N_2 adsorption isotherms at -196°C by the multipoint BET method taking 0.162 nm^2 as the cross-sectional area. Prior to these experiments, the materials were degassed under helium flow overnight at 200°C using a Micrometrics Flow Prep 060 and all experiments were carried out at a relative pressure range (p/p°) of 0.05 to 0.9. Infrared (IR) spectra were recorded on a Perkin Elmer Precisely, equipped with a Universal ATR sampling accessory using a diamond crystal. The powdered material was placed on the crystal and a force of 120 psi was applied to ensure proper contact between the material and the crystal. The spectra were analyzed using Spectrum 100 software. Ex-situ pyridine adsorbed FT-IR experiments were carried out on a Perkin Elmer ATR spectrometer at room temperature. Prior to analysis, pyridine adsorption experiments were carried out by placing a drop of pyridine on a small amount of the catalyst, followed by evacuation in air for 1 h to remove the reversibly adsorbed pyridine. The metal content was determined by ICP-OES analysis using a PerkinElmer Optima 5300 DV spectrometer, while ^{31}P NMR spectra were recorded on a Bruker Advance 400 MHz spectrometer where chemical shifts were reported relative to 85% H_3PO_4 in D_2O, used as an external standard at 298 K.

5.2.3 Catalytic testing

The solvent free oxidation of benzyl alcohol was studied in a 10 mL round bottom flask at room temperature. In a typical experiment, 10 mmol of benzyl alcohol, 10 mmol of 70% TBHP and 0.05 g of the catalyst were placed in the flask, under stirring (Scheme 1). The reaction was constantly monitored by a Perkin Elmer Auto gas chromatograph equipped with a flame ionization detector (GC-FID). The catalyst was recycled and re-used for the reaction by repeating the procedure described.

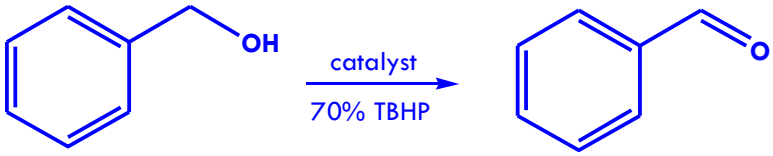

Figure 5.1 Scheme showing catalytic oxidation of benzyl alcohol**.**

5.3 Results and discussion

5.3.1 X-ray diffraction studies

X-ray diffraction profiles of the parent and the metal exchanged heteropolyacid catalysts are shown in Figure 5.2. The pure phosphomolybdic acid (PMA), Cu-PMA and Zn-PMA catalyst exhibits diffraction peaks at 8.2°, 9.1°, 26.5° and 28.8° represents characteristic diffraction peaks of primary structure of Keggin ion [29]. However, in the case PTA, Cu-PTA and Zn-PTA catalysts the characteristic Keggin ion of the parent PTA together with other additional peaks were observed.

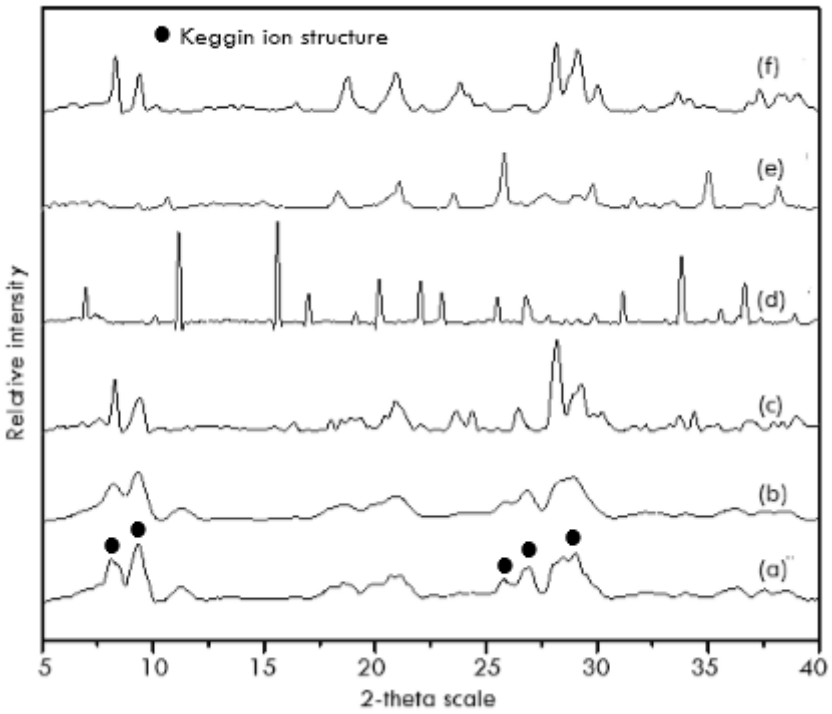

Figure 5.2 XRD profile of (a) PMA, (b) Cu-PMA, (c) Zn-PMA, (d) PTA, (e) Cu-PTA, (f) Zn-PTA catalysts.

5.3.2 Infrared spectroscopy

The infrared spectra of the parent and synthesized metal exchanged heteropolyacid catalysts were recorded in the region 1200-600 cm^{-1} (Figure 5.3). Bands at 1056, 958, 891, 760 cm^{-1} are assigned to P-O, Mo=O, Mo-O_t-Mo, Mo-O_c-Mo for PMA, whereas at 1075, 977, 906, 764 cm^{-1} attributed to P-O, W-O, W-O_b-W and W-O_c-W for PTA, respectively. The Cu and Zn exchanged heteropolyacid catalysts exhibits IR band shifts in the Keggin ion bands suggesting that Cu and Zn was successfully incorporated in the primary structure of Keggin ion.

The ex-situ pyridine studies of pure and synthesized Cu and Zn metal exchanged heteropolyacid catalysts were recorded (1400-1600 cm^{-1}) to investigate the acidic sites of the catalysts (Figure 5.4). The infrared bands located at 1529-1538, 1483-1487, 1439-1442 cm^{-1} represents Brønsted (B), Brønsted + Lewis (B+L) and Lewis (L) acidic sites, respectively. The B/L acidic sites ratio increased significantly for the metal exchanged-PMA catalysts, but decreased in the case of PTA catalysts.

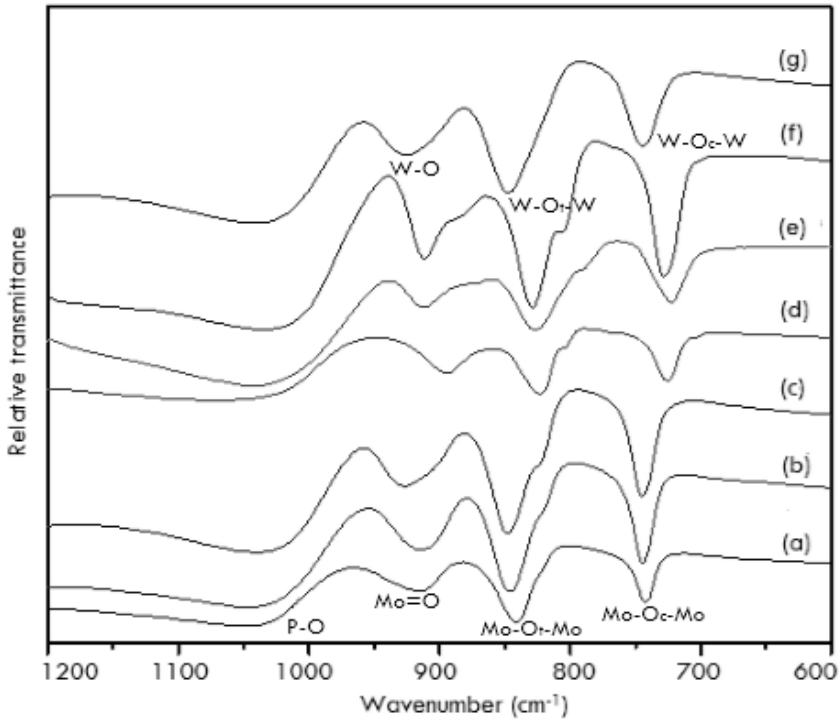

Figure 5.3 FT-IR spectra of (a) PMA, (b) Cu-PMA, (c) Zn-PMA, (d) PTA, (e) Cu-PTA, (f) Zn-PTA and (g) regenerated Zn-PMA catalysts.

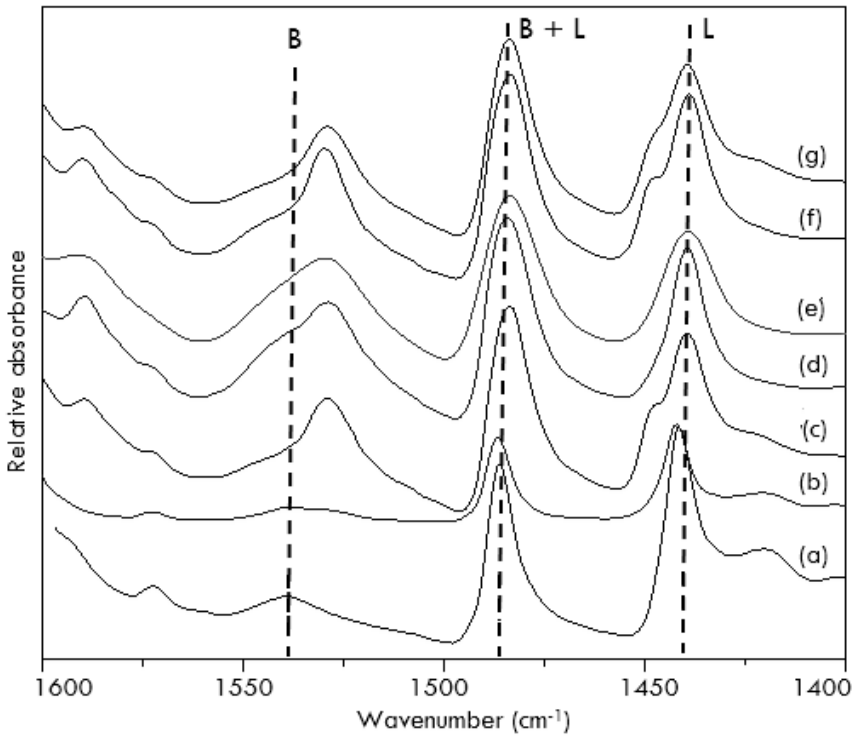

Figure 5.4 Pyridine infrared spectra of (a) PMA, (b) Cu-PMA, (c) Zn-PMA, (d) PTA, (e) Cu-PTA, (f) Zn-PTA and (g) regenerated Zn-PMA catalysts (B = Brønsted, L = Lewis)

5.3.3 ^{31}P NMR spectroscopy

The ^{31}P NMR spectra of the parent, Cu and Zn metal exchanged heteropolyacid catalysts show the presence of single signal at -3.89 ppm due to the phosphorus atoms in the PMA, whereas for PTA it was observed at -15.20 ppm. After exchange with Cu and Zn, the catalysts exhibit slight shift in the peak, which has no effect in the phosphorus environment which is maintained and these results match well with studies conducted by other researchers [28, 29].

5.3.4 Chemical composition and BET surface studies

ICP analysis and BET surface area of the metal exchanged heteropolyacid catalysts results are tabulated in Table 5.1. These findings are shows that theoretical metal loadings of exchanged catalysts correlates well with experimental values. The regenerated catalyst shows minimal change in the metal content. There was an increase in the surface area of the copper exchanged catalysts compared to its parent, whereas a decrease was observed for the Zn catalysts, probably due to metal size.

Table 5.1 BET surface area, ICP analysis and B/L acidic sites of Cu and Zn exchanged heteropolyacid catalysts.

Catalyst	Surface area (m^2/g)	Cu/Zn loadings Calc. (%)	Cu/Zn loadings Expt. (%)	B/L ratio
PMA	2.5	--	--	0.44
Cu-PMA	6.9	1.5	1.42	0.46
Zn-PMA	2.1	1.5	1.46	0.59
PTA	4.5	--	--	0.60
Cu-PTA	7.5	1.5	1.45	0.54
Zn-PTA	1.8	1.5	1.49	0.55
regenerated Zn-PMA	2.0	1.5	1.44	0.58

B/L = Brønsted/Lewis

5.3.5 Catalytic activity studies

The catalytic properties were studied considering various reaction parameters such as nature of catalyst, catalyst loading, TBHP concentration, type of oxidant, amount of reactant and reaction temperature. Time on stream and regeneration experiments were also conducted.

The catalytic oxidation of benzyl alcohol was carried out over the Cu and Zn exchanged heteropolyacid catalysts under a nitrogen atmosphere and the results are presented in Table 5.2. Blank experiments conducted under same reaction conditions showed an 8.0 % benzyl alcohol conversion with high selectivity towards benzaldehyde. The parent heteropolyacids, phosphomolybdic acid showed a 14.5 % conversion, whereas phosphotungstic acid a 13.5 % conversion. In both cases, benzaldehyde was the major product obtained with very high selectivity. Among the Cu and Zn exchanged heteropolyacid catalysts, Zn-PMA catalysts performed slightly better compared to parent and other metal exchanged heteropolyacid catalysts, probably due to a slightly higher B/L acidic site ratio.

The catalytic properties of different amounts of Zn-PMA catalysts were studied and results are presented in Table 5.3. These findings indicate that as the loading increases from 0.025 to 0.05 g, the catalytic activity increased. Catalysts with higher amounts resulted in a decrease in the catalytic activity. The optimum catalyst amount was taken as 0.05 g. This was taken further in studies involving other parameters.

Table 5.2 Catalytic results of benzyl alcohol oxidation over parent and metal exchanged heteropolyacid catalysts.

Catalyst	Conversion (%)	Selectivity (%)		TON
		benzaldehyde	benzoic acid	
Blank	8.0	94	6	--
PMA	14.5	96	4	30
Cu-PMA	23.0	95	5	48
Zn-PMA	25.2	85	15	53
PTA	13.5	98	2	28
Cu-PTA	22.0	96	4	46
Zn-PTA	23.9	94	6	50

Reaction conditions: benzyl alcohol (10 mmol), TBHP (10 mmol), catalyst (0.1 g), reaction temperature = room temperature, reaction time = 24 h, TON = number of moles of products/number of moles of catalyst. (Experiments done in triplicate).

Table 5.3 Catalytic results of benzyl alcohol oxidation over various catalytic amounts of Zn exchanged phosphomolybdic acid catalysts.

Catalyst amount (g)	Conversion (%)	Selectivity (%)	
		benzaldehyde	benzoic acid
0.025	23.4	76	24
0.05	40.2	83	17
0.1	25.2	85	15
0.2	26.1	86	14

Reaction conditions: benzyl alcohol (10 mmol), TBHP (10 mmol), reaction temperature = room temperature, reaction time = 24 h. (Experiments done in triplicate).

An increase in the TBHP concentration resulted in an increase in the oxidation activity, but a decrease in the selectivity towards benzaldehyde and optimum value was determined to be 10 mmol TBHP (Table 5.4).

The oxidation ability of various oxidants such air, H_2O_2 and TBHP for benzyl alcohol oxidation were assessed over Zn-PMA catalysts (Figure 5.5). These findings indicate that TBHP was most efficient during the oxidation reaction. However, air was more selective, although the activity was rather poor at room temperature.

Table 5.4 Catalytic results of benzyl alcohol oxidation with various amounts of TBHP over Zn exchanged phosphomolybdic acid catalysts.

TBHP (mmol)	Conversion (%)	Selectivity (%)	
		benzaldehyde	benzoic acid
5	21.8	98	2
10	40.2	83	17
20	47.3	76	24
30	50.4	74	26

Reaction conditions: benzyl alcohol (10 mmol), TBHP (5-30 mmol), catalyst (0.05 g), reaction temperature = room temperature, reaction time = 24 h. (Experiments done in triplicate).

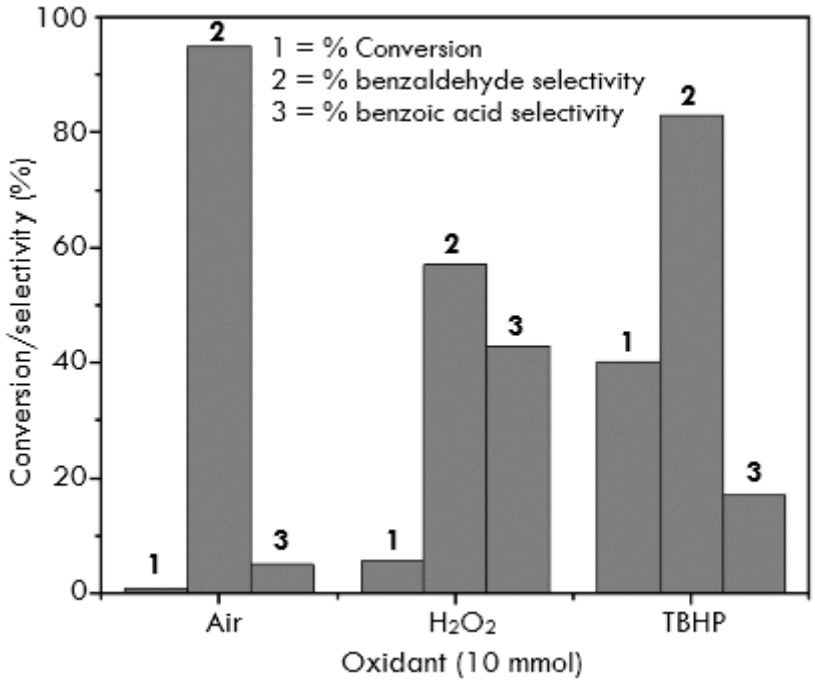

Figure 5.5 The oxidation of benzyl alcohol over the Zn-PMA catalyst using various oxidants.

The effect of benzyl alcohol concentration over Zn-PMA catalysts were studied under same reaction conditions and results are presented in Table 5.5. The conversion was highest for a 2% feedstock, however the selectivity towards benzaldehyde was low and more benzoic acid was observed. There was a decrease in conversion at higher concentrations of benzyl alcohol, probably due to dilution.

Table 5.5 Catalytic oxidation results with various concentrations of benzyl alcohol over Zn exchanged phosphomolybdic acid catalysts.

Benzyl alcohol (mmol)	Conversion (%)	Selectivity (%)	
		Benzaldehyde	Benzoic acid
2	75	76	24
4	58.3	79	21
8	46.8	80	20
10	40.2	83	17

Reaction conditions: TBHP (10 mmol), catalyst (0.05g), reaction temperature = room temperature, reaction time = 24 h. (Experiments done in triplicate).

Effect of reaction time was studied during benzyl alcohol oxidation reaction and results are shown in Figure 5.6. From the figure, the activity increased with an increase in reaction time, however there was a decrease in the selectivity towards benzaldehyde, probably due to over oxidation to benzoic acid which showed a relative increase over time.

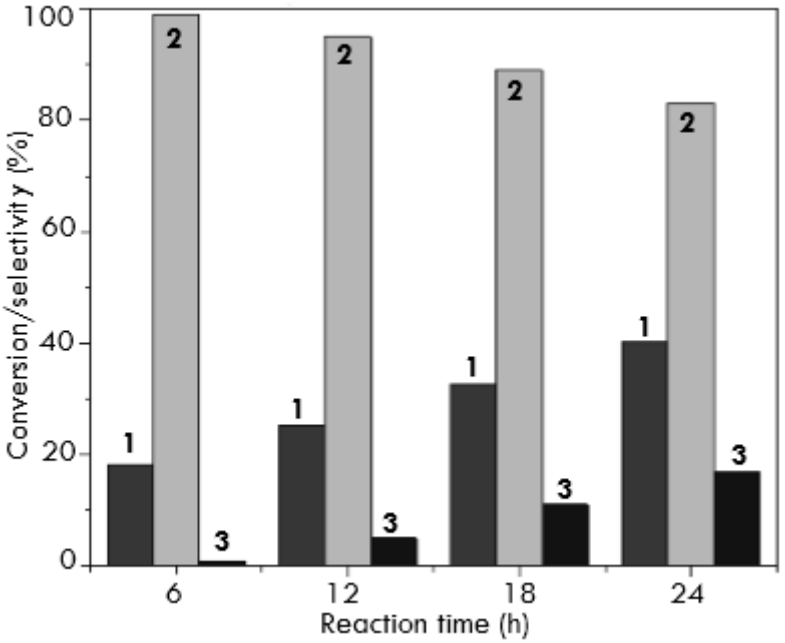

Figure 5.6 Oxidation of benzyl alcohol over Zn-PMA catalysts as a function of time. (1 = % Conversion, 2 = % benzaldehyde selectivity and 3 = % benzoic selectivity).

Once regenerated, the Zn-PMA catalyst was subjected to further studies and the results are shown in Figure 5.7. There is a slight decrease in the activity over three cycles which correlates with the acidity of used catalysts. Also, there is minimal change in Zn content after regeneration.

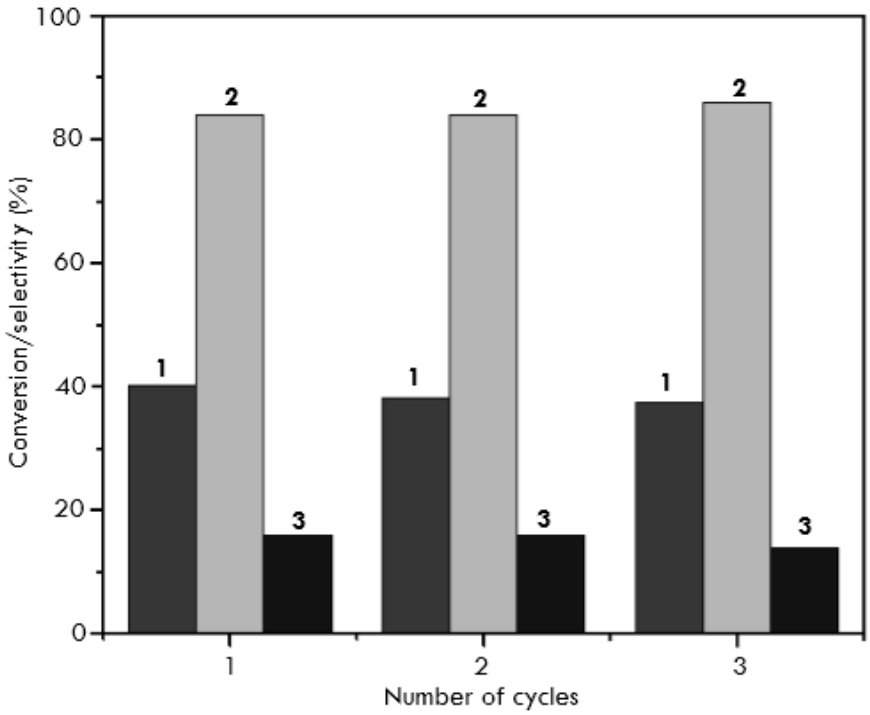

Figure 5.7 Oxidation of benzyl alcohol over Zn-PMA catalysts over three cycles. (1 = % conversion, 2 = % benzaldehyde selectivity and 3 = % benzoic selectivity).

5.4 Conclusion

Zn exchanged heteropolyacid catalysts exhibit higher oxidation ability than Cu catalysts in the conversion of benzyl alcohol to benzaldehyde and this is related to the acidity of the catalysts. XRD and infrared results confirm that the primary structure of Keggin ion is retained even after metals are incorporated in its structure, while pyridine adsorbed infrared spectroscopy showed that the incorporation of metal in PMA resulted in an increase in the B/L acidic sites ratio, whereas it decreased for the metal exchanged PTA catalysts. ^{31}P NMR spectra clearly shows that the phosphorus environment is retained, indicating that metal successfully exchanged with protons but did not interfere with the primary structure of heteropolyacid. The Zn exchanged PMA catalysts produced a 97.4 % conversion of benzyl alcohol with a 76 % benzaldehyde selectivity.

References

[1] Franz, G.; Sheldon, R.A. *Ullmann's Encyclopedia of Industrial Chemistry,* 5th Ed. VCH Weinheim: Germany; **1991**; p. 261.

[2] Xia, Q.H.; Ge H.Q.; Ye, C.P.; Liu Z.M.; Su K.X. Advances in Homogeneous and Heterogeneous Catalytic Asymmetric Epoxidation. *Chem. Rev.* **2005**, 105, 1603-1662.

[3] Gerhartz, W. *Ullmann's Encyclopedia of Industrial Chemistry*, 5th Ed. VCH Weinheim: Germany; **1985;** p. 469.

[4] Fey, F.; Fischer, H.; Bachmann, S.; Albert, K.; Bolm, C. Silica-Supported TEMPO Catalysts: Synthesis and Application in the Anelli Oxidation of Alcohols. *J. Org. Chem.* **2001**, 66, 8154-8159.

[5] Sheldon, R.A. Heterogeneous Catalytic Oxidation and Fine Chemicals. *Stud. Surf. Sci. Catal.* **1991**, 59, 33-54.

[6] Regen, S.L.; Koteel, C. Activation through impregnation. Permanganate-coated solid supports. *J. Am. Chem. Soc.* **1977**, 99, 3837-3838.

[7] Chen, G.; Zhou, Y.; Long, Z.; Wang, X.; Li, J.; Wang, J. Mesoporous Polyoxometalates -Based ionic Hybrid As a Triphasic Catalyst for Oxidation of Benzyl Alcohol with H_2O_2. *ACS Appl. Mater. Interfaces.* **2014**, 6, 4438-4446.

[8] Pathan, S.; Patel, A. Keggin type transition metal substituted phosphomolybdates: heterogeneous catalysts for selective aerobic oxidation of alcohols and alkenes under solvent free condition. *Catal. Sci. Technol.* **2014**, 4, 648-656.

[9] Farsani, M.R.; Jalilian, F.; Yadollahi, B.; Rudbari, H.A. A Comparative Study on Keggin and Wells-Dawson Sandwich type polyoxometalates in the oxidation of alcohols with 30% hydrogen peroxide. *Polyhedron* **2014**, 76, 102-107.

[10] Tundo, P.; Romanelli, G.P.; VAzquez, P.G.; Arico, F. Multiphase oxidation of alcohols and sulfides with hydrogen peroxide catalyzed by heteropolyacids. *Catal. Commun.* **2010**, 11, 1181-1184.

[11] Nikbakht, E.; Yadollahi, B.; Farsani, M.R. Green oxidation of alcohols in water by polyoxometalate nano capsule as catalyst. *Inorg. Chem. Commun.* **2015**, 55, 135-138.

[12] Nadealian, Z.; Mirkhani, V.; Yadollahi, B.; Moghadam, M.; Tangestaninejad, S.; Baltork, I.M. Selective oxidation of alcohols to aldehydes using inorganic–organic hybrid catalyst based on zinc substituted polyoxometalate and ionic liquid. *J. Coord. Chem.* **2012**, 65, 1071-1081.

[13] Bordoloi, A.; Sahoo, S.; Lefebvre, F.; Halligudi, S.B. Heteropoly acid-based supported ionic liquid-phase catalysts for the selective oxidation of alcohols. *J. Catal.* **2008**, 259, 232-239.

[14] Palermo, V.; Villabrillle, P.I.; Gvazquez, P.; Caceres, C.V.; Tundo, P.; Romanell, G.P. Role of vanadium and pyridine in heteropoly compounds for selective oxidation of alcohols with hydrogen peroxide. *J. Chem. Sci.* **2013**, 125, 1375-1383.

[15] Haimov, A.; Neumann, R. Polyethylene glycol as a non-ionic liquid solvent for polyoxometalate catalyzed aerobic oxidation. *Chem. Commun.* **2002**, 876-877.

[16] Choi, J.H.; Kang, T.H.; Bang, Y.; Song, J.H.; Song, I.K. Electrochemical and UV-Visible spectroscopy studies of $K_6As_2W_{18-x}Mo_xO_{62}$ (x = 0-3) and Well-Dawson heteropolyacid catalysts for oxidative dehydrogenation of benzyl alcohol. *Catal. Commun.* **2014**, 55, 29-33.

[17] Farhadi, S.; Zaidi, M. Polyoxometalate-zirconia (POM/ZrO_2) nanocomposite prepared by sol-gel process: A green and recyclable photocatalyst for efficent and selective aerobic oxidation of alcohols into aldehydes and ketones. *Appl. Catal. A: Gen.* **2009**, 354, 119-126.

[18] Hasannia, S.; Yadollahi, B. Zn-Al LDH nanostructures pillared by Fe substituted Keggin type polyoxometalates: Synthesis, characterization and catalytic effect in green oxidation of alcohols. *Polyhedron* **2015**, 99, 260-265.

[19] Leng, Y.; Zhao, P.; Zhang, M.; Wang, J. Amino functionalized bipyridine-heteropolyacid ionic hybrid: A recylable catalyst for solvent-free oxidation of benzyl alcohol with H_2O_2. *J. Mol. Catal. A: Chem* **2012**, 358, 67-72.

[20] Park, D.R.; Song, J.H.; Lee, S.H.; Song, S.H.; Kim, H.; Jung, J.C.; Song, I.K. Redox properties of $H_3PMo_xW_{12-x}O_{40}$ and $H_6P_2Mo_xW_{18-x}O_{62}$ heteropolyacid catalysts and their catalytic activity for benzyl alcohol oxidation. *Appl. Catal A: Gen.* **2008**, 349, 222-228.

[21] Zhao, H.; Zeng, L.; Li, Y.; Liu, C.; Hou, B.; Wu, D.; Feng, N.; Zheng, A.; Xie, X.; Su, S.; Yu, N. Polyoxometalate-based ionic complexes immobilized in mesoporous silica as prepared a one-pot procedure: Efficent and reusable catalysts for H_2O_2-mediated alcohol oxidations in aqueous media. *Micro. Meso. Mater.* **2013**, 172, 67-76.

[22] Fan, J.; Pu, F.; Sun, M.; Liu, Z.W.; Han, X.Y.; Wei, J.F.; Shi, X.Y. Immobilized bis-layered ionic liquids/peroxotungstates as an efficient catalyst for selective oxidation of alcohols in neat water. *New J. Chem.* **2016**, 40, 10498-10503.

[23] Ma, W.; Tong, Q.; Wang, J.; Yang, H.; Zhang, M.; Jiang, H.; Wang, Q.; Liu, Y.; Cheng, M. Synthesis and characterization of titanium(IV)/graphene oxide foam: a sustainable catalyst for the oxidation of benzyl alcohol to benzaldehyde. *RSC Adv.* **2017**, 7, 6720-6723.

[24] Choudhary, V.R.; Dumbre, D.K.; Bhargava, S.K. Oxidation of Benzyl Alcohol to Benzaldehyde by *tert*-Butyl Hydroperoxide over Nanogold Supported on TiO_2 and other Transition and Rare-Earth Metal Oxides. *Ind. Eng. Chem. Res.* **2009**, 48, 9471-9478.

[25] Khabazzadeh, H.; Saidi, K.; Seyedi, N. Cu-exchanged heteropolyacids as efficient and reusable catalysts for preparation of 1-amidoalkyl-2-naphthols, *J. Chem. Sci*. **2009**, 121, 429-433.

[26] Patil, U.; Saih, Y.; Hamad, E.A.; Hamieh, A.; Pelletier, J.D.A.; Basset, J.M. Low temperature activation of methane over a zinc-exchanged heteropolyacid as an entry to its selective oxidation to methanol and acetic acid. *Chem. Commun.* **2014**, 50, 12348-12351.

[27] Jagadeeswaraiah, K.; Kumar, C.R.; Prasad, P.S.S.; Lingaiah, N. Incorporation of Zn^{2+} ions into the secondary structure of heteropoly tungstate: catalytic efficiency for synthesis of glycerol carbonate from glycerol and urea. *Catal. Sci. Technol.* **2014**, 4, 2969-2977.

[28] Rao, B.S.; Kumari, P.K.; Dhanalakshmi, D.; Lingaiah, N. Selective conversion of furfuryl alcohol into butyl levulinate over zinc exchanged heteropoly tungstate supported on niobia catalysts. *J. Mol. Catal.* **2017**, 427, 80-86.

[29] Viswanadham, B.; Pedada, J.; Friedrich, H.B.; Singh, S. The Role of Copper Exchanged Phosphomolybdic Acid Catalyst for Knoevenagel Condensation. *Catal. Lett.* **2016**, 146, 1470-1477.

[30] Pope, M.T. *Heteropoly and Isopoly Oxometalates*, 13th Ed. Springer: Berlin, Germany; **1983**; p 180.

CHAPTER SIX

SUMMARY AND CONCLUSIONS

Efficient and eco-friendly heteropolyacid (HPA) catalysts were employed for the synthesis of ethyl acetate and benzaldehyde through esterification ad selective oxidation, respectively, at room temperature without the use of organic solvents. In all the studies the HPA catalysts were prepared by known methods and the metal incorporated catalysts by simple ion-exchange. In all the studies, two main heteopolyacids were prepared, viz. phosphomolybdic acid (PMA) and phosphotungstic acid (PTA). A number of metals such as potassium, cesium, rubidium, copper and zinc were successfully incorporated into the HPAs. In all the catalysts, the diagnostic Keggin structure of the HPAs were present, supported by X-ray diffraction and infra-red spectroscopy. The materials also showed a variance in the type of acidity present. Pyridine-FTIR showed that the incorporation of an alkali metal into the HPAs decreased the acidity and this directly influenced the catalysis. The results show that the strength of the acidity is quite prominent for the pure PTA and at low loadings of the alkali metal due to a combination of strong B and L sites. The acidic strength diminishes gradually as the content of alkali metal is increased. With respect to surface properties of the catalysts such as surface area, pore volume and pore, the BET surface area of the catalysts increased with an increase in the metal loadings, with a few exceptions. From adsorption isotherms, type IV isotherms with hysteresis loops were obtained which indicated presence of mesoporous materials. The surface morphology the metal exchanged HPA catalysts exhibited a well- defined spherical morphology, while from HR-TEM images, the metal exchanged catalysts display well defined particles with sizes ranging from 300 to 450 Å, whereas for the HPA, particles varied between 18000 to 20000 Å. From BF-STEM analysis, the metal content in the Keggin anion matches theoretical loadings. These results were reinforced with data obtained by flame photometry and ICP analysis.

For the esterification studies, blank studies, carried out under conditions similar to the catalytic reactions showed a 2% yield towards ethyl acetate. The bare phosphotungstic acid catalyst gave a 78% yield, whereas the Cs exchanged PTA catalysts with 0.5 and 1 wt.% loadings gave yields of

74 and 72 %, respectively. The slight decrease in the yield for the Cs exchanged PTA catalysts when compared to the bulk PTA catalyst was attributed to a decrease in acidity of these catalysts due to the exchange of the acidic protons in the PTA with Cs. It was also shown that a higher density of the Keggin ion results in improved catalytic activity. In general, the Cs exchanged heteropolyacid catalysts performed better than the K exchanged catalysts and this was attributed to a greater acidic nature of the Cs exchanged catalysts. Varying the mole ratios of reactants and catalyst amounts influenced activity. A 1:2 mole ratio of acetic acid to ethanol gave the best activity towards ethyl acetate, compared to a decrease in the mole ratios, where ethanol is in excess. The ethyl acetate yield was 55% when 0.05 g of catalyst was used, however this yield increased to about 72% when the catalyst amount was doubled. There was no further increase in the yields with further incremental increases in the amount of catalyst. Time on stream studies showed an increase in acetic acid conversion with increase in time, but reaches its maximum of 84% after 48 h at room temperature. Used catalysts were maintained their Keggin structure as shown by further characterization and performed well in subsequent esterification studies.

During benzaldehyde synthesis, a number of different catalysts were employed. Styrene oxidation was carried out using potassium, cesium and rubidium PMA catalysts. Blank reactions showed a 2 % conversion with a 73% and 18 % selectivity towards benzaldehyde and styrene oxide, respectively, recorded at room temperature for 24 h, whereas the pure PMA showed a 4.5 % conversion, with similar selectivity as the blank. Among the potassium exchanged catalysts, 2KPMA showed highest activity with an 80% selectivity towards benzaldehyde and this was attributed to the availability of active sites because of the large surface area. The surface acidity of the catalyst was also assumed to have played a role, more particularly the nature of acidic sites of the catalyst, in this case, the Brønsted acidic sites. The reaction over the Rb and Cs exchanged PMA catalysts under similar reaction conditions indicated a similar trend in activity to the 2KPMA catalyst, but not as efficient. The order of reactivity of styrene oxidation followed the order, K > Rb > Cs. Varying the TBHP concentration showed an increase in the activity with oxidant concentration. Thereafter, only a slight increase in the activity was observed, but the selectivity decreased marginally because of the formation of the undesired diol. The styrene conversion increased with an increase in the catalyst amount, however, the selectivity towards benzaldehyde decreased significantly due to over oxidation of benzaldehyde to benzoic acid. Of the various

oxidants studied, TBHP was the only active oxidant at room temperature, producing a conversion of 8.5% and an 80% selectivity towards benzaldehyde. H_2O_2 and air showed no activity at room temperature. Time on stream studies that were carried out showed that the selectivity towards benzaldehyde and styrene oxide was 77% and 28%, respectively. Over time, the selectivity towards benzaldehyde increased while there was a decrease in styrene oxide selectivity, indicating that the formation of benzaldehyde occured via styrene oxide. This result supported the assumption that there are two pathways for benzaldehyde formation, one is C=C cleavage and the other is the cleavage of styrene oxide to produce benzaldehyde. To obtain validity, the oxidation styrene oxide showed the formation of phenyl acetaldehyde together with benzaldehyde.

In the catalytic oxidation of benzyl alcohol, blank experiments showed 8 % benzyl alcohol conversion with high selectivity towards benzaldehyde. The parent heteropolyacids, phosphomolybdic acid showed a 14.5 % conversion, whereas phosphotungstic acid, 13.5 % conversion. In both cases, benzaldehyde was the major product obtained with very high selectivity. Among the Cu and Zn exchanged heteropolyacid catalysts, Zn-PMA catalysts performed slightly better compared to parent and other metal exchanged heteropolyacid catalysts. The use of different amounts of Zn-PMA catalysts indicated that as the loading increases from 0.025 to 0.05 g, the catalytic activity increased. Catalysts with higher amounts resulted in a decrease in the catalytic activity, with the optimum catalyst amount being 0.05 g. Reaction time, oxidant and reactant concentrations impacted on the overall catalysis.

APPENDIX A

Journal of the Iranian Chemical Society
https://doi.org/10.1007/s13738-018-1341-z

ORIGINAL PAPER

Synergistic role of Brønsted and Lewis acidity in alkali metal-exchanged heteropolyacid catalysts for esterification of acetic acid at room temperature

Jhansi Pedada[1] · Holger B. Friedrich[1] · Sooboo Singh[1]

Received: 8 September 2017 / Accepted: 5 March 2018

Abstract
A series of Cs exchanged phosphotungstic acid (PTA) catalysts were synthesized by the ion exchanged method and were characterized by X-ray diffraction, FT-IR spectroscopy, pyridine adsorbed FT-IR spectroscopy, SEM, BF-TEM, ICP-OES and BET surface area analysis. For comparison purposes, K exchanged PTA, Cs and K exchanged phosphomolybdic acid (PMA) catalysts were also prepared. XRD diffractograms showed that the crystallites of the Keggin ion are maintained, while FT-IR spectra also revealed the characteristic bands of the Keggin ion at all metal loadings of all the catalysts. From pyridine adsorbed FT-IR spectroscopy, it was observed that the Brønsted and Lewis acidity were significantly maintained at lower metal loadings, whereas STEM analysis showed a uniform distribution of the elements which correlated well with the theoretical atomic values of the loaded metals for all the catalysts, which were verified by ICP results. The efficiency of various metal-exchanged heteropolyacid catalysts was assessed for the esterification reaction using various substrates, and the Cs exchanged phosphotungstic acid catalysts showed superior activity compared to the other catalysts. In particular, the Cs exchanged phosphotungstic acid with a 1 wt% loading showed the highest activity and was most tolerant to the presence of water that was produced in the reaction. The catalytic activity correlates well with the Brønsted and Lewis acidity, as well as Keggin ion density of the catalysts.

Keywords Esterification · Brønsted and Lewis acidity · Cs-PTA · Keggin ion · Room temperature

Catalysis Letters
https://doi.org/10.1007/s10562-018-2352-1

The Role of Alkali Metal Exchanged Phosphomolybdic Acid Catalysts in the Solvent Free Oxidation of Styrene to Benzaldehyde at Room Temperature

Jhansi Pedada[1] · Holger B. Friedrich[1] · Sooboo Singh[1]

Received: 17 October 2017 / Accepted: 7 March 2018

Abstract
A series of alkali metal exchanged phosphomolybdic acid catalysts were synthesized by ion exchange, characterized by various physico-chemical techniques and used in the solvent free oxidation of styrene to benzaldehyde. XRD and infrared results showed that the primary structure of the Keggin ion usually present in phosphomolybdic acid is retained after metal exchange. HR-TEM analysis show a well-constructed spherical morphology of the materials with a lower degree of crystalinity. Type IV isotherms with mesoporous structure are observed from nitrogen adsorption–desorption isotherm studies and ex situ pyridine adsorption experiments reveal that Brønsted acidic sites increased after metal exchange. The K exchanged phosphomolybdic acid catalysts were most efficient in the conversion of styrene to benzaldehyde and the order of reactivity of the alkali metal exchanged phosphomolybdic acid catalysts was K > Rb > Cs. Insight into the reaction pathway by investigating the oxidation styrene oxide was obtained. The results show that phenyl acetaldehyde together with benzaldehyde are produced, providing some evidence that styrene oxidation proceeds via C=C cleavage to selectively produce benzaldehyde. The catalyst was easily recovered and was reused for up to three cycles showing stable activity.

APPENDIX B

Catal Lett (2016) 146:364–372
DOI 10.1007/s10562-015-1646-9

Efficient Solvent Free Knoevenagel Condensation Over Vanadium Containing Heteropolyacid Catalysts

Balaga Viswanadham[1] · Pedada Jhansi[1] · Komandur V. R. Chary[2] · Holger B. Friedrich[1] · Sooboo Singh[1]

Received: 3 August 2015 / Accepted: 28 October 2015 / Published online: 20 November 2015

Abstract Various V/P mole ratios of vanadium substituted Keggin-type phosphomolybdic acids were synthesized by the hydrothermal method. These materials were characterized using several physico-chemical techniques such as X-ray diffraction, FT-IR, N_2-sorption, Raman spectroscopy, ^{31}P MAS NMR, SEM and NH_3-TPD. FT-IR, Raman spectroscopy and ^{31}P NMR results confirm the formation of the primary structure of the Keggin ion and its crystalline nature is shown clearly by XRD. NH_3-TPD results reveal that the acidity of the materials systematically decreases with increasing vanadium content. The Knoevenagel reaction carried out over vanadium substituted phosphomolybdic acid with various V/P mole ratios indicate that the higher V/P mole ratio exhibits better catalytic performance under solvent free conditions. The catalytic properties correlate with the structural properties and the acidity of the materials.

Graphical Abstract

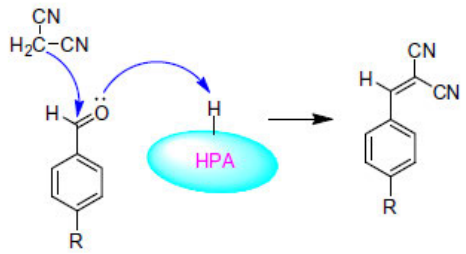

Keywords Vanadium-substituted phosphomolybdic acid · Knoevenagel reaction · Solvent free reaction · Acidity

1 Introduction

In recent years, there has been increasing emphasis on the use and design of environment-friendly solid acid catalysts to reduce the amount of toxic waste and by-products arising from chemical processes prompted by stringent environment protection laws. The challenge is to perform heterogeneous catalysis reactions leading to C–C bond formation which are widely employed in organic synthesis in a solvent free system [1]. The Knoevenagel reaction is an important C–C bond forming reaction that is widely used in the synthesis of important intermediates or end-products for perfumes, pharmaceuticals, calcium antagonists and polymers [2, 3]. The reaction is catalyzed by bases, acids or materials containing both acidic and basic sites [4]. Bases such as

✉ Balaga Viswanadham
balagiav@ukzn.ac.za; visubalaga@gmail.com

[1] Catalysis Research Group, School of Chemistry and Physics, University of KwaZulu-Natal, Durban 4000, South Africa

[2] Catalysis Division, Indian Institute of Chemical Technology, Hyderabad 500007, India

ammonia, the primary amines, secondary amines and their salts, Lewis acids such as $CuCl_2$, $ZnCl_2$ and SmI_2 and the ZnY zeolites are some of the examples that have been employed in the Knoevenagel condensation reaction [5–9]. Numerous types of heterogeneous catalysts containing both acidic and basic sites have been reported in the literature [10–15]. Activated Mg–Al hydrotalcite was used for the first time in condensation reactions producing excellent yields. However, all the reactions were carried out using toluene and DMF as solvents [16]. Joshi et al. [17] studied the effect of incorporating other alkali metals in NaX- type zeolites in deciding the activity in the Knoevenagel condensation reaction. They found that an increase in the cation kinetic diameter improved activity by 50 %. In a number of studies conducted by Corma and co-workers [18–21], solid base catalysts such as zeolites, sepiolites and hydrotalcites have been used to prepare prepolymers of malononitrile with a series of ketones. In all the condensation reactions studied, they proposed that the controlling step was not the proton abstraction as assumed, but the attack of the carbonyl group by the carbanion. In the studies mentioned, although some reactions are carried out in heterogenous medium, all of the catalytic reactions required the presence of solvents. To avoid the use of organic solvents, water as a desirable solvent was investigated [22, 23]. However, in the bulk phase production of fine chemicals, large amounts of water are required which needs purification post reaction for environmental reasons. Thus, it has become imperative to develop catalytic systems that are efficient in organic reactions without the use of a solvent. Metzger [24] and Tanaka and Toda [25] emphasized very emphatically in their paper and review, respectively, the importance in carrying out solvent free reactions. Pillai et al. [26] studied the Knoevenagel reaction using iridium and platinum hydroxyapatites. Hydroxyapatites (HAp) are bifunctional materials with both acidic and basic sites in the crystal lattice. Their results showed that the IrHAp catalyzed reactions gave higher yields than PtHAp catalyzed reactions, but both IrHAp and PtHAp catalyzed reactions were very efficient in the Knoevenagel reaction without the use of a solvent, with the overall production of excellent yields.

In our work, we report the solvent free liquid phase Knoevenagel condensation of benzaldehyde and substituted benzaldehydes with malononitrile over vanadium substituted phosphomolybdic acid catalysts with various V/P mole ratios. The aim of this investigation is to study the effect of V/P mole ratio of the catalyst during the Knoevenagel condensation reaction and the effect of substituent on the benzaldehyde on the catalysis.

2 Experimental

2.1 Catalyst Synthesis

The solid acid catalysts containing vanadium, $H_4PMo_{11}VO_{40}$ (PMoV1), $H_5PMo_{10}V_2O_{40}$ (PMoV2) and $H_6PMo_9V_3O_{40}$ (PMoV3) were prepared using V_2O_5 (Sigma Aldrich), $H_3PMo_{12}O_{40}$ (Sigma Aldrich), MoO_3 (Fluka) and H_3PO_4 (S.D Fine-Chem. Ltd.) according to the method reported previously [27]. For the detailed synthesis of PMoV1, 14.4 g of MoO_3 and 0.91 g of V_2O_5 were placed in 250 mL distilled water, refluxed at 100 °C with stirring, followed by the drop wise addition of 1.15 g of 85 % H_3PO_4. The resulting slurry was maintained at this temperature, under reflux, for 24 h. The solid was collected after evaporation of the slurry in a vacuum heater set at 60 °C. A similar procedure was followed for the synthesis of PMoV2 and PMoV3.

2.2 Catalyst Characterization

Powder X-ray diffraction patterns of samples were obtained with Bruker D8 Advance diffractometer, using Cu Kα radiation (1.5406 Å) at 40 kV and 30 mA. The measurements were recorded in steps of 0.045° with a count time of

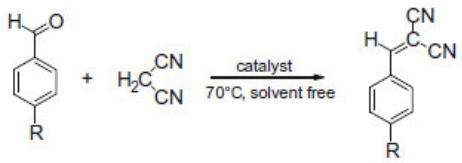

Scheme 1 Knoevenagel condensation of benzaldehyde with malononitrile over heteropolyacids

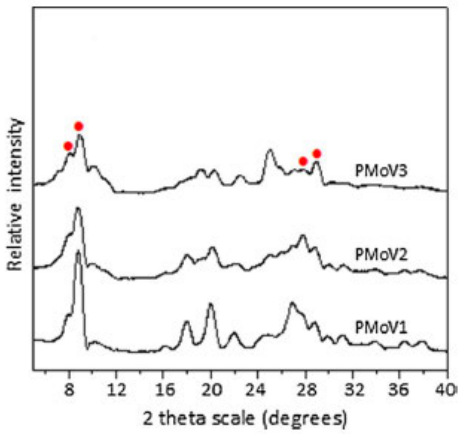

Fig. 1 X-ray diffraction patterns of PMoV1, PMoV2 and PMoV3 catalysts

0.5 s in the range of 2–40°. BET surface area and NH_3 temperature programmed studies of the catalysts were conducted on a Micromeritics Auto Chem 2910 instrument. For TPD studies, about 50 mg of sample was pretreated at 200 °C for 2 h by passing through helium at 50 mL/min). After pretreatment, the sample was saturated with a mixture of 10 % NH_3 in helium at 80 °C for 1 h and subsequently flushed with helium flowing at 50 mL/min to remove physisorbed ammonia. The entire TPD analysis was carried out from ambient temperature to 700 °C at a ramp rate of 10 °C/min. Ex-situ pyridine adsorbed FT-IR experiments spectra of samples were carried out to investigate the nature of acidity, such as Brønsted and Lewis acid sites present on the catalyst. The spectra were recorded on a Perkin-Elmer ATR spectrometer at room temperature. Prior to analysis, pyridine adsorption experiments were carried out by placing a drop of pyridine on a small amount of the catalyst followed by evacuation in air for 1 h to remove the reversibly adsorbed pyridine. FT-IR spectra of catalysts were recorded on the Nicolet 670 spectrometer by the KBr disc method,

Table 1 Results of BET surface area and NH_3-TPD analysis

Catalyst	BET surface area (m^2/g)	Acidity (mmol/g) NH_3		
		Weak (A)	Moderate (B)	Strong (C)
PMoV1	8	0.6	0.3	1.7
PMoV2	4.5	0.7	0.5	1.2
PMoV3	2	0.4	0.6	0.9

Desorption temperature: A = 50–150 °C, B = 150–300 °C, C = 300–500 °C

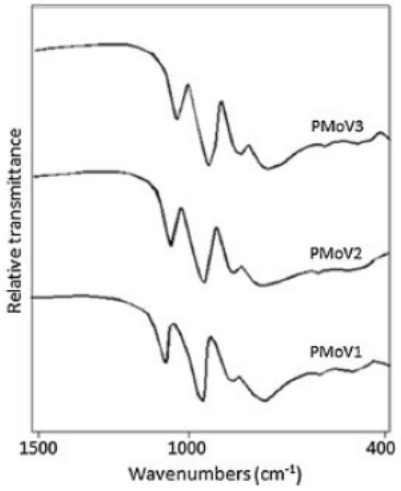

Fig. 2 FT-IR spectra of PMoV1, PMoV2 and PMoV3 catalysts

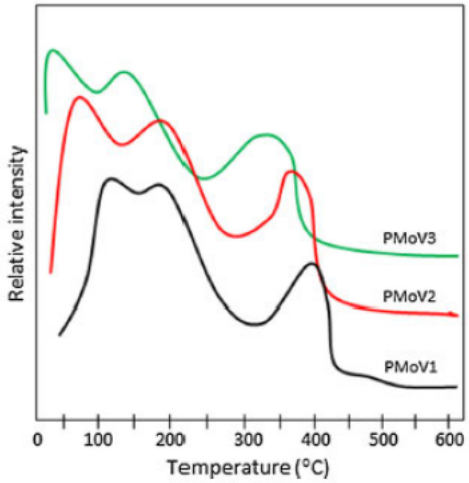

Fig. 4 NH_3 -TPD profile of PMoV1, PMoV2 and PMoV3 catalysts

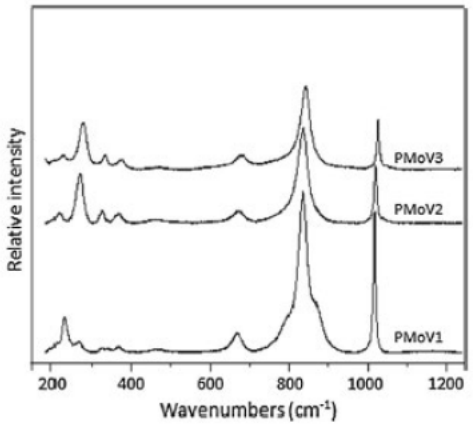

Fig. 3 Raman spectra of PMoV1, PMoV2 and PMoV3 catalysts

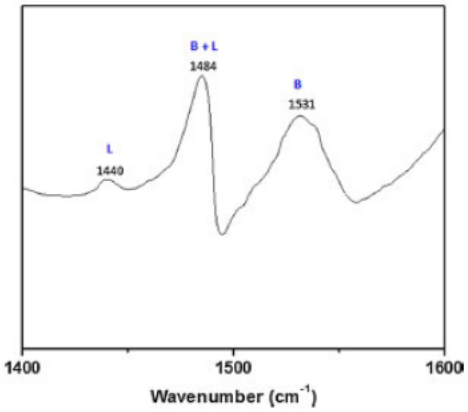

Fig. 5 The pyridine adsorbed FT-IR spectrum of the PMoV3 catalyst

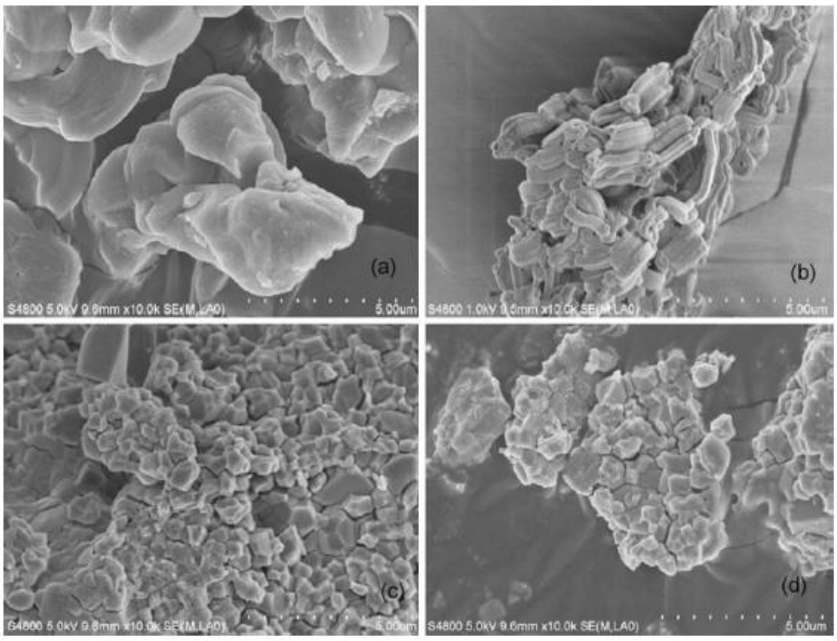

Fig. 6 SEM images of **a** PMA, **b** PMoV1, **c** PMoV2 and **d** PMoV3 catalysts

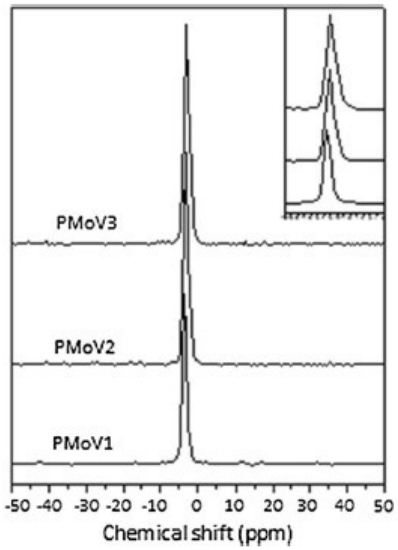

Fig. 7 ^{31}P MAS NMR of PMoV1, PMoV2 and PMoV3 catalysts

whereas The Raman spectra were collected using a Horbia–Jobin–Yvon LabRam high resolution spectrometer equipped with a confocal microscope with 2400/900 grooves/mm gratings and a notch filter. The visible laser excitation at 532 nm (visible/green) was supplied by a Yag double diode pumped laser (20mW). The surface morphology of materials was examined by scanning electron microscopy (SEM) with a Hitachi S-4800 microscope. Solid state ^{31}P MAS NMR spectra were recorded at ambient temperature using 4 mm diameter zirconia rotors with a spinning rate of 7 kHz on a Jeol ECA-500 NMR spectrometer.

2.3 Catalytic Activity

The Knoevenagel condensation of benzaldehyde and its derivatives was carried out in a 25 mL reaction flask, equipped with a condenser, at 70 °C without solvent (Scheme 1). In typical reaction, 10 mmol of benzaldehyde, 10 mmol of malononitrile and 2 mol % of the catalyst were placed in the flask and refluxed at 70 °C. The reaction was constantly monitored by thin layer chromatography (TLC) and after completion of reaction, the resulting mixture was analysed by GC–MS using a HP 6890 Series Gas Chromatograph coupled with a mass selective detector. The catalyst was then recycled and used for the same reaction.

3 Results and Discussion

3.1 Characterization Results

The XRD profiles the vanadium substituted phosphomolybdic acid catalysts are shown in Fig. 1. The Bragg

Table 2 Catalytic results over PMA and different V/P mole ratio of vanadium containing PMA catalyst

Entry	R	Catalyst (2 mol%)	Product	Time (min)	Con. (%)	Sel. (%)	Yield (%)
1	H	-	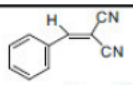	50	8	100	8
2	OMe	-	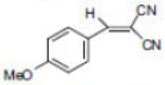	50	6	100	6
3	Cl	-	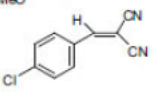	50	7	100	7
4	NO_2	-	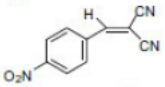	50	10	100	10
5	H	PMA	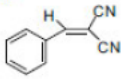	50	80	100	80
6	OMe	PMA	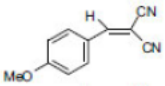	25	70	100	70
7	Cl	PMA	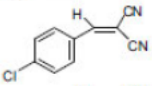	30	60	100	60
8	NO_2	PMA	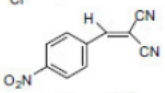	55	85	100	85
9	H	PMoV1	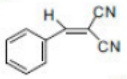	45	86	100	86
10	OMe	PMoV1	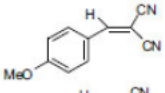	40	85	100	85
11	Cl	PMoV1	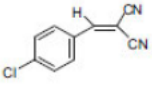	50	63	100	63
12	NO_2	PMoV1	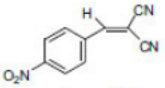	45	90	100	90
13	H	PMoV2	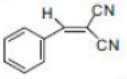	30	90	100	90
14	OMe	PMoV2	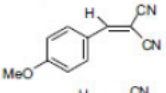	45	88	100	88
15	Cl	PMoV2	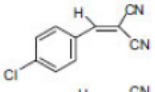	40	76	100	76
16	NO_2	PMoV2	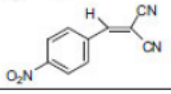	35	94	100	94

Table 2 continued

Entry	R	Catalyst (2 mol%)	Product	Time (min)	Con. (%)	Sel. (%)	Yield (%)
17	H	PMoV3	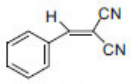	10	96	100	96
18	OMe	PMoV3	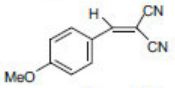	55	94	100	94
19	Cl	PMoV3	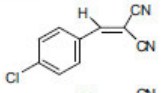	30	85	100	85
20	NO_2	PMoV3	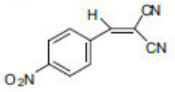	15	99	100	99

Reactions were carried out with benzaldehyde (10 mmol), malononitrile (10 mmol) with catalysts (2 mo%), solvent free, temperature = 70 °C. Yield based GC–MS analysis

diffraction wide angle reflections at $2\theta = 8.3°$, 9.0°, 27.8° and 29.1° are observed and these peaks correspond to the crystalline nature of the Keggin type heteropolyacid [27]. The characteristic diffraction peaks are retained with increasing V/P mole ratios [28].

The pure and vanadium substituted PMA catalysts were characterized by FT-IR spectroscopy in the range of 400–1500 cm^{-1} and the spectra are shown in Fig. 2. The catalysts exhibit well defined IR bands in the range of 1100–700 cm^{-1}. The bands are assigned to P–O, Mo=O and Mo–O–Mo vibrations and are located at 1080–1060, 990–960 and 900–760 cm^{-1}, respectively [29, 30]. There is a slight shift in IR bands with increase of the V/P mole ratio of V substituted PMA catalysts, indicating that vanadium is incorporated in the Keggin ion structure of PMA catalyst. These results agree well with the XRD patterns obtained for the catalysts.

The structure of the Keggin ion in vanadium containing PMA catalysts with various V/P mole ratios, characterized by Raman spectroscopy, in the range 200–1200 cm^{-1}, is shown in Fig. 3. All the samples possess a Raman band at 1010 cm^{-1} which is characteristic for the Keggin structure. Other bands at 849, 817, 656 and 286 cm^{-1} are assigned to Mo–O_t, Mo–O_b–Mo, Mo–O_c–Mo and Mo–O_a, respectively [31]. There is a significant shift in the characteristic Keggin ion Raman bands towards the higher region with an increase in the V/P mole ratio, suggesting that vanadium is incorporated into the PMA catalysts.

The results of the BET surface area of the vanadium substituted phosphomolybdic acid catalyst with different V/P mole ratios are summarized in Table 1. From the results, the surface area decreases as V/P mole ratio of the catalyst is increased, probably due to bulk crystallite formation. These catalysts appear to be more crystalline.

Figure 4 shows the ammonia TPD profile of the PMoV1, PMoV2 and PMoV3 samples. All the samples exhibit three types of acid sites, located between 50 and 150 °C, 150 and 300 °C and 300 and 500 °C. The peak observed between 50 and 150 °C is attributed to weak acidic sites, the peak located between 150 and 300 °C, to moderate acidic sites and the peak between 300 and 500 °C, exclusively to strong acidic sites (Table 1). An increase in V/P mole ratio in the vanadium substituted phosphomolybdic acid catalysts shows a significant decrease in acidity.

The nature of the acidic sites was evaluated by pyridine adsorbed FT-IR spectroscopy on the PMoV3 catalyst (Fig. 5). It is shown that most are Brønsted acidic sites with a few Lewis acidic sites.

Scanning electron microscopy images of pure PMA and the vanadium substituted phosphomolybdic acid catalysts are shown in Fig. 6. The surface morphology of the PMA and PMoV1 compounds appears as cylindrical particles, whereas PMoV2 and PMoV3 have a cubic-like morphology. In addition, a bulk-like structure formation is observed for the PMoV3.

To understand the coordination and the chemical environment of P in the catalysts, ^{31}P MAS NMR was studied. The results are shown in Fig. 7. With an increase in the V/P mole ratio, a change in the chemical shift from −3.9 δ for PMoV1 catalyst to −2.5 δ for PMoV3 is observed, attributed to the change in the local environment of ^{31}P with an increase in the V/P mole ratio of the catalyst [32–34]. When these catalysts were compared to the acidity of PMA, PMoV1 was found to be more acidic than PMA, whereas at higher loadings of vanadium, the catalysts were less acidic than the pure PMA catalyst.

Table 3 Catalytic results of regenerated PMoV3 catalyst

Recycle entry	R	Product	Con. (%)	Sel. (%)	Yield (%)
1	H	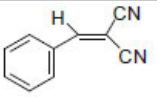	99	100	99
	OMe	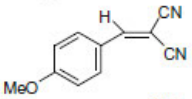	96	100	96
	Cl	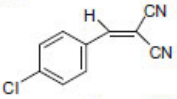	84	100	84
	NO_2	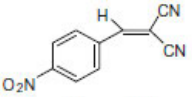	96	100	96
2	H	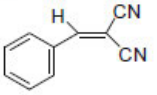	95	100	95
	OMe	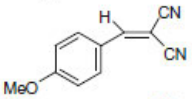	92	100	92
	Cl	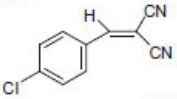	82	100	82
	NO_2	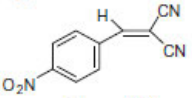	93	100	93
3	H	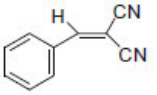	92	100	92
	OMe	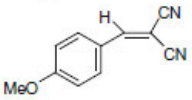	90	100	90
	Cl	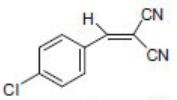	78	100	78
	NO_2	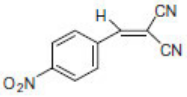	89	100	89

3.2 Catalytic Activity Studies

The catalytic properties of pure PMA and vanadium substituted phosphomolybdic acid samples with different V/P mole ratios was tested for the liquid phase Knoevenagel condensation reaction, without solvent at 70 °C. The blank reactions gave up to 5 to 10 % yield towards the desired product in 50 min. Aldehyde conversion increased significantly with increasing vanadium content in the heteropolyacid (Table 2). The higher aromatic aldehyde

Table 4 Catalytic results comparison of Knoevenagel reaction over various catalysts

Catalyst	Catalyst amount (mol%)	Reaction temperature (°C)	Solvent	Reaction time (min)	Yield (%)	Ref
$InCl_3$	10	60	Toluene/ AC_2O	480	94	35
$H_3PW_{12}O_{40}$	1	100	H_2O	15	91	22
$H_6PMo_9V_3O_{40}$ (PMoV3)	2	70	–	10	96	Present work

conversion and yield towards the desired condensation product are observed in the case of higher V/P mole ratio of the PMoV3 catalyst. These results suggest that conversion of a particular aldehyde and yield towards the desired product can be controlled by changing the vanadium content, resulting in altering the acidity of the catalyst. The results clearly show that the catalyst with a lower acidity exhibits superior catalytic performance.

The Knoevenagel reaction was further studied with compounds containing activating and deactivating groups substituted on the benzaldehyde. The results, given in Table 2, clearly show that higher conversions and yields are obtained with benzaldehyde and 4-nitro benzaldehyde than the methoxy and chloro substituted benzaldehyde. This is mainly due to the withdrawing group decreasing the electron density around the carbonyl group and therefore enhancing the conversion in presence of the heteropolyacid.

There was evidence no leaching of vanadium during the reaction. This was confirmed by ICP-AES analysis on the fresh and used catalyst. In both cases, the P/Mo/V atomic ratio was determined to be 1.00/9.01/3.05. The used catalyst was regenerated and studied for 3 cycles and the results are reported in Table 3. There was a slight difference in the activity and selectivity towards the desired products for all 3 cycles.

From Table 4, Ogiwara et al. [35] reported that combination of a catalytic amount of $InCl_3$ in acetic anhydride remarkably promotes the Knoevenagel condensation of an aldehyde with an activated methylene group, producing a 94 % yield. Oskooie et al. [22], on the other hand, showed 91 % yield for the condensation reaction using phosphotungstic acid in water. Both these processes use solvents and require higher reaction temperatures to attain the yields mentioned. In our study, the PMoV3 catalyst consistently produces a yield of about 96 % of the condensation product in a solvent free environment at a reaction temperature of 70 °C. It is assumed that due to the presence of largely Brønsted acidic sites, as shown by pyridine adsorbed FT-IR spectroscopy, the reaction is understood to proceed via Brønsted acidic sites or protons present in the catalyst (Fig. 5).

4 Conclusion

Keggin-type vanadium substituted phosphomolybdic acid catalysts have been synthesized with different vanadium to phosphorous mole ratios and characterized successfully by powder XRD, FT-IR and Raman spectroscopy. NH_3-TPD results confirmed that the acidity of the catalysts decreases with an increase in the V/P mole ratio and these results are supported by ^{31}P NMR analysis. The catalytic properties strongly depend on the amount of vanadium incorporated into PMA, the higher the V/P mole ratio, the higher the catalytic activity. The vanadium containing PMA catalysts are competitive, in most cases superior for the Knoevenagel reaction under a solvent free condition when compared to most catalytic systems even employing solvents.

Acknowledgments B Viswanadham thanks to the University of KwaZulu-Natal for the award of the AES Postdoctoral Research Fellowship.

References

1. Trost BM (1991) Comprehensive organic synthesis. Elsevier, Oxford, p 133
2. Knoevenagel L (1898) Ber 31:258
3. Enders D, Muller S, Demir AS (1988) Tetrahedron Lett 29:6437
4. Reeves RL, Patai S (1996) The chemistry of carbonyl compounds. Interscience Publishers, New York 567
5. Jones G (1967) Org React 15:204
6. Attanasi O, Fillippone P, Mei A (1983) Syn Commun 13:1203
7. Shanthan Rao P, Venkatratnam RV (1991) Tetrahedron Lett 32:5821
8. Bao W, Zhang Y, Wang J (1996) Syn Commun 26:3025
9. Saravanamurugan S (2006) Appl Catal A Gen 298:8
10. Boullet FT, Focucad A (1982) Tetrahedron Lett 23:4927
11. Macquarrie DJ, Clark JH, Lambert A, Gmode JE, Priest A (1997) React Funct Polym 35:153
12. Brunel D (1993) Micropor Mesopor Mater 27:329
13. Hein RW, Astle MJ, Shelton JR (1961) J Org Chem 26:4874
14. Moison H, Boullet FT, Focaud A (1987) Tetrahedron 43:537
15. Bigi F, Chesini L, Maggi R, Sartori G (1999) J Org Chem 64:1033
16. Kantam ML, Choudary BM, Reddy CV, Rao KK, Figueras F (1998) Chem Commun 1033
17. Joshi UD, Joshi PN, Tamhankar SS, Joshi VV, Rode CV, Shiralkar VP (2003) Appl Catal A Gen 239:209

18. Climent MJ, Corma A, Forens V, Frau A, Lopez RG, Iborra S, Primo J (1996) J Catal 163:392
19. Corma A, Fornes V, Aranda RMM, Garcia H, Primo J (1990) Appl Catal 59:237
20. Corma A, Aranda RMM, Sanchez F, Guinst M, Barrault J, Bouchoule C, Duprez D, Maurel R, Montassier C (1991) Stud Surf Sci Catal 62:503
21. Corma A, Aranda RMM (1993) Appl Catal A 105:271
22. Oskooie HA, Heravi MM, Derikvand F, Khorasani M (2006) Syn Commu 36:2819
23. Bhunia S, Saha D, Koner S (2011) Langmuir 27:15322
24. Metzger JO (1998) Ang Chem Inter Ed 37:2975
25. Tanaka K, Toda F (2000) Chem Rev 100:1025
26. Pillai MK, Singh S, Jonnalagadda SB (2011) Kinet Catal 52:536
27. Fumin Z, Maiping G, Hanqing G, Jun W (2007) Front Chem Eng China 1:296
28. Sen R, Bera R, Ashis B, Gutlich P, Ghosh S, Mukherjee AK, Koner S (2008) Langmuir 24:5970
29. Ilkenhans T, Herzag B, Braun T, Schlogl R (1995) J Catal 153:275
30. Zhang J, Tang Y, Li G, Hu C (2005) Appl Catal A Gen 278:251
31. Predoeva A, Damyanova S, Gaigneaux EM, Petrov L (2007) Appl Catal A Gen 319:14
32. Raj NKK, Deshpande SS, Ingle RH, Raja T, Manikandan P (2004) Catal Lett 24:1001
33. Yue ZY, Bao B, Liu RL, Xi HS, Yong H (2006) Chin J Chem 24:1001
34. Tang Y, Zhang J (2006) J Serb Chem Soc 71:111
35. Ogiwara Y, Takahashi K, Kitazawa T, Sakai N (2015) J Org Chem 80:3101

Catal Lett (2016) 146:1470–1477
DOI 10.1007/s10562-016-1777-7

The Role of Copper Exchanged Phosphomolybdic Acid Catalyst for Knoevenagel Condensation

Balaga Viswanadham[1] · Jhansi Pedada[1] · Holger B. Friedrich[1] · Sooboo Singh[1]

Received: 18 May 2016 / Accepted: 19 May 2016 / Published online: 2 June 2016

Abstract Cu exchanged heteropolyacid catalysts were synthesized by ion exchange method and characterized using various physico-chemical techniques such as X-ray diffraction (XRD), FT-IR, Raman, BET surface area, temperature programmed desorption (TPD) of ammonia, ^{31}P NMR, pyridine adsorbed FT-IR spectroscopy, ICP-AES and STEM analysis. XRD diffractograms shows crystallites of heteropolyacid, while FT-IR and Raman spectra indicate that the Keggin ion is retained in the catalysts. ^{31}P NMR, ammonia TPD and pyridine adsorbed FT-IR spectra results suggest that acidity decreases once Cu was incorporated in the heteropolyacid catalyst. For the Knoevenagel condensation reaction, the Cu exchanged phosphomolybdic acid (Cu–PMA) exhibits better catalytic performance than the phosphomolybdic acid (PMA) catalyst and this is related closely with the structural and acidic properties of the catalyst.

Graphical Abstract

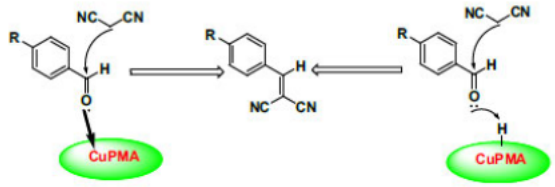

✉ Balaga Viswanadham
Balagiav@ukzn.ac.za

[1] Catalysis Research Group, School of Chemistry and Physics, University of KwaZulu-Natal, Durban 4000, South Africa

Keywords Cu exchanged PMA · Bi-functional · Raman spectroscopy · TPD · Py-FTIR · ^{31}P NMR · Acidity

1 Introduction

In recent years, the use of heteropolyacids (HPAs) or polyoxometalates as heterogeneous catalysts has received considerable interest in different areas of organic synthesis, mainly due to their tuneable acid and oxidation functionalities [1, 2]. Heterogeneous catalysts are preferred over conventional homogeneous acid catalysts as they can be easily recovered from the reaction mixture by simple separation. As a result, heteropoly-acid catalysts can be reused after activation or without activation, leading to a more economically sustainable process under solvent free conditions [3]. Heteropoly-acid catalysts are used in several reactions such as oxidation and acid catalyzed transformations [4–11]. Among these reactions, the Knoevenagel condensation reaction is an important C–C bond forming reaction and its products are extensively used as intermediates in the manufacture of perfumes, pharmaceuticals and polymers [12, 13]. This reaction was also studied extensively using catalysts possessing acidic, basic or both acidic and basic functionalities and among them were ammonia, the primary amines, secondary amines and its salts, Lewis acids such as metal halides and zeolites [14–23]. It has been proposed that in the acid catalyzed reaction, the rate determining step is the attack of a proton on the carbonyl oxygen, thereafter the attack of the electron deficient carbon in carbonyl group by an active methylene group. In the base catalyzed reaction, the rate determining step is the abstraction of a proton from the active methylene group to produce a carbanion

which then proceeds to attack the carbonyl group [23]. Hydroxyapatites, which have both acidic and basic sites, proceeds by either of the two pathways mentioned [22]. In addition, metal promoted hydroxyapatites showed superior catalytic performance for this reaction [22, 24]. In studies conducted by Viswanadham et al. [4] and Khorasani and co-workers [25], using vanadium substituted phosphomolybdic acid and phosphotungstic acid catalysts respectively, it was shown that the reaction proceeds via the attacking of a proton on the carbonyl oxygen lone pair. In the view of several researchers, heteropolyacid catalysts were found to be robust, easily recyclable and showed better catalytic properties than other catalysts. Recently, copper has received attention and has been the metal of choice in a variety of catalyst formulations. These copper catalysts were used in well-known named reactions such as the Ullman reaction, the Sandmeyer reaction and Click chemistry [26–28]. Stark and coauthors [29] studied the Knoevenagel reaction over various catalysts incorporating metals such as Fe, Co, Cu, Ag and Au. Among these catalysts, the copper substituted catalyst produced better catalytic results. In addition, they showed that copper concentration in the catalyst influenced the catalytic activity in reaction.

In this work, we report the solvent free liquid phase Knoevenagel condensation of aromatic aldehydes with malononitrile over copper exchanged heteropolyacids with the main aim to study the effect of copper exchanged HPA and the effect of the substituent on the aromatic aldehyde during the condensation reaction. This study is also investigates the relationship between the acidity of catalyst and activity.

2 Experimental

2.1 Catalyst Synthesis

$H_3PMo_{12}O_{40}$ and $H_3PW_{12}O_{40}$, copper sulphate hydrate and barium hydroxide were procured from Sigma-Aldrich (RSA). The Cu exchanged catalysts were synthesized according to a method described previously [30]. Using this procedure, 0.18 g of barium hydroxide was added to an aqueous mixture of 2.0 g of phosphomolybdic acid in 5 mL distilled water. Thereafter, 0.16 g of $CuSO_4 \bullet 5H_2O$ was added to replace barium with copper by precipitating the barium as $BaSO_4$. The $Cu_{1.5}PMo_{12}O_{40}$ solid was recovered by centrifugation and dried 100 °C for 10 h in an oven. The $Cu_{1.5}PW_{12}O_{40}$ was synthesised by the method described earlier.

2.2 Catalyst Characterization

Powder XRD patterns of samples were obtained with Bruker D8 Advance diffractometer, using Cu Kα radiation (1.5406 Å) at 40 kV and 30 mA. The measurements were recorded in steps of 0.045° with a count time of 0.5 s in the range of 2°–40°. BET surface areas of the catalyst were determined using a Micromeritics AutoChem 2910 instrument with nitrogen physisorption at −196 °C, taking 0.0162 nm^2 as the cross-sectional of dinitrogen. FT-IR spectra were recorded on a GC-FT-IR Nicolet 670 spectrometer by the KBr disc method and pyridine adsorption experiments were also studied [5]. The Raman spectra of the samples were collected with a Horbia-Jobin-Yvon LabRam-HR spectrometer equipped with a confocal microscope, 2400/900 grooves/mm gratings and a notch filter. The Visible Laser excitation a 532 nm (visible/green) was supplied by a Yag doubled diode pumped laser (20 mW). The scattered photons were focused on to a single stage monochromator and measured with a UV-sensitive LN_2 cooled CCD detector (Horbia-Jobin-Yvon CCD-3000 V). Distribution of elements in the catalysts was examined by STEM analysis. Solid state ^{31}P NMR spectra were recorded at ambient temperature by using 4 mm diameter zirconia rotors with a spinning rate of 7 kHz on an ECA-500 NMR spectrometer (JEOL Ltd). Temperature programmed desorption (TPD) studies of NH_3 were conducted on AutoChem 2910 (micromeritics, USA) instrument. In a typical experiment for TPD studies, about 50 mg of oven dried sample (dried at 100 °C for 2 h) was placed in a U-shaped quartz sample tube. Prior to TPD studies, the catalyst sample was pretreated at 200 °C for 2 h by passing helium (99.999 %, 50 mL/min). After pretreatment, the sample was saturated with high purity 10 % ammonia in helium (50 mL/min) at 80 °C for 1 h and subsequently flushed with helium flow (50 mL/min) to remove physisorbed ammonia. TPD analysis was conducted from ambient temperature to 600 °C at a heating rate of 10 °C/min. The composition of catalysts was determined by ICP-AES analysis using a PerkinElmer Optima 5300 DV spectrometer and UV–Vis spectra was recorded on the PerkinElmer Lambda 35 UV–Vis spectrophotometer.

2.3 Catalytic Activity

The Knoevenagel condensation was carried out in a 25 mL round bottom flask at 70 °C, under reflux, in a solvent free condition with aromatic aldehyde and malonitrile/ethyl cyanoacetate as reactants in the presence of a catalyst (Scheme 1).

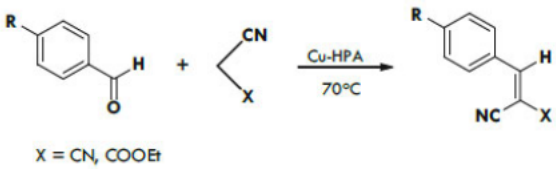

X = CN, COOEt

Scheme 1 Knoevenagel reaction over Cu exchanged heteropolyacid catalysts

In this reaction, 10 mmol of aldehyde and 10 mmol of malononitrile with 2 mol% of catalyst were added to the flask and the reaction was carried out at 70 °C. The reaction was monitored by thin layer chromatography, and upon completion, the mixture was cooled to room temperature. Distilled water was added so that the catalyst which is soluble in water can be separated easily from the product which remains in the organic layer. The products were analyzed by a HP 6890 GC–MS equipped with a mass selective detector (5973 Mass Selective Detector).

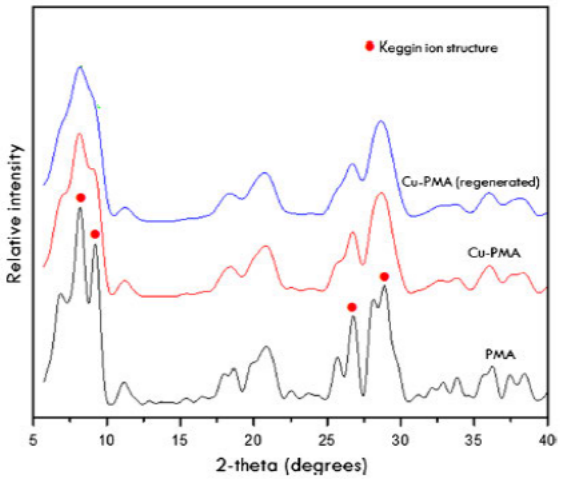

Fig. 1 XRD patterns of PMA, Cu–PMA (fresh) and Cu–PMA (regenerated) catalysts

3 Results and Discussion

3.1 Catalyst Characterization

3.1.1 XRD Studies

XRD patterns of the phosphomolybdic acid (PMA), copper exchanged PMA (Cu–PMA) and regenerated Cu–PMA catalysts are shown in Fig. 1. These patterns showed diffraction peaks at 8.2°, 9.1°, 26.5° and 28.8° and were assigned to the characteristic diffraction peaks of Keggin ion structure [4]. There was a significant decrease in the intensity of characteristic peaks once copper was incorporated into the phosphomolybdic acid. The Keggin ion structure was retained although the crystalinity is decreased slightly for the copper exchanged catalysts.

3.1.2 Elemental Composition and BET Surface Area

ICP-AES analysis of the Cu–PMA catalysts resulted in the P:Mo:Cu atomic ratio to be 1.00:11.98:1.48. The used catalyst was regenerated and when studied for five cycles showed an atomic ratio of 1.00:11.91:1.45 when compared to fresh catalyst, indicating minimal leaching. The Keggin anion density was calculated previously and reported by Viswanadham et al. [5] and it was observed that PMA shows more Keggin ion density than the Cu–PMA catalyst. The BET surface area of pure PMA, fresh and regenerated Cu–PMA is shown in Table 1. The surface area increased significantly for the copper exchanged catalysts. These results correlate with the crystalinity which is lower in the case of the copper exchanged PMA than the pure PMA catalyst and this could be related to the Keggin ion density, impacting on the BET surface area of the catalysts. The BET surface area of the regenerated catalysts decreased slightly when compared to fresh Cu–PMA catalyst.

3.1.3 Fourier Transform Infrared and Raman Spectroscopy

The IR spectra of the PMA, fresh Cu–PMA and regenerated Cu–PMA catalysts are shown in Fig. 2. PMA shows

Table 1 Results of BET surface area and NH_3-TPD analysis

Catalyst	BET surface area (m^2/g)	Acidity (mmol/g)		
		Weak (A)	Moderate (B)	Strong (C)
PMA	2.5	0.6	0.2	1.6
Cu–PWA	7.9	0.5	0.5	1.2
Cu–PMA	6.5	0.5	0.8	0.7
Cu–PMA (regenerated)	6.0	0.6	0.7	0.7

Desorption temperature: A = 50–150°C, B = 150–300°C, C = 300–500°C

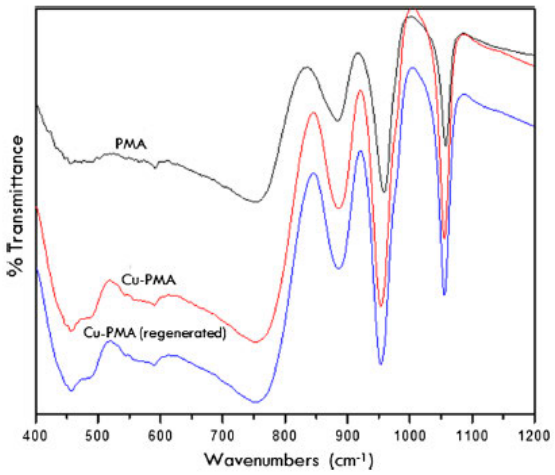

Fig. 2 FT-IR spectra of PMA, Cu–PMA (fresh) and Cu–PMA (regenerated) catalysts

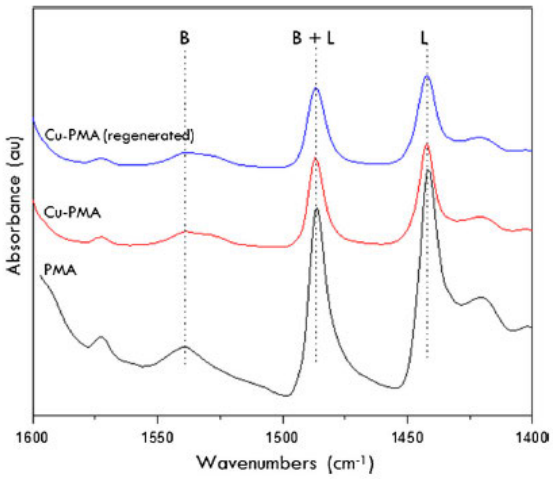

Fig. 4 Pyridine adsorbed FT-IR spectra of PMA, Cu–PMA (fresh) and Cu–PMA (regenerated) catalysts

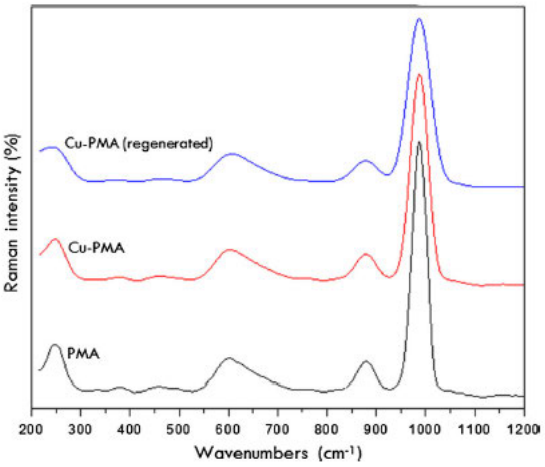

Fig. 3 Raman spectra of PMA, Cu–PMA (fresh) and Cu–PMA (regenerated) catalysts

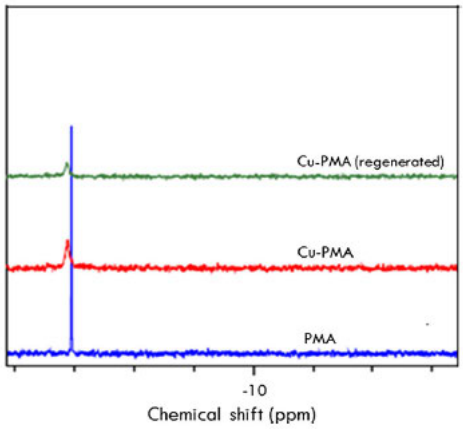

Fig. 5 ^{31}P NMR of PMA, Cu–PMA (fresh) and Cu–PMA (regenerated) catalysts

characteristic Keggin ion IR bands at 1059, 959, 884 and 756 cm^{-1} which are assigned to P–O, Mo=O and Mo–O_c–Mo and Mo–O_e–Mo respectively [4]. There is a shift in these bands for the fresh and regenerated Cu–PMA catalysts located at 1057, 957, 886, 754 cm^{-1} which is minimal, suggesting that the Keggin ion of heteropolyacid is intact after copper exchange.

From Raman spectra (Fig. 3), the pure PMA shows typical Keggin ion bands at 987, 880, 603 and 245 cm^{-1} which were assigned to M–O_t, Mo–O_b–Mo, Mo–O_c–Mo and Mo–O_a, respectively [4]. In the case of fresh and regenerated Cu–PMA catalysts, these bands are retained, further illustrating that these catalysts retained the Keggin ion structure.

3.1.4 Catalyst Acidity

Ammonia TPD of PMA shows three types of acid sites which are located at 50–150, 150–300 and 300–500 °C corresponding to weak, moderate and strong acidic sites, respectively (Table 1). With the addition of copper, there is a decrease in the strong acid sites resulting in an overall decrease in the surface acidity which could promote the overall activity.

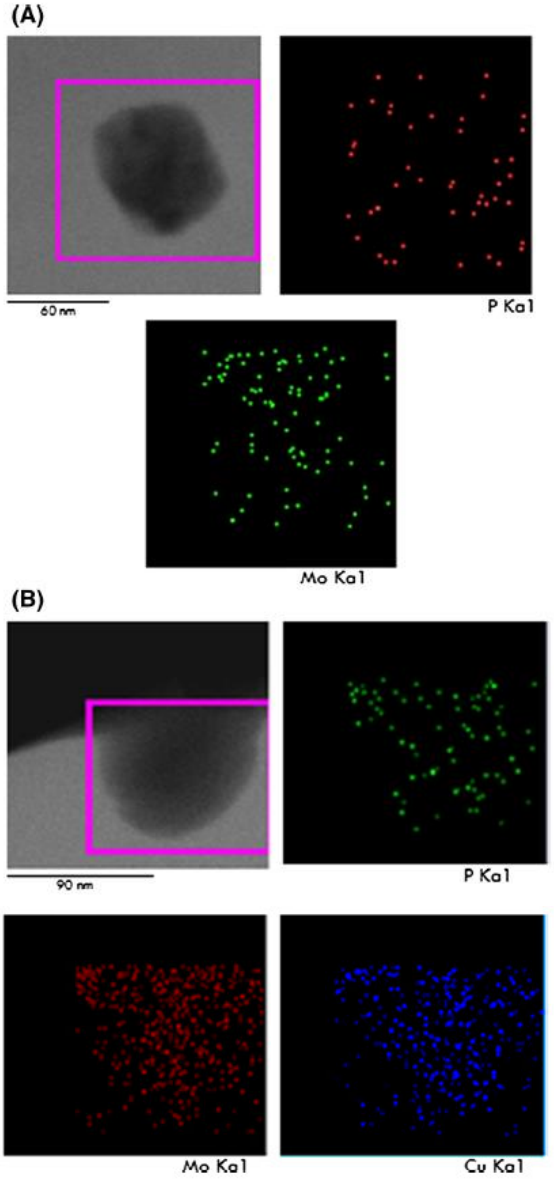

Fig. 6 STEM images of **a** PMA, **b** Cu–PMA catalysts

The ex situ pyridine adsorbed FT-IR spectra of pure PMA, fresh and regenerated Cu–PMA catalysts were recorded in the range of 1600–1400 cm^{-1} (Fig. 4). Bands at 1538, 1486 and 1442 cm^{-1} were attributed to Brønsted, Brønsted and Lewis and Lewis acidic sites, respectively. Brønsted and Lewis acidic sites decreased in the copper exchanged PMA catalysts when compared to pure PMA catalyst. The regenerated catalyst possessed similar acidity when compared to the fresh Cu–PMA catalyst.

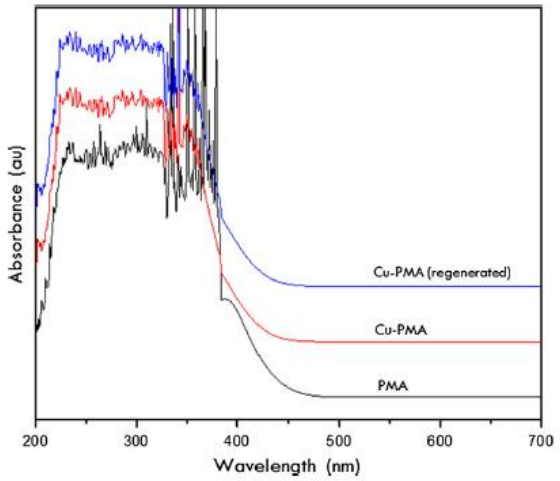

Fig. 7 UV–Vis spectra of PMA, Cu–PMA (fresh) and Cu–PMA (regenerated) catalysts

3.1.5 ^{31}P NMR Analysis

^{31}P NMR analysis of pure PMA, fresh and regenerated Cu–PMA catalysts was studied to understand the chemical environment of P in the catalysts and the results are shown in Fig. 5. The pure PMA shows a −3.9 ppm chemical shift value, whereas the Cu–PMA catalysts exhibit a ppm value at −3.6. The result suggests a slight change in the local environment of ^{31}P after copper exchange although the Keggin ion structure of the catalysts is maintained [4].

3.1.6 STEM Analysis

BF-STEM imaging with chemical analysis was conducted to map the structure and relative distribution of the elements (Fig. 6). PMA and Cu–PMA shows uniform distribution of all the elements in these materials.

3.1.7 UV–Vis Spectroscopy

In the UV–Vis spectra of the catalysts (Fig. 7), PMA catalyst exhibits an edge band at 468 nm and in the case of fresh and regenerated Cu–PMA catalyst, this band is observed at 461 nm due to O → Mo charge transfer band of $PMo_{12}O_{40}$. This concurs with the findings of Barteau et al. [31] and this suggests that copper exchanges with protons and not with Mo.

3.2 Catalytic Activity Studies

Catalytic control experiments were conducted and the results are shown in Table 2. Blank experiments conducted

Table 2 Catalytic results of Knoevenagel condensation over copper exchanged heteropolyacid catalyst

Entry	R	Catalyst [2 mol%]	Product	Time (min)	Con. (%)
1	H	Blank	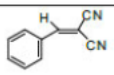	30	3
2	H	Blank	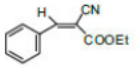	30	1
3	H	$CuSO_4$ $5H_2O$	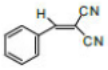	30	14
4	H	PMA	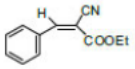	30	15
5	H	PWA	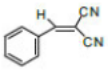	30	55
6	H	PMA	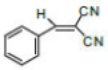	30	65
7	OMe	PMA	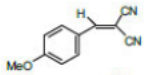	25	50
8	Cl	PMA	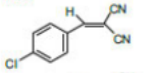	30	70
9	NO_2	PMA	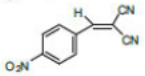	30	75
10	H	Cu-PWA	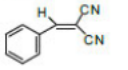	20	80
11	OMe	Cu-PWA	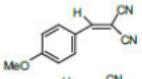	30	70
12	Cl	Cu-PWA	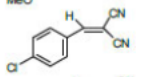	25	84
13	NO_2	Cu-PWA	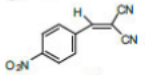	20	91
14	H	Cu-PMA	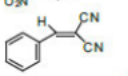	15	95
15	OMe	Cu-PMA	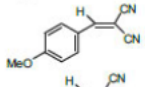	30	92
16	Cl	Cu-PMA	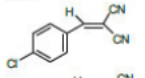	20	96
17	NO_2	Cu-PMA	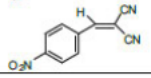	10	99

Reactions were carried out with aromatic aldehyde (10 mmol), malononitrile (10 mmol) with catalysts (2 mol%) in solvent free at 70 °C

Table 3 Catalytic results of the 2 mol % Cu–PMA catalyst over five cycles

Recycle entry	R	Product	Con. (%)
1	H	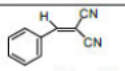	93
	OMe	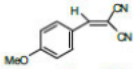	90
	Cl	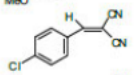	94
	NO_2	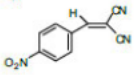	98
2	H	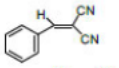	90
	OMe	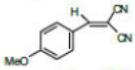	88
	Cl	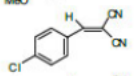	92
	NO_2	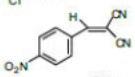	97
3	H	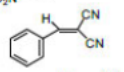	89
	OMe	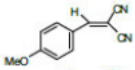	86
	Cl	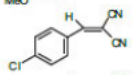	90
	NO_2	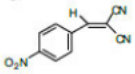	96
4	H	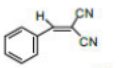	88
	OMe	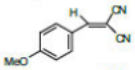	85
	Cl	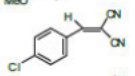	89
	NO_2	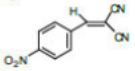	95
5	H	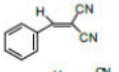	88
	OMe	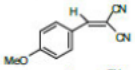	85
	Cl	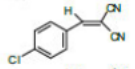	89
	NO_2	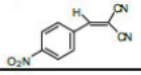	95

Reactions were carried out with benzaldehyde (10 mmol), malononitrile (10 mmol) with catalysts (2 mol %) in solvent free at 70 °C

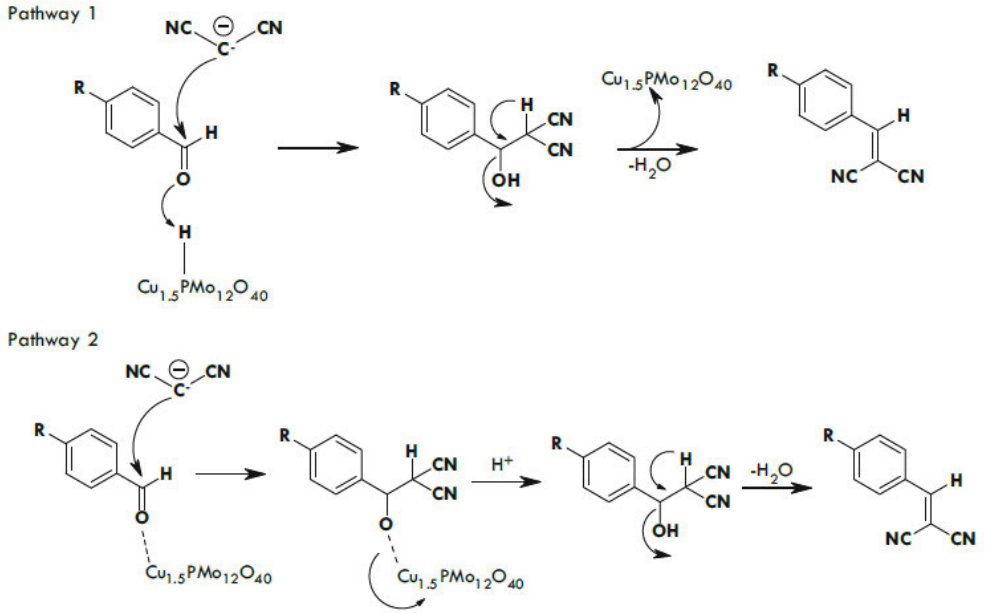

Scheme 2 Proposed reaction mechanism for the Knoevenagel condensation over Cu–PMA catalysts

at 70 °C with benzaldehyde and malononitrile as reactants produced a 3 % conversion and 100 % product selectivity, whereas using $CuSO_4$ gave a conversion of 14 % conversion with same selectivity. The PWA catalyst was less active than the PMA catalyst. The reaction between benzaldehyde and other active methylene compounds such as ethyl cyanoacetate was also studied. The findings indicate that malononitrile is a more active methylene group than ethyl cyanoacetate, suggesting that the methylene group contributes to the overall activity during the reaction.

The effect of copper exchange in the catalysts was studied initially for the Knoevenagel reaction under solvent free conditions at 70 °C and the results are presented in Table 2. The aldehyde conversion increased considerably suggesting that the increase in the formation of the desired product can be controlled by exchanging protons of PMA with copper, thereby altering the acidity of the catalyst. In other words, activity increased with a decrease in the strong acidic sites of the catalyst. The results correlate with BET surface area since Cu–PMA presents more available active sites than the PMA catalyst. The role of the strong acidic sites is further illustrated in the Cu–PWA catalyst. There are more strong acidic sites in the Cu–PWA catalyst than the Cu–PMA catalyst, and from catalytic results, it is observed that Cu–PMA shows superior activity (Table 2). In all cases, there was complete selectivity to the desired product.

The catalytic activity is also assessed according to the effect of activating and deactivating groups present on benzaldehyde (denoted R in Table 2). The result clearly illustrates that deactivating groups in the aromatic aldehyde exhibits higher activity than other groups due to the withdrawing group decreasing the electron density around the carbonyl group and thereby enhancing the activity when compared to electron releasing group present on benzaldehyde.

The catalytic properties of the regenerated catalyst were studied up to five cycles and the results are shown in Table 3. These findings show that there is very little change in the activity during these cycles suggesting that the catalysts are relatively stable and no loss of metal through leaching, as evidenced by ICP-AES analysis.

A possible reaction pathway for the copper exchanged phosphomolybdic acid catalysed Knoevenagel condensation reaction is shown in Scheme 2. It is proposed that the reaction occurs through two pathways. The first pathway shows the proton on the Cu–PMA catalyst is attacked by the carbonyl oxygen to further minimize electron density around carbonyl carbon. This is followed by attack of the active methylene group to produce the product. Pathway 2 shows that the copper in catalyst partially binds with the carbonyl oxygen to reduce the electron density around the carbonyl carbon followed by the addition of the active methylene group in malononitrile to the carbonyl carbon to

produce an adduct [30]. In the both pathways water is removed.

4 Conclusion

In this study, we have demonstrated the efficiency of eco-friendly heterogeneous bi-functional copper exchanged phosphomolybdic acid catalysts for the Knoevenagel condensation. Both copper and protons in the catalyst contribute to the superior activity of the copper exchanged catalysts when compared to the pure phosphomolybdic acid. XRD patterns show that crystalline nature of Keggin ion while FT-IR and Raman spectroscopy reveal that the Keggin structure is retained after exchange of copper in the PMA catalysts. Ammonia TPD, ^{31}P NMR and pyridine adsorbed FT-IR spectra results confirmed the activity is related to the acidity of the catalysts. Regeneration and further testing up to five cycles demonstrated the stable nature of the catalysts.

Acknowledgments Authors thank to the University of KwaZulu-Natal for financial support.

References

1. Kozhevnikov IV (1998) Chem Rev 98:171
2. Mizuno N, Misono M (1998) Chem Rev 98:199
3. Trost BM (1991) Comprehensive organic synthesis. Elsevier, Oxford, p 133
4. Viswanadham B, Jhansi P, Chary KVR, Friedrich HB, Singh S (2016) Catal Lett 146:364
5. Viswanadham B, Kumar VP, Chary KVR (2014) Catal Lett 144:744
6. Viswanadham B, Srikanth A, Chary KVR (2014) J Chem Sci 126:445
7. Viswanadham B, Srikanth A, Kumar VP, Chary KVR (2015) J Nanosci Nanotech 15:5391
8. Alharbi W, Kozhevnikova EF, Kozhevnikov IV (2015) ACS Catal 5:7186
9. Alharbi K, Kozhevnikova EF, Kozhevnikov IV (2015) Appl Catal A 504:457
10. Abdullah A, Hossein B, Elena K, Ivan K (2015) ACS Catal 5:5512
11. Walaa A, Esther B, Elena K, Ivan K (2014) J Catal 319:174
12. Knoevenagel L (1998) Ber 31:258
13. Enders D, Muller S, Demir AS (1988) Tetrahedron Lett 29:6437
14. Reeves RL, Patai S (1996) The chemistry of carbonyl compounds. Interscience Publishers, New York, p 567
15. Jones G (1967) Org React 15:204
16. Attanasi O, Fillippone P, Mei A (1983) Syn Commun 13:1203
17. Rao PS, Venkatratnam RV (1991) Tetrahedron Lett 32:5821
18. Bao W, Zhang Y, Wang J (1996) Syn Commun 26:3025
19. Saravanamurugan S (2006) Appl Catal A 298:8
20. Metzger JO (1998) Ang Chem Int Ed 37:2975
21. Tanaka K, Toda F (2000) Chem Rev 100:1025
22. Pillai MK, Singh S, Jonnalagadda SB (2011) Kinet Catal 52:536
23. Fioravanti S, Pellacani L, Tardella PA, Vergari MC (2008) Org Lett 10:1449
24. Pillai MK, Singh S, Jonnalagadda SB (2010) Syn Comm 40:3710
25. Oskooie HA, Heravi MM, Derikvand F, Khorasani M (2006) Syn Commun 36:2819
26. Nakamura E, Mori S (2000) Ang Chem Int Ed 39:3750
27. Johnson JS, Evans DA (2000) Acc Chem Res 33:325
28. Beletskaya IP, Cheprakov AV (2004) Coord Chem Rev 248:2337
29. Schneider EM, Zeltner M, Kranzlin N, Grass RN, Stark WJ (2015) Chem Comm 51:10695
30. Margandan B, Pushparaj H, Mani G, Mei MP, Hyun TJ (2011) J Ind Eng Chem 17:628
31. Barteau KP, Lyons JE, Song IK, Barteau MA (2006) Top Catal 41:55

Journal of Molecular Catalysis A: Chemical 425 (2016) 116–123

Contents lists available at ScienceDirect

Journal of Molecular Catalysis A: Chemical

journal homepage: www.elsevier.com/locate/molcata

Research Paper

Tuning surface composition of Cs exchanged phosphomolybdic acid catalysts in C—H bond activation of toluene to benzaldehyde at room temperature

Viswanadham Balaga*, Jhansi Pedada, Holger B. Friedrich, Sooboo Singh

Catalysis Research Group, School of Chemistry & Physics, University of KwaZulu-Natal-Durban, South Africa

ARTICLE INFO

Article history:
Received 3 July 2016
Received in revised form 3 October 2016
Accepted 4 October 2016
Available online 4 October 2016

Keywords:
Cesium
Phosphomolybdic acid
Ion-exchange
C—H bond activation
Brønsted acidity

ABSTRACT

A series of Cs exchanged phosphomolybdic (PMA) catalysts were synthesised by the ion exchange method. The prepared materials were characterized by various physico-chemical techniques such as X-ray diffraction, FT-IR, Raman spectroscopy, pyridine adsorbed FT-IR spectroscopy, ^{31}P NMR, BET surface area, nitrogen isotherms, TEM and STEM analysis. XRD results show crystallites of the Keggin ion of heteropolyacid catalysts. FT-IR and Raman spectra data reveal that the Keggin structure of PMA catalyst is maintained even after the exchange of the protons with Cs ions. Pyridine adsorbed FT-IR spectra show that available Brønsted acidic sites increases after Cs is incorporated in PMA. TEM analysis shows that the spherical shape remains intact after Cs exchange and STEM analysis shows a uniform distribution of elements in the Cs exchanged PMA catalyst. Nitrogen isotherms studies reveal a type IV isotherms for the Cs exchanged catalyst. The Cs exchanged phosphomolybdic acid (CsPMA) showed better catalytic performance than the phosphomolybdic acid (PMA) catalyst when evaluated for the C—H bond activation of toluene to benzaldehyde. The catalyst was easily recovered and reused for five cycles with stable activity.

1. Introduction

Polyoxometalates (POMs) or heteropolyacids (HPAs) are well known solid acid catalysts due to their tunable bi-functional acid and redox properties for various acid and oxidation reactions, respectively [1,2]. Recently, HPAs have been received considerable attention in many acid catalyzed and oxidation reactions with industrial applications [3–15]. HPAs are well known strong Brønsted acidity materials, however one of its major drawbacks is the low surface area which may impact on its catalytic performance. This can be resolved, to a certain extent, by modifying the textural properties and acidic functionalities of the compound, simply by exchanging or replacing the protons of HPA, specifically PMA with a large cation such as cesium Cs. Cs exchanged PMA catalysts are water tolerant solid acid catalysts which possess a higher surface area than the PMA catalysts and were studied in number of reactions including carbonylation, dehydration, condensation, alkylation, acylation, isomerization of *n*-butane, hydration of olefins and biodiesel synthesis [16–22]. In the view of several organic transformations carried out over Cs containing Keggin HPA catalysts, we proceeded to investigate the selective C—H bond activation of toluene to produce benzaldehyde at room temperature over Cs exchanged phosphomolybdic acid catalysts.

The catalytic selective oxidation of toluene to the benzaldehyde has great importance in both basic and applied research due to its extensive applications in academic and industrial chemistry. Benzaldehyde is a versatile aromatic carbonyl compound used in the perfumery, cosmetics and agrochemical industries. It is currently produced by liquid phase chlorination of toluene followed by hydrolysis [21,22] and also by the partial oxidation of toluene [23]. Among the two processes, oxidation of toluene is the more preferable route since chlorination of toluene followed by hydrolysis is a non-eco-friendly method. However, the oxidation of toluene in the gas phase leads to the formation of carbon oxides instead of benzaldehyde as the major product. Liquid phase oxidation or activation of toluene to benzaldehyde at room temperature could address these problems and at the same time, promote the selective synthesis of benzaldehyde as an eco-friendly process. Various studies involve the synthesis of benzaldehyde from toluene at room temperature and among them, heteropolyacid (HPA) has received considerable attention due to its eco-friendly and bi-functional nature [24–28]. Liu et al. [24] synthesised a tripodal tridentate copper(II) complex, CuImph (Imph = bis(4-imidazolyl methyl)benzylamine) to mimic the active site of copper enzymes

* Corresponding author.
E-mail addresses: visubalaga@gmail.com, Balagiav@ukzn.ac.za (V. Balaga).

http://dx.doi.org/10.1016/j.molcata.2016.10.007
1381-1169/

that mediate the oxidation of aliphatic C—H bonds under mild conditions. Their results show high reactivity and selectivity toward toluene aliphatic C—H bond oxidation, converting the toluene initially to benzyl alcohol and subsequently to benzaldehyde as the major product in a kinetic consecutive reaction. No evidence for benzoic acid is obtained. Wurtele et al. [26], on the other hand used copper peroxo complexes which they found to be stable at room temperature for the aliphatic C—H bond oxidation of toluene. To test the potential of these complexes, they reacted four peroxo complexes with toluene at room temperature under air and observed the formation of benzaldehyde in yields of up to 20%, along with small amounts of benzyl alcohol.

Our present work is related to effect of Cs exchanged phosphomolybdic acid catalysts for the selective C—H bond activation of toluene to benzaldehyde at room temperature. These materials were characterized by various techniques to investigate its surface, structural and acidic functionalities and its correlation with the catalytic activity.

2. Experiential

2.1. Catalyst synthesis

A series of Cs exchanged phosphomolybdic acid catalysts with various Cs content, ranging from 1 to 3 wt% loadings were prepared by ion exchanged method. In a typical synthesis, for a 1 wt% loading, 0.326 g of Cs_2CO_3 (Sigma Aldrich, SA) was dissolved in 10 mL of double distilled water. This solution was added drop wise to a solution of 3.65 g of $H_3PMo_{12}O_{40}$ (Sigma Aldrich, SA) made up in 15 mL of double distilled water. The resulting mixture was centrifuged to remove the precipitate which was the washed repeatedly with double distilled water. The solid was dried at 200 °C for 10 h. These prepared catalysts which had the formulae, $Cs_{1.0}PMo_{12}O_{40}$, $Cs_{2.0}PMo_{12}O_{40}$ and $Cs_{3.0}PMo_{12}O_{40}$ were labelled as CsPMA-1, CsPMA-2 and CsPMA-3, respectively.

2.2. Catalyst characterization

Powder X-ray diffraction patterns of samples were obtained with a Bruker D8 Advance diffractometer, using a Cu Ka radiation source (1.5406 Å) at 40 kV and 30 mA. The measurements were recorded in steps of 0.045° with a count time of 0.5 s in the range of 2–60°. The surface area of catalysts was determined using N_2 adsorption isotherms at −196 °C by the multipoint BET method taking 0.162 nm^2 as its cross-sectional area. The pore size distribution was measured by N_2 adsorption-desorption isotherms using a Micrometrics ASAP 2020 multi-point BET surface area analyzer. Prior to these experiments, the materials were degassed under helium flow overnight at 200 °C using a Micrometrics Flow Prep 060 and all experiments were carried out at a relative pressure range (p/p°) of 0.05 to 0.9. Infrared (IR) spectra were recorded on a Perkin Elmer Precisely equipped with a Universal ATR sampling accessory using a diamond crystal. The powdered material was placed on the crystal and a force of 120 psi was applied to ensure proper contact between the material and the crystal. The spectra were analyzed using Spectrum 100 software. Ex-situ pyridine adsorbed FT-IR experiments were carried out to investigate the nature of acidity, such as Brønsted and/or Lewis acid sites present on the catalyst. The spectra were recorded on a Perkin-Elmer ATR spectrometer at room temperature. Prior to analysis, pyridine adsorption experiments were carried out by placing a drop of pyridine on a small amount of the catalyst, followed by evacuation in air for 1 h to remove the reversibly adsorbed pyridine. Raman spectra were collected using a Horbia-Jobin-Yvon LabRam high resolution spectrometer equipped with a confocal microscope

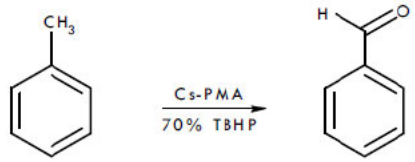

Scheme 1. Oxidation of toluene to benzaldehyde over Cs exchanged phosphomolybdic acid catalyst.

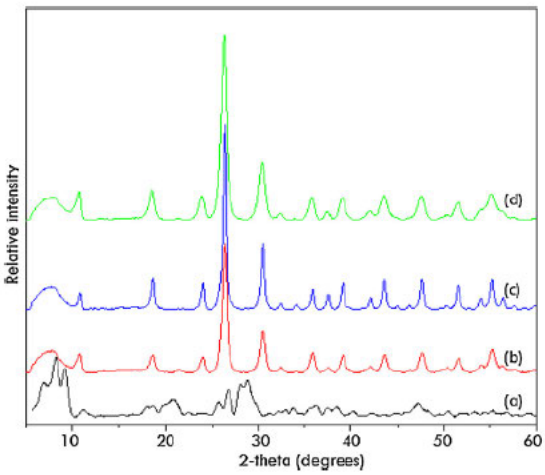

Fig. 1. XRD profile of (a) PMA, (b) CsPMA-1, (c) CsPMA-2, (d) CsPMA-3 catalysts.

with 2400/900 grooves/mm gratings and a notch filter. The visible laser excitation at 532 nm (visible/green) was supplied by a Yag double diode pumped laser (20 mW). Transmission electron microscopy (TEM) images were obtained on a Jeol JEM-1010 electron microscope. The images were captured and analyzed using iTEM software. Distribution and chemical analysis of elements in the materials was examined by STEM analysis. ^{31}P NMR spectra of catalyst were recorded on a Bruker Advance 400 MHz spectrometer and chemical shifts were reported relative to 85% H_3PO_4 in D_2O used as an external standard at 298 K.

2.3. Catalytic testing

Solvent free liquid phase oxidation of toluene was carried out in a 10 mL round bottom flask at room temperature. In a typical run, 10 mmol of toluene, 2 mL of 70% TBHP and 4 mol% of the catalyst were placed in the flask, under stirring (Scheme 1) and the reaction was constantly monitored by GC. The catalyst was then recycled and used for the same reaction.

3. Results & discussion

3.1. Catalyst characterization

3.1.1. X-ray diffraction

X-ray diffraction patterns of pure PMA and synthesised Cs exchanged PMA catalysts are shown in Fig. 1. These profiles indicate that PMA shows the triclinic structure, whereas the Cs exchanged PMA catalyst possesses the cubic structure of the Keggin ion of a heteropolyacid. The XRD profile also shows that in the pure PMA, the Keggin ion, usually found around a 2-theta value of 9–10° is

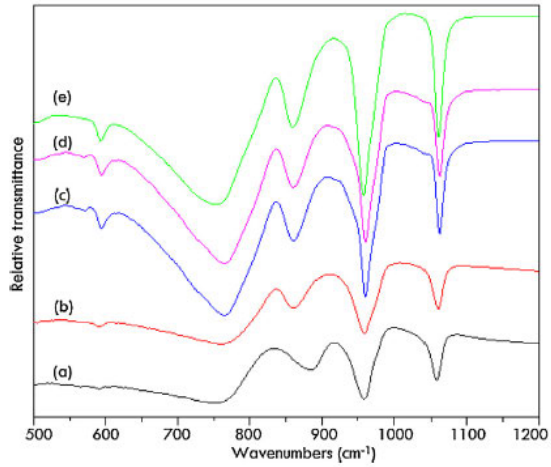

Fig. 2. FT-IR spectra of (a) PMA, (b) CsPMA-1, (c) CsPMA-2, (d) Reg. CsPMA-2, (e) CsPMA-3 catalysts.

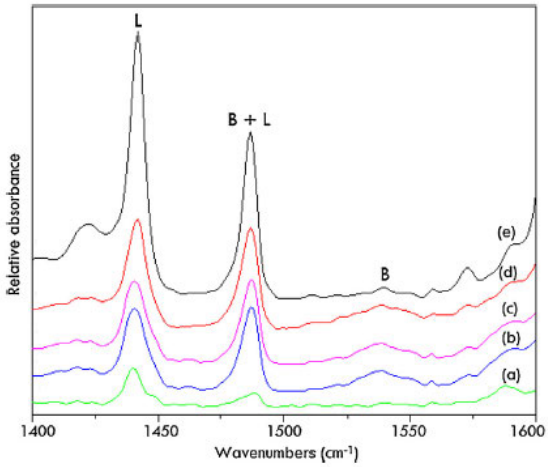

Fig. 4. Pyridine adsorbed FT-IR spectra of (a) CsPMA-3, (b) CsPMA-2, (c) regenerated CsPMA-2, (d) CsPMA-1, (e) PMA catalysts.

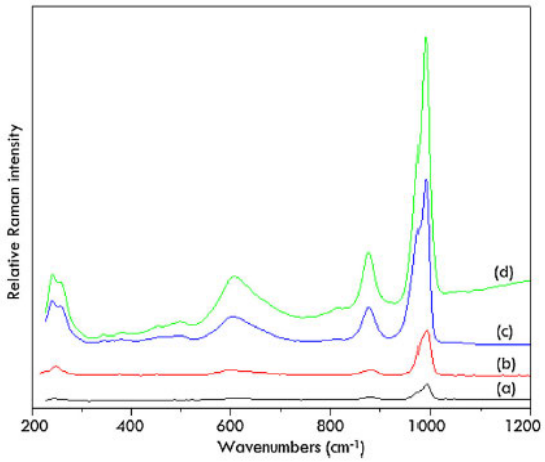

Fig. 3. Raman spectra of (a) PMA, (b) CsPMA-1, (c) CsPMA-2, (d) CsPMA-3 catalysts.

more pronounced when compared to the Cs exchanged PMA, consistent with findings in literature [29].

3.1.2. FT-IR spectroscopy

The FT-IR spectra of PMA and Cs-PMA catalysts shows four characteristic bands in the 500–1200 cm^{-1} region. The bands for the pure PMA at 760, 889, 961, 1058 cm^{-1} are attributed to Mo-Oc-Mo, Mo-O_t-Mo, Mo = O and P-O, respectively [3,4,6,7]. In Cs exchanged catalysts, a slight shift in the bands found at 754–767, 860, 960–962 and 1060–1061 are assigned to Mo—Oc—Mo, Mo—O_t—Mo, Mo═O and P—O, respectively. The shift of the peaks of about 2 to 7 cm^{-1} indicates that Cs successfully exchanges with protons in PMA, maintaining the characteristic Keggin ion of the heteropolyacid, even at higher loadings of cesium [30] (Fig. 2).

3.1.3. Raman spectroscopy

From Fig. 3, the characteristic Keggin ion band is present at 989–992 cm^{-1} for the PMA and the CsPMA catalysts. The more intense bands at 239, 600–603, 814 and 876–884 cm^{-1} are assigned to Mo-O_a, Mo-O_c-Mo, Mo-O_b-Mo and Mo-O_t, respectively [3,4,6,7]. It is also established that Keggin ion remains intact, even at higher loading of Cs. The findings in Raman spectroscopy complements the observations made in FT-IR spectroscopy.

3.1.4. Pyridine adsorbed FT-IR spectroscopy

The nature of the acidity in the catalysts was studied by *ex situ* pyridine FT-IR spectroscopy and the results are shown in Fig. 4. The IR band at 1538 cm^{-1} is assigned to Brønsted acidic sites. The peak observed at 1486 cm^{-1} is due to both Brønsted and Lewis acidic sites, whereas the band is observed at 1441 cm^{-1} is attributed to Lewis acidic sites of the catalysts. From Fig. 4, it is also apparent that Brønsted acidic sites increased slightly with an increase in the Cs content in PMA catalysts, but decreased considerably at higher Cs content. Lewis acidity is predominant at higher Cs content. A combination of both Brønsted and Lewis acidic sites decreased at higher Cs loadings.

Brønsted acidity is observed more in the case of CsPMA-2 catalyst rather than other loadings, which might be due to a large surface area exhibited by the CsPMA-2 catalyst, resulting in the availability of more protons on the surface area of catalyst.

3.1.5. Nitrogen adsorption-desorption isotherms

Textural properties of PMA and the synthesised Cs exchanged PMA catalysts are tabulated in Table 1. The surface area of the catalysts increases with an increase in Cs content up to the CsPMA-2 catalyst. All the Cs exchanged catalysts exhibits a type IV isotherm and a hysteresis loop associated with mesoporous materials [31]. At higher Cs loadings, the BET surface area decreased substantiantly with a slight increase in pore size, probably due to agglomeration. The high BET surface area of the CsPMA-2 catalyst results in a lower Keggin anion density as reflected by the lower crystallinity of Keggin ion units when compared to other Cs loadings. These results correlate well with X-ray diffraction studies which shows that pure PMA is more crystalline than the Cs exchanged PMA catalysts. The particle size obtained from sorption experiments shows large particle sizes for the PMA catalyst compared to the Cs exchanged PMA catalysts (Fig. 5).

3.1.6. ^{31}P NMR spectroscopy

^{31}P NMR spectra of PMA and the Cs exchanged PMA catalysts were recorded in D_2O solvent (Fig. 6). The pure PMA catalyst showed a chemical shift at −3.9 ppm, whereas in the case of Cs

Table 1
Textural properties and Cs content of Cs-PMA catalysts.

Catalyst	BET surface area (m^2/g)	Pore volume (cm^3/g)	Pore diameter (Å)	Particle size (Å)	Cs content theoretical per Keggin ion (atomic%)	Cs content practical per Keggin ion (atomic%)[a]	Keggin anion density (HPA/nm^2)
PMA	2.7	0.01	128	21662	–	–	1.2
CsPMA-1	25	0.03	80	1950	1.0	0.9	0.12
CsPMA-2	146	0.14	40	409	2.0	2.1	0.019
CsPMA-3	80	0.08	50	756	3.0	2.9	0.033

[a] Cs content obtained from STEM analysis.

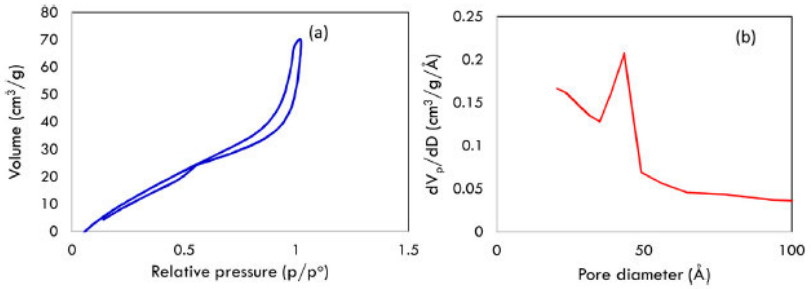

Fig. 5. Nitrogen adsorption-desorption isotherm (a) and BJH pore size distribution (b) of the CsPMA-2 catalyst.

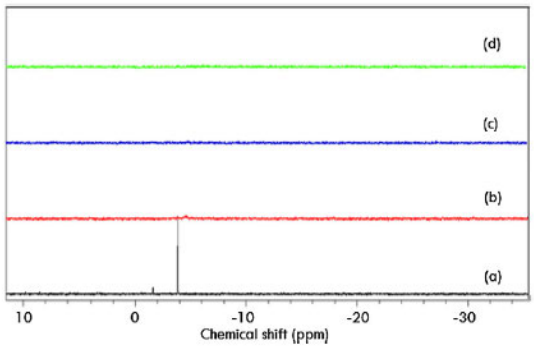

Fig. 6. ^{31}P NMR of (a) PMA, (b) CsPMA-1, (c) CsPMA-2, (d) CsPMA-3 catalysts.

exchanged PMA catalysts, this peak disappears indicating that the Cs exchanged PMA is not soluble in the D_2O solvent, providing evidence that the Cs exchanged catalysts have no impurities such as the starting material which is PMA.

3.1.7. TEM analysis

The internal morphology of pure PMA and the CsPMA catalysts was studied by TEM analysis and the results are shown in Fig. 7. There is every indication that the pure PMA has a spherical structure and this structure was maintained with the Cs exchanged compounds.

3.1.8. STEM analysis

BF-STEM imaging with chemical analysis of fresh and regenerated CsPMA-2 catalyst was conducted to map the structure and relative spatial distribution of the elements present in the catalysts (Fig. 8) and to obtain the Cs content in the Keggin anion (Table 1).

Table 2
Catalytic results over Cs exchanged phosphomolybdic acid catalysts.[a]

Catalyst	Conversion (%)	Selectivity (%)		TON[b]
		Benzaldehyde	Benzyl alcohol	
Blank	–	–	–	–
PMA	0.6	53	47	1.09
CsPMA-1	0.7	85	15	1.37
CsPMA-2	0.9	98	2	1.88
CsPMA-3	0.5	78	22	1.10

[a] Reaction conditions: Toluene (10 mmol), TBHP (2 mL), Catalyst = 0.1 g, Reaction temperature = RT, Reaction time = 24 h.
[b] TON=Number of moles of products/Number of moles of catalysts.

3.2. Catalytic activity studies

The catalytic activation of C—H bond in toluene was studied over Cs exchanged PMA catalysts under nitrogen atmosphere and the results are tabulated in Table 2.

Initially, blank reactions were studied at same reaction conditions, however there was no activity recorded. The phosphomolybdic acid showed a 0.6% conversion and 53% towards benzaldehyde. Among the various Cs exchanged PMA catalysts, the CsPMA-2 catalyst showed the highest conversion with almost maximum selectivity towards benzaldehyde compared to the other Cs/P ratios, probably due to the larger number of available active sites as reflected by the high surface area of the catalyst. Surface acidity of the catalyst also plays a role. At a higher Cs loading, i.e. for CsPMA-3, the catalyst is more crystalline leading to a decrease in the surface acidity resulting in lower activity, similar to that observed for the CsPMA-1 and pure PMA catalyst. It is also interesting to note that the higher turnover number of CsPMA-2 leads to better activity compared to the other loadings and the PMA itself. The catalytic results are strongly associated with the nature of acidity of the catalyst. From pyridine adsorbed FT-IR studies, more surface Brønsted acidic sites are observed in the case of CsPMA-2 catalyst than the other Cs containing materials including the pure PMA catalyst. The mesoporous nature of CsPMA-2 catalyst with its high pore volume and surface area also favours formation of benzaldehyde compared other catalysts.

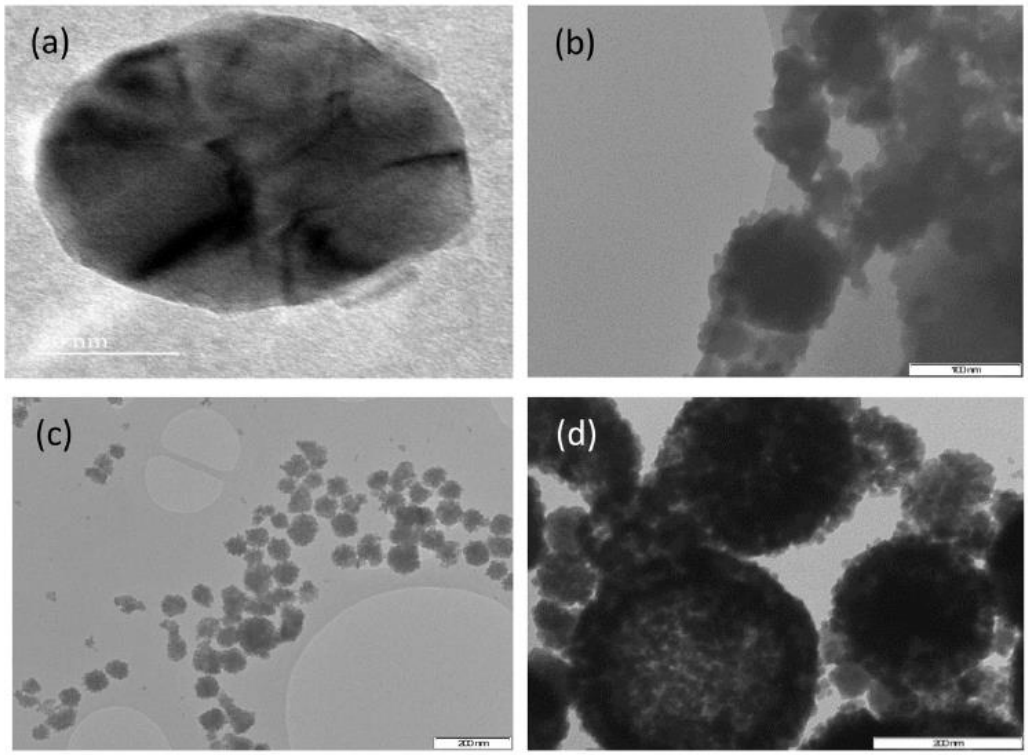

Fig. 7. TEM images of (a) PMA (b) CsPMA-1, (c) CsPMA-2 and (d) CsPMA-3 catalysts.

Table 3
Catalytic results over CsPMA-2 catalysts with various amounts of TBHP.[a]

TBHP (mL)	Conversion (%)	Selectivity (%)		
		Benzaldehyde	Benzyl alcohol	Benzoic acid
1	0.5	96	4	–
2	0.9	98	2	–
4	1.0	99	–	1
6	1.1	97	–	3

[a] Reaction conditions: Toluene (10 mmol), TBHP (1–6 mL), Catalyst = 0.1 g, Reaction temperature = RT, Reaction time = 24 h.

Table 4
Catalytic results over various loadings of CsPMA-2 catalysts.[a]

Catalyst (g)	Conversion (%)	Selectivity (%)		
		Benzaldehyde	Benzyl alcohol	Benzoic acid
0.05	0.4	96	4	–
0.1	0.9	98	2	–
0.2	1.1	90	1	9
0.3	1.1	85	–	15

[a] Reaction conditions: Toluene (10 mmol), TBHP (2 mL), Catalyst = 0.05–0.3 g, Reaction temperature = RT, Reaction time = 24 h.

Table 5
Catalytic results over CsPMA-2 catalysts with different concentrations of toluene.[a]

Concentration of toluene (mmol)	Conversion (%)	Selectivity (%)	
		Benzaldehyde	Benzyl alcohol
2	1.6	46	54
4	1.3	75	25
8	1.1	90	10
10	0.9	98	2

[a] Reaction conditions: Toluene (2–10 mmol), TBHP (2 mL), Catalyst = 0.1 g, Reaction temperature = RT, Reaction time = 24 h.

The oxidation of toluene over the CsPMA-2 catalyst was studied with various volumes of the oxidant, TBHP and the results are presented in Table 3. These results are show that the activity increases significantly when the volume of the oxidant is doubled from 1 mL to 2 mL. Thereafter, there is a slight increase in the activity as the volume of the oxidant increased. An increase in the concentration of TBHP results in the formation of benzoic acid at the expense of benzaldehyde.

The effect of amount of catalyst used on the activity was investigated and the results are given in Table 4. The conversion of toluene increased with an increase in the amount of the catalyst. Although the conversion increased with an increase of catalyst loadings, the selectivity towards benzaldehyde selectivity decreased substantiantly, probably be due to further oxidation of benzaldehyde to benzoic acid at higher concentration of the heteropolyacid at room temperature. The above findings also show that 0.1 g of catalyst is the optimum amount required.

We also studied effect of toluene concentration over the CsPMA-2 catalyst under similar reaction conditions (Table 5). These findings show that an increase in the concentration of reactant results in a decrease in the conversion but selectivity towards benzaldehyde increases significantly. The effect of various oxidants was studied and results are shown in Fig. 9. TBHP is the most efficient oxidant that can activate the C—H bond in the presence of the heteropolyacid catalyst.

Time on stream experiments were conducted to investigate the influence of time on the activity of the CsPMA-2 catalyst. From Fig. 10, at the outset, conversion of toluene and selectivity towards benzaldehyde is low, but increases significantly over time.

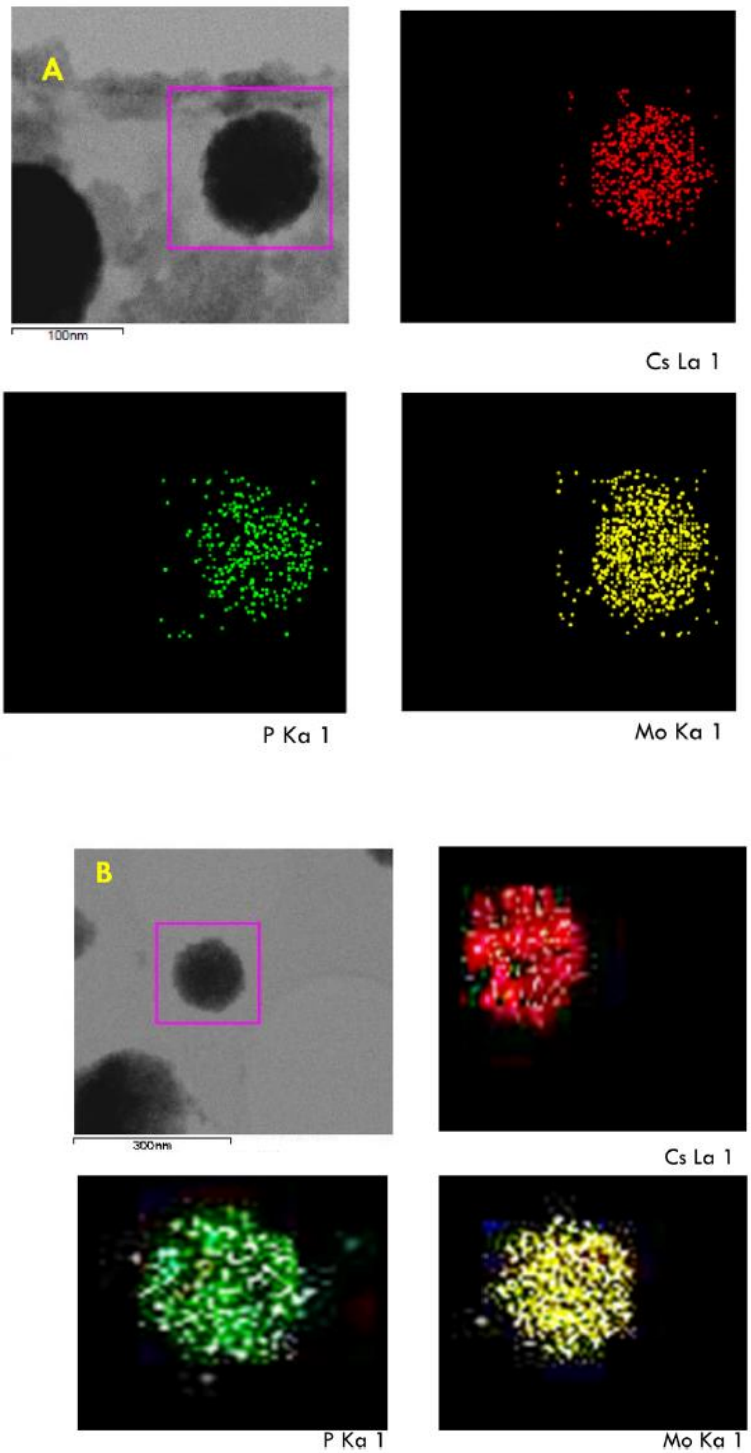

Fig. 8. STEM images of (A) fresh and (B) regenerated CsPMA-2 catalyst. These findings show that theoretical Cs loadings are well correlated with experimental atomic% data obtained from STEM chemical analysis. The fresh and regenerated CsPMA-2 shows uniform spatial distribution of all the elements and shows a 2.1 Cs atomic% of the catalyst.

The catalyst was subjected to a number of cycles to study its stability (Fig. 11). Before regeneration, the catalyst was separated, filtered and washed several times with organic solvent to remove any organic moiety on the surface of the catalyst and dried in an oven over night. The catalyst was characterized by FT-IR (Fig. 2) to observe any structural changes and pyridine adsorbed FT-IR (Fig. 4) to investigate any change in the surface acidity. STEM analysis was also conducted to observe any change in the Cs content of the regenerated catalyst. All these analyses showed no change in terms of structure, surface acidity and concentration in the regenerated

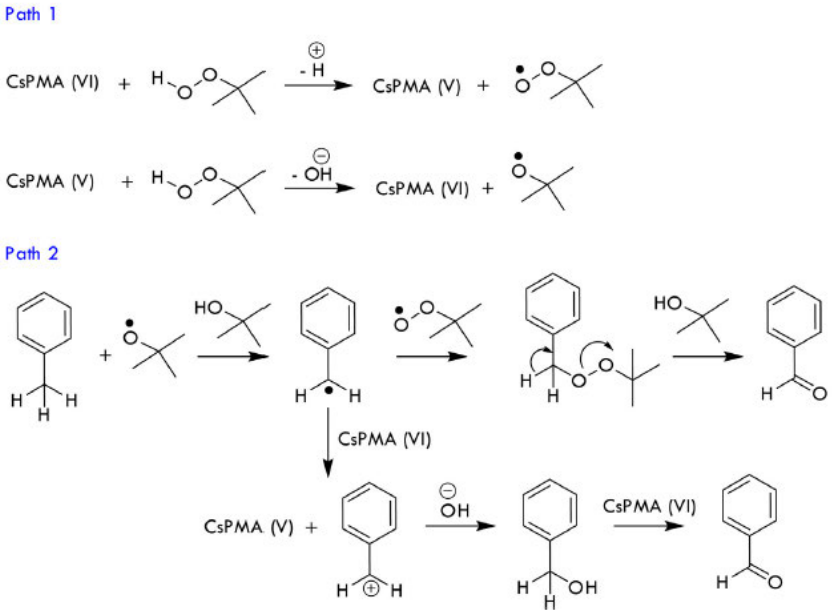

Scheme 2. Proposed reaction mechanism of C—H bond activation of toluene to benzaldehyde over Cs exchanged phosphomolybdic acid (Cs-PMA) catalysts.

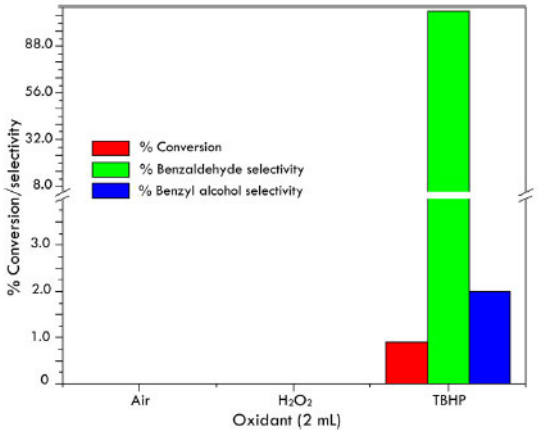

Fig. 9. Catalytic results with various oxidants over CsPMA-2 catalyst.

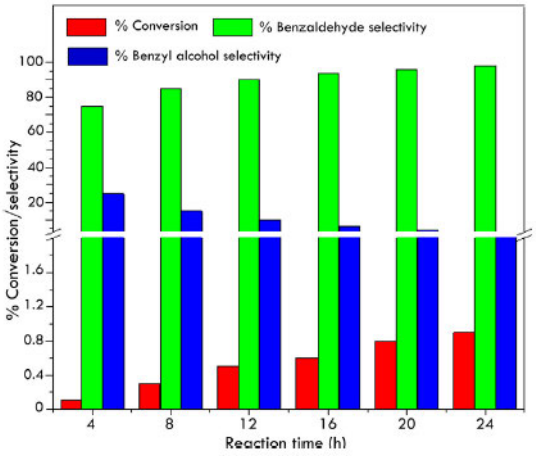

Fig. 10. Time on stream studies over the CsPMA-2 catalyst.

CsPMA-2 catalyst as a result consistent results were obtained over the five cycles investigated.

The reaction was also studied at various reaction temperatures and the results indicate that the formation of benzaldehyde increased with an increase in reaction temperature. However, as the temperature was increased to 120 °C, the benzaldehyde selectivity decreased sharply and benzoic acid was observed as the major product. Brutchey et al. [32] studied toluene oxidation over Co supported SBA-15 using TBHP as oxidant showed a 8% conversion with a 64% selectivity towards benzaldehyde at 80 °C. However, in our study, the Cs exchanged PMA catalyst achieved a 86% selectivity towards benzaldehyde for a 3.1% conversion at 80 °C, showing that the CsPMA-2 catalyst is highly selective towards benzaldehyde compared to Co-SBA-15 catalyst at a lower reaction temperature (Table 6).

Table 6
Catalytic results over CsPMA-2 catalysts at various reaction temperature.[a]

Temperature (°C)	Conversion (%)	Selectivity (%)		
		Benzaldehyde	Benzyl alcohol	Benzoic acid
RT	0.9	98	2	–
80	3.1	86	4	10
120	5.0	61	5	34

[a] Reaction conditions: Toluene (10 mmol), TBHP (2 mL), Catalyst = 0.1 g, Reaction time = 24 h.

3.3. Proposed reaction mechanism

The selective synthesis of benzaldehyde over Cs-PMA catalysts could be due to the proposed pathways shown in Scheme 2 [33].

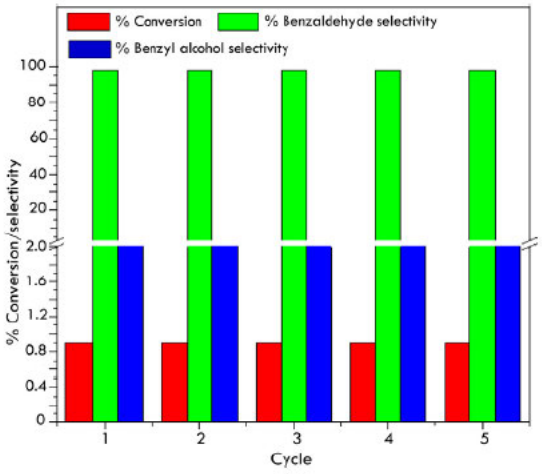

Fig. 11. Conversion of toluene and selectivity towards benzaldehyde and benzyl alcohol over the CsPMA-2 catalyst for 5 cycles.

Initially, in path 1, the Cs-PMA catalyst reacts with TBHP to form *tert*-butyl peroxy and *tert*-butyloxy radicals. In path 2, these radicals react with toluene and produce benzaldehyde as the major product. However, the benzyl radical reacts with the catalyst to from the benzyl cation by a transfer of an electron to the catalyst which later reacts with the hydroxyl ion to form benzyl alcohol [33]. The formation of the benzaldehyde from benzyl alcohol over phosphomolybdic acid catalysts occurs through the transfer of two electrons and two protons from the benzyl alcohol to the catalyst to produce benzaldehyde [34].

4. Conclusion

In the present investigation, we have demonstrated an eco-friendly heterogeneous Cs exchanged phosphomolybdic acid catalysts exhibiting remarkable benzaldehyde selectivity and significant conversion than the pure PMA catalyst during C—H bond activation of toluene. BET surface area and pore size distribution studies shows that the mesoporous nature of CsPMA-2 catalyst results in higher selectivity towards desired product. FT-IR and Raman spectroscopy reveal that Keggin structure is maintained even after the exchange of Cs in PMA. ^{31}P NMR spectra strongly indicate the water tolerant nature of HPA catalysts, while pyridine FT-IR shows that surface acidity is related to the catalytic activity of the Cs exchanged catalysts. STEM images show an even spatial distribution of metals in both the fresh and regenerated CsPMA-2 catalyst. The catalyst maintains its structure and acidity even after recycling up to 5 times.

Acknowledgment

Authors thank the University of KwaZulu-Natal for financial support.

References

[1] I.V. Kozhevnikov, Chem. Rev. 98 (1998) 171.
[2] N. Mizuno, M. Misono, Chem. Rev. 98 (1998) 199.
[3] B. Viswanadham, P. Jhansi, K.V.R. Chary, H.B. Friedrich, S. Singh, Catal. Lett. 146 (2016) 364.
[4] B. Viswanadham, J. Pedada, H.B. Friedrich, S. Singh, Catal. Lett. 146 (2016) 1470.
[5] B. Viswanadham, V.P. Kumar, K.V.R. Chary, Catal. Lett. 144 (2014) 744.
[6] B. Viswanadham, A. Srikanth, K.V.R. Chary, J. Chem. Sci. 126 (2014) 445.
[7] B. Viswanadham, A. Srikanth, V.P. Kumar, K.V.R. Chary, J. Nanosci. Nanotech. 15 (2015) 5391.
[8] S. Yamaguchi, S. Sumimoto, Y. Ichihashi, S. Nishiyama, S. Tsuruya, Ind. Eng. Chem. 44 (2005) 1.
[9] G. Wang, Y. Han, F. Wang, Y. Chu, X. Chen, Reac. Kinet. Mech. Cat. 115 (2015) 679.
[10] L. Marosi, G. Cox, A. Tenten, H. Hibst, J. Catal. 194 (2000) 140.
[11] Z. Long, Y. Zhou, G. Chen, W. Ge, J. Wang, Sci. Report 4 (2014) 3651.
[12] Z. Fumin, G. Maiping, G. Hanqing, W. Jun, Chin. J. Chem. Eng. 15 (2007) 895.
[13] P. Sharma, A. Patel, Ind. J. Chem. 48A (2009) 964.
[14] I.K. Song, J.K. Lee, G.I. Park, W.Y. Lee, Stu. Sur. Sci. Catal. 110 (1997) 1183.
[15] M. Misono, Chem. Comm. 13 (2001) 1141.
[16] A. Srikanth, B. Viswanadham, V.P. Kumar, N.R. Anipindi, K.V.R. Chary, Appl. Petrochem. Res. 6 (2016) 145.
[17] P. Guyraud, N. Essyem, J.C. Vedrine, Catal. Lett. 56 (1999) 35.
[18] A. Corma, M. Martinez, C. Martinez, J. Catal. 164 (1996) 422.
[19] N. Essayem, G. Coudurier, M. Fournier, J.C. Vedrine, Catal. Lett. 34 (1995) 223.
[20] K. Narasimharao, D.R. Brown, A.F. Lee, A.D. Newman, P.F. Siril, S.J. Tavener, K. Wilson, J. Catal. 248 (2007) 226.
[21] T. Okuhara, H. Watanabe, T. Nishimura, K. Inumaru, M. Misono, Chem. Mater. 12 (2000) 2230.
[22] M. Kimura, T. Nakato, T. Okuhara, Appl. Catal. 165 (1997) 227.
[23] B. Friedrich, W. Elaine, Benzaldehyde in Ullmann's Encyclopedia of Industrial. Chemistry, Wiley-VCH, 2002.
[24] C.C. Liu, T.S. Lin, S.I. Chan, C.Y. Mou, J. Catal. 322 (2015) 139.
[25] M. Mahyari, M.S. Laeini, A. Shaabani, Chem. Comm. 50 (2014) 7855.
[26] C. Wurtele, O. Sander, V. Lutz, T. Waitz, F. Tuczek, S. Schindler, J. Am. Chem. Soc 131 (2016) 7544.
[27] S. Bose, A. Pariyar, A.N. Biswas, P. Das, P. Bandyopadhyay, Catal. Comm. 12 (2001) 1193.
[28] K.T.V. Rao, P.S.N. Rao, P. Nagaraju, P.S.S. Prasad, N. Lingaiah, J. Mol. Catal. A: Chem. 303 (2016) 84.
[29] H.R. Ghalebi, S. Aber, A. Karimi, J. Mol. Catal. A: Chem. 415 (2016) 96.
[30] M. Sun, J. Zhang, C. Cao, Q. Zhang, Y. Wang, H. Wan, Appl. Catal. A: Gen. 349 (2008) 212.
[31] J.B. McMonagle, J.B. Moffat, J. Coll. Interface Sci. 101 (1984) 479.
[32] R.L. Brutchey, I.J. Drake, A.T. Bell, T. Don Tilley, Chem. Commun. (2005) 3736.
[33] A.M. Khenkin, R. Neumann, J. Am. Chem. Soc. 123 (2001) 6437.
[34] A. Patel, S. Pathan, Ind. Eng. Chem. Res. 51 (2012) 732.

APPENDIX C

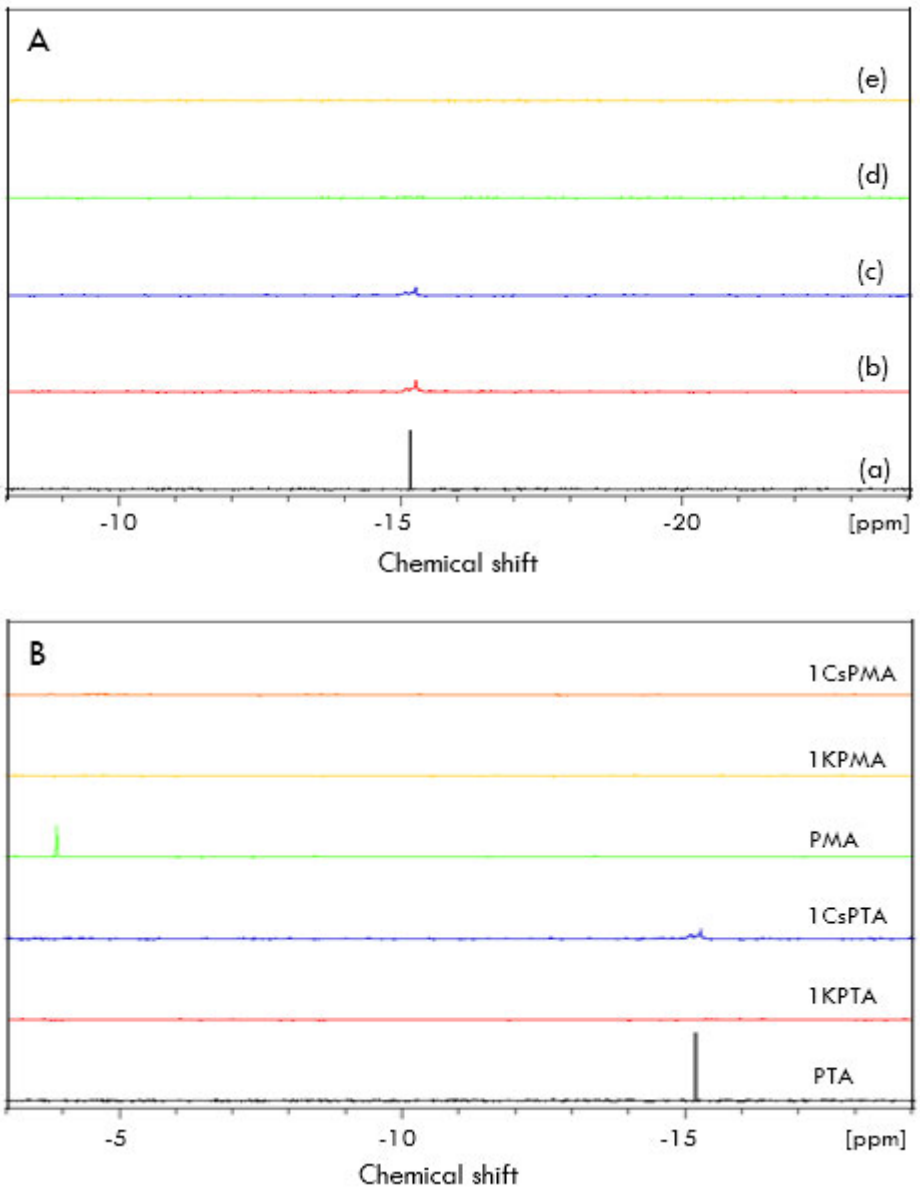

Figure C3.1 ^{31}P NMR spectra of (a) PTA, (b) 0.5CsPTA, (c) 1CsPTA, (d) 2CsPTA and (e) 3CsPTA catalysts (A) and of K and Cs exchanged heteropolyacid catalysts (B).

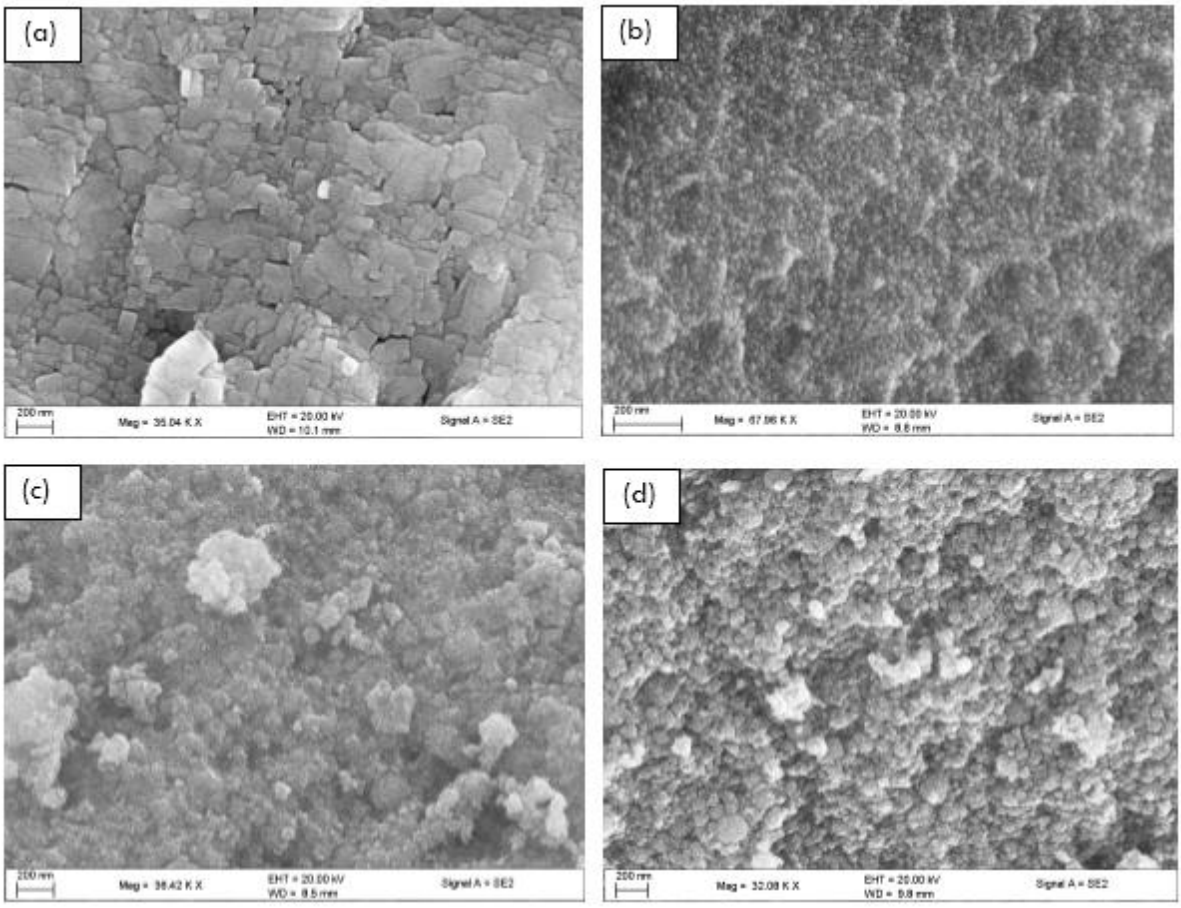

Figure C3.2 SEM images of (a) PTA, (b) 1CsPTA, (c) 2CsPTA and (d) 3CsPTA catalysts.

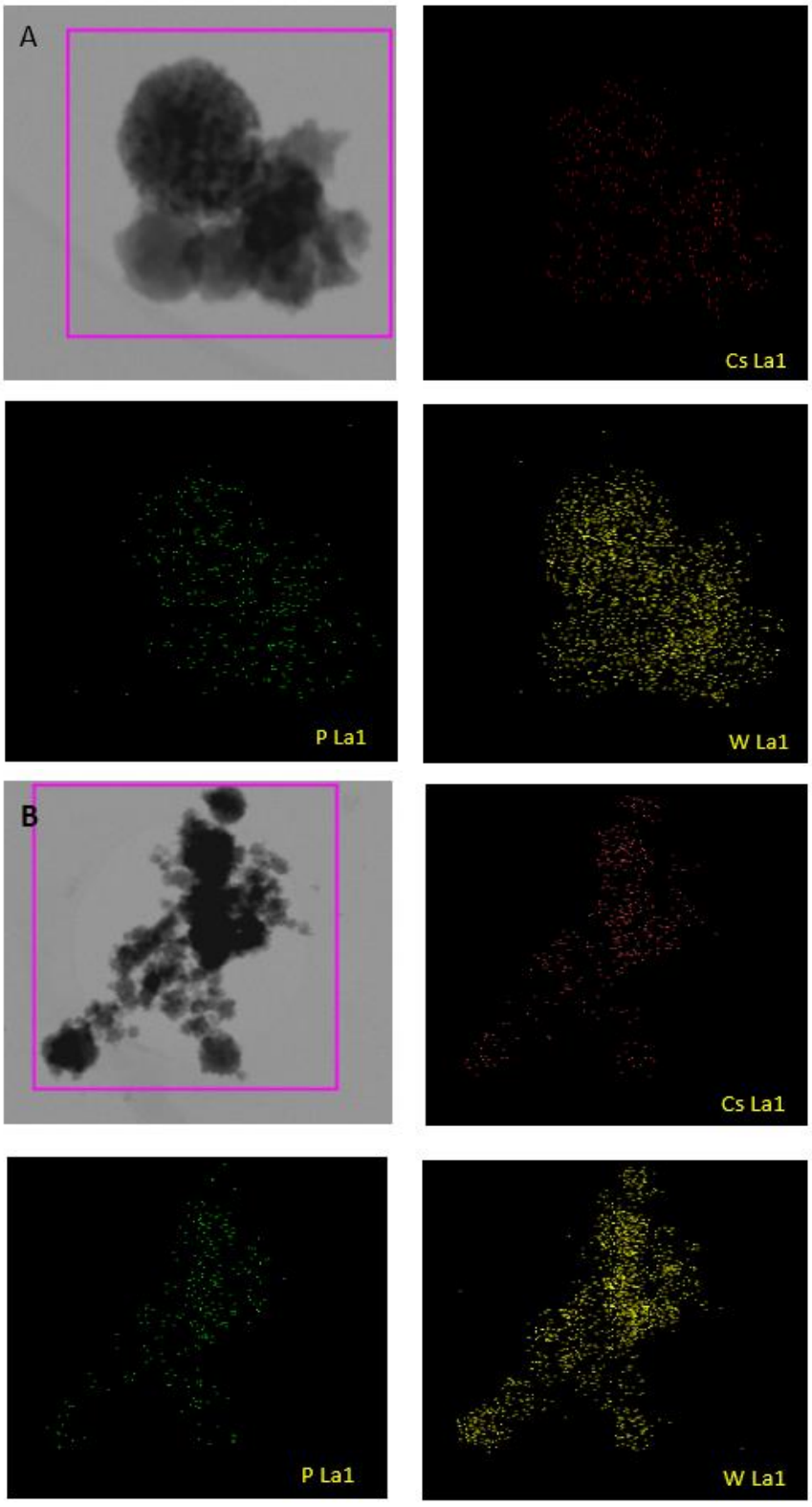

Figure C3.3 BF-STEM analysis of (A) 2CsPTA and (B) 3CsPTA catalysts.

Table C4.1 Catalytic results over 2KPMA catalysts using various amounts of TBHP[a].

TBHP (mmol)	Conversion (%)	Selectivity (%)		
		benzaldehyde	styrene oxide	others[b]
5	5.0	75	14	11
10	8.5	80	16	4
15	8.7	80	16	4
20	8.9	78	16	6

[a]Reaction conditions: styrene (10 mmol), catalyst = 0.1 g, reaction temperature = RT, reaction time = 24 h;
[b]others = 1-phenylethane -1,2-diol, phenyl acetaldehyde, benzoic acid; reactions done in triplicate.

Table C4.2 Catalytic results with different amounts of 2KPMA catalysts[a].

Catalyst	Conversion (%)	Selectivity (%)		
		benzaldehyde	styrene oxide	others[b]
0.05	5.6	78	16	6
0.1	8.5	80	16	4
0.2	8.6	75	15	10
0.3	8.7	69	14	17

[a]Reaction conditions: styrene (10 mmol), TBHP (10 mmol), reaction temperature = RT, reaction time = 24 h;
[b]Others = 1-phenylethane -1,2-diol, phenyl acetaldehyde, benzoic acid; reactions done in triplicate.

Table C4.3 Catalytic results over 2KPMA catalyst with variation in the concentration of styrene[a].

Styrene (mmol)	Conversion (%)	Selectivity (%)		
		benzaldehyde	styrene oxide	others[b]
2	22.6	88	9	4
4	17.5	85	10	5
6	14.7	84	12	4
8	11.9	81	13	6
10	8.5	80	16	4

[a]Reaction conditions: styrene (2-10 mmol), TBHP (10 mmol), catalyst = 0.1 g, reaction temperature = RT, reaction time = 24 h; [b]others = 1-phenylethane -1,2-diol, phenyl acetaldehyde; reactions done in triplicate.

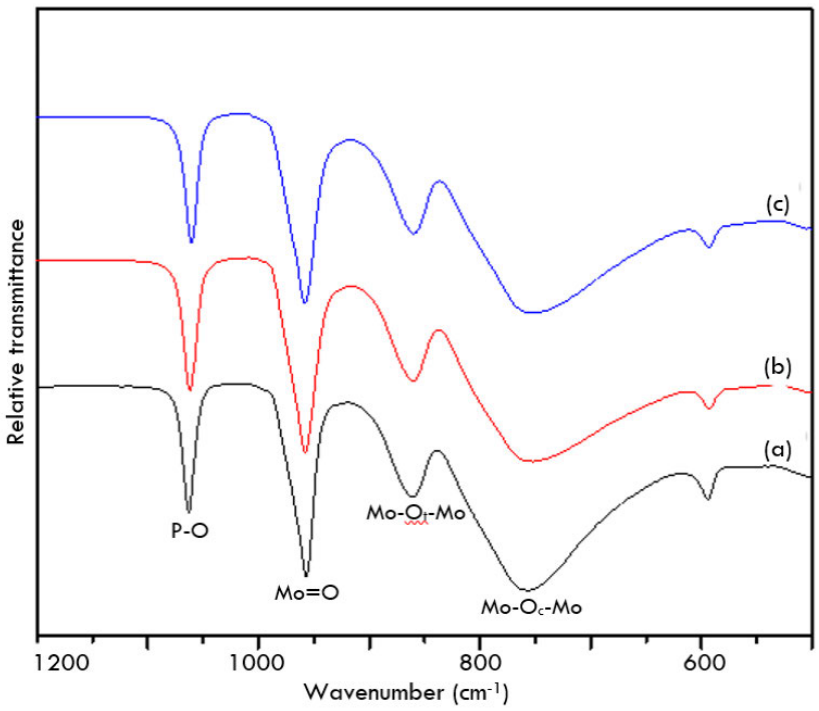

Figure C4.1 Infrared spectra of (a) 2KPMA, (b) 2RbPMA and (c) 2CsPMA catalysts.

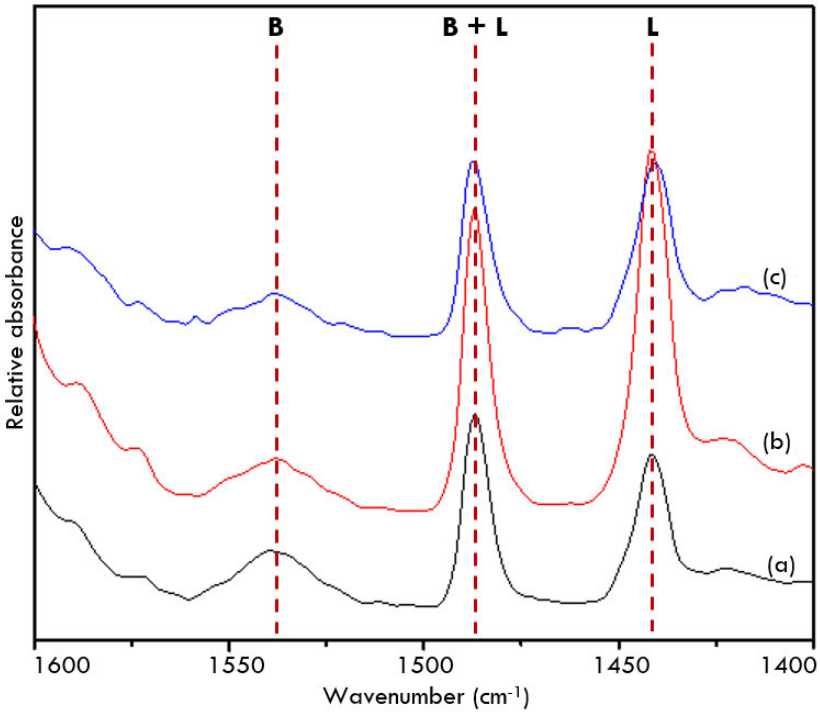

Figure C4.2 Pyridine infrared spectra of (a) 2KPMA, (b) 2RbPMA and (c) 2CsPMA catalysts.

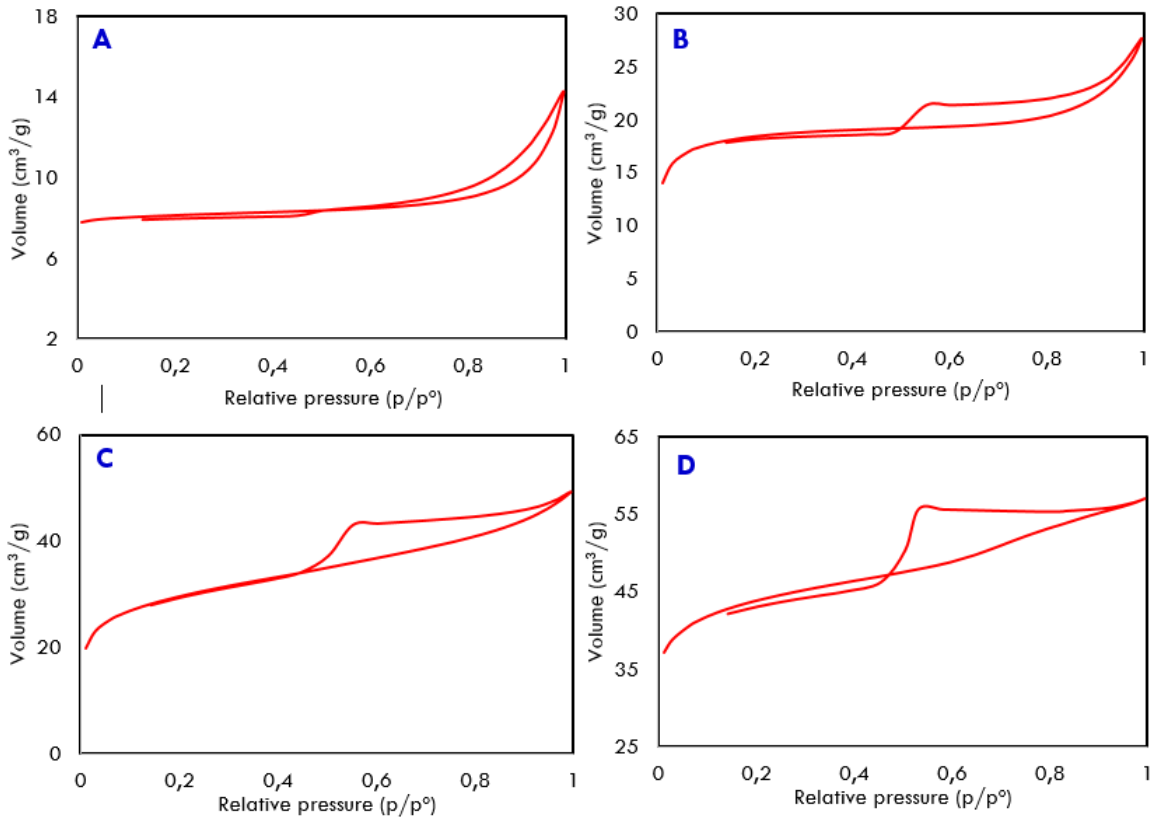

Figure C4.3 N_2 isotherms of (A) PMA, (B) 1KPMA, (C) 2KPMA and (D) 3KPMA catalysts.

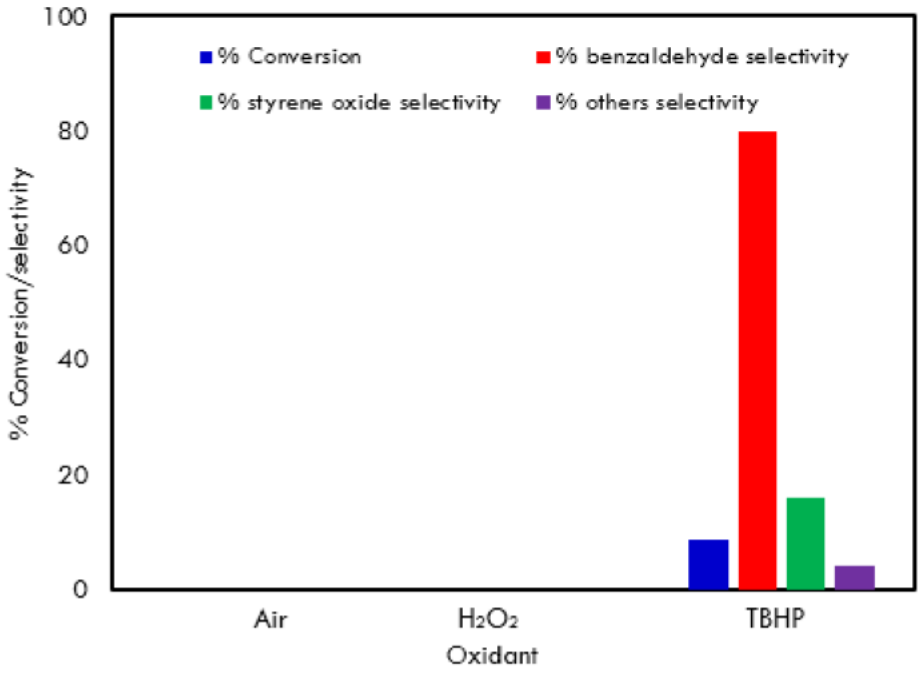

Figure C4.4 Catalytic results of styrene oxidation over 2KPMA using various oxidants at room temperature.

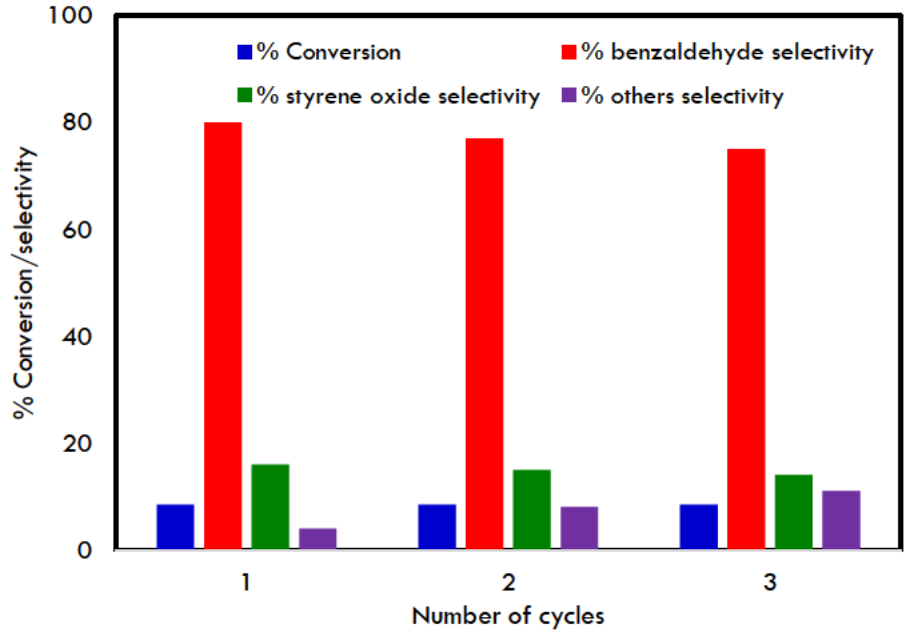

Figure C4.5 Catalytic recycling results of styrene oxidation over 2KPMA catalysts at room temperature.